KWAME NKRUMAH UNIVERSITY OF SCIENCE AND TECHNOLOGY,

KUMASI

Vegetation dynamics in the southwest of Burkina Faso in response to rainfall variability and land use

by

Benewinde Jean-Bosco ZOUNGRANA

(MSc. GIS and Remote Sensing of Environmental Management)

A thesis submitted to the Department of Civil Engineering, College of Engineering,

in partial fulfilment of the requirements for the degree of

DOCTOR OF PHILOSOPHY

in

Climate Change and Land Use

April, 2016

DEDICATION

Dedicated to:

- ✓ My father, Poko Boniface ZOUNGRANA, may your soul rest in peace.
- ✓ My mother, brothers and sisters.

DECLARATION

I hereby declare that this submission is my own work towards the PhD in Climate Change and Land Use and that, to the best of my knowledge, it contains no material previously published by another person, nor material which has been accepted for the award of any other degree of the University, except where due acknowledgment has been made in the text.

Benewinde Jean-Bosco ZOUNGRANA,

ID: PG8393212 Signature Date

Certified by

Dr. Leonard K. AMEKUDZI (Main supervisor) Signature Date
Department of Physics
Kwame Nkrumah University of Science and
Technology (KNUST), Kumasi, Ghana

Prof. Dr. Christopher CONRAD (First co-supervisor) Signature Date
Remote Sensing Unit
Institute of Geography and Geology
University of Würzburg, Germany

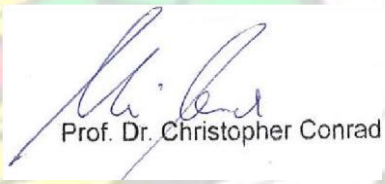

Prof. Evariste Dapola DA (second co-supervisor) Signature Date
Department of Geography
University of Ouagadougou

Prof. Yaw Adubofour-Tuffour Signature Date

Head of Department

ABSTRACT

Assessing vegetation dynamics is relevant for ensuring sustainable development especially in regions where natural vegetation is altered by anthropogenic land use and rainfall variability. This is particularly crucial in the Sudan savannah of West Africa where vegetation dynamics remains poorly understood and is subject to debate. The main objective of this study was to evaluate the response of vegetation dynamics to rainfall variability and land use in the southwest of Burkina Faso. For this purpose, Landsat data (1999, 2006 and 2011) and ancillary data were used to determined changes in Land Use/Cover (LULC) with random forest classifier. Standardised Precipitation Index (SPI) and correlation analysis were used to determine rainfall variability and the relationship between vegetation indices (NDVI and EVI) and rainfall respectively. Lastly, the integration of temporal persistence analysis and Mann-Kendall's trend test was employed to detect trends in vegetation based on MODIS NDVI 250 m data (2000-2013). Local perceptions have also been determined. The results revealed that multi-temporal LULC classification significantly outperformed mono-temporal data classification. However, combining mono-temporal imagery and ancillary data significantly enhanced the accuracy to the level of multi-temporal classification. In the period 1999-2011, LULC dynamics in the study area was mainly characterised by expansion of agricultural area and bare surface and reduction of woodland and mixed vegetation. In all the decades within the period 1981-2012, the study area was frequently under near normal conditions of rainfall with intermittent occurrence of extreme events. A non-significant increasing rainfall trend was predominant mainly in the periods 1981-2012 and 2001-2012. Vegetation dynamics was found to be strongly related to rainfall, and NDVI was slightly more sensitive to rainfall than EVI. This research also showed that the study area (83.8%) was dominated by inconsistent dynamics of vegetation in the period 2000-2013. Decreasing trajectory (14%) was prominent among the detected trends and was particularly found in agricultural area and also in areas under high and moderate human footprint. Greening trend (2.2%) was observed mainly in woodland and areas less affected by human footprint. Human was identified as the main driver of vegetation trends in the study area. The perception of local population of vegetation trends was in agreement with the remote sensing observation. In general, between 2000 and 2013, the vegetation of the study area was found to have reduced, and this is more because of unsustainable land use than rainfall conditions. These findings call for more sustainable land use management practices in this part of Burkina Faso.

ACKNOWLEDGMENT

First and foremost, I would like to give thanks and praises to the Almighty God for His abundant grace, mercies and protection throughout the three years of study.

My sincere thanks to German Federal Ministry of Education and Research (BMBF) which funded this PhD research through West African Science Service Center on Climate Change and Adapted Land use (WASCAL).

I am extremely grateful to my supervisors, Dr. Leonard K. AMEKUDZI, Prof. Dr. Christopher CONRAD and Prof. Dr. Evariste Dapola DA whose guidance, suggestions and comments, significantly helped to shape this PhD thesis.

Dr. Michael THIEL, thank you very much for your assistance and devotion to make this PhD a reality. Many thanks to the vibrant team of the Department of Remote Sensing at University of Wuerzburg, for your great friendship during my stay in Germany.

Dr. Gerald FORKUOR, a friend and mentor, I cannot forget your support and advices during my training in Germany and all along my research, stay blessed.

Special thanks to WASCAL-CCLU advisory board members and lecturers at KNUST, particularly Prof. Samuel Nii Odai, Dr. Wilson Agyei Agyare, Prof. Eric Kwabena Forkuo, Prof. Kyere Boateng and all my colleagues for this enthusiasm three years that we spent together.

My thanks also go to Dr Barry Boubacar, Director of WASCAL Competence Center in Ouagadougou and to all the staff for the support during my field work.

Finally, I am grateful to my family and to Marie-Pierre COMPAORE, for supporting me in prayers, and by way of encouragement.

TABLE OF CONTENT

LIST OF TABLES

LIST OF FIGURES

ACRONYMS

ASTER	Advanced Spaceborne Thermal Emission and Reflection Radiometer
BNDT	Base Nationale des Données Topographiques
BUNASOLS	Bureau National des Sols du Burkina Faso
DEM	Digital Elevation Model
DLR	German Aerospace Center
EVI	Enhanced Vegetation Index
FAO	Food and Agriculture Organization of the United Nations
FLAASH	Fast Line-of-sight Atmospheric Analysis of Spectral Hypercubes
GIMMS	Global Inventory Modeling and Mapping Studies
GPCC	Global Precipitation Climatology Centre
GPCP	Global Precipitation Climatology Project
INSD	Institut National de la Statistique et de la Démographie
IPCC	Intergovernmental Panel on Climate Change
ISODATA	Iterative Self-Organizing Data Analysis
ITCZ	Intertropical Convergence Zone
LAI	Leaf Area Index
LULC	Land Use/Cover
LULCC	Land Use/Cover Change
MDA	Mean Decrease Accuracy
MDG	Mean Decrease Gini
MLC	Maximum Likelihood Classification
MODIS	Moderate Resolution Imaging Spectroradiometer
NDVI	Normalised Difference Vegetation Index
NPP	Net Primary Productivity
NOAA/AVHRR	National Oceanic and Atmospheric Administration/ Advanced Very High Resolution Radiometer
RESA	RapidEye Science Archive Team
RS	Remote Sensing
SAVI	Soil Adjusted Vegetation Index

SPI	Standardized Precipitation Index
SPOT	Satellite Pour l'Observation de la Terre
SRTM	Shuttle Radar Topography Mission
TM	Thematic Mapper
TSAVI	Transformed Soil Adjusted Vegetation Indices
UN REDD	United Nations Programme on Reducing Emissions from Deforestation and Forest Degradation
UNCCD	United Nation Convention to Combat Desertification
UNESCO	United Nations Educational, Scientific and Cultural Organization
UNFCCC	United Nations Framework Convention on Climate Change
USGS	United States Geological Survey
UTM	Universal Transverse Mercator projection
WASCAL	West African Science Service Center on Climate Change and Adapted Land Use
WGS 84	World Geodesic System 1984

Chapter 1: General Introduction

1.1. Background

Vegetation refers to all plant life in a given area (Thackway and Lesslie, 2006). It regulates the energy exchange between the earth-atmosphere interfaces (Middleton and Thomas, 1997; Mennis, 2001) and influences several processes such as water cycle, absorption and reemission of solar radiation (Lambin and Ehrlich, 1996; Compaore, 2006). Vegetation also plays an important role in carbon sequestration. Indeed, vegetation (e.g. forest) constitutes a carbon sink that captures carbon dioxide from the atmosphere and stores it in biomass through the process of photosynthesis (Zeng *et al.,* 2013).

Change in vegetation cover is known to have an effect at local, regional and global scale (Amri *et al.*, 2011). However, climate variability and land use change affect vegetation cover. In West Africa, among climate variables, rainfall is the most influencing element of vegetation dynamics (Knauer *et al.*, 2014). The devastating effects of rainfall variability on vegetation include the recurrence of periods of drought (Bouriaud *et al.*, 2005). Indeed, diebacks of trees caused by drought have been recently observed in many forests of the world which affects ecosystem form and function (Galiano *et al.*, 2010). Land use change is also an important threat to natural vegetation and a key factor of the global environmental change (Lambin, 1997). It is characterised by the expansion of human activities (e.g. agriculture, logging and mining) on the land. Several forests worldwide have lost portions of their natural vegetation because of anthropogenic activities; this is the case of the Amazon forest (Morton *et al.*, 2006; Skole and Tucker, 1993; Galford *et al.*, 2010) and Congo basin forest (Bamba, 2010).

Vegetation response to those disturbances which is seen as its quantitative change over the years, is likely to be heterogeneously distributed on the land, and therefore, needs to be spatially monitored. Remote Sensing (RS) is indispensable to assess changes in vegetation, as it has the

most appropriate tools for monitoring vegetation and providing updated spatiotemporal data on the earth's surface at diverse scales. Satellites, such as National

Oceanic and Atmospheric Administration/ Advanced Very High Resolution Radiometer (NOAA/AVHRR) and Landsat, record from the space information on the earth's surface which are used to compute diverse vegetation indices employed to assess changes in vegetation. Besides, several studies have noted the usefulness of RS tools and techniques for monitoring vegetation change (e.g. Lanfredi *et al.*, 2004; Simoniello *et al.*, 2008; Washington-Allen *et al.*, 2008; Cui *et al.*, 2013). For example, Simoniello *et al.* (2008) analysed the time series 1982–2003 of 8 km GIMMS AVHRR-NDVI data of the Italian territory to characterise vegetation resilience. Washington-Allen *et al.* (2008) also used digital RS data (Landsat data) to quantify ecological resilience of drylands. The traditional methods (e.g. literature reviews, field work and ancillary data analysis) are less efficient to monitor vegetation dynamics because they are time consuming and often too expensive for large scale analyse (Xie, 2008). RS technique, that is faster, has known important technology progresses that offer economic benefits to study vegetation changes, especially over large areas (Langley *et al.*, 2001; Nordberg and Evertson 2003; Xie, 2008).

Therefore, the present research aims at using RS to investigate vegetation cover dynamics in the savannah of southwest Burkina Faso. The study was initiated under the West African Science Service Center on Climate Change and Adapted Land Use (WASCAL) programme on climate change and land use. The programme focuses on capacity building to help develop the knowledge necessary for sustainable land use and management in the face of climate change (WASCAL, 2015).

1.2. Problem statement and justification

Rainfall variability and land use change influence vegetation cover (Bouriaud *et al.*, 2005; Nacoulma *et al.*, 2011), especially in regions exposed to climate change and population growth

like West Africa. Land use change within this region is related to agriculture through cropland expansion (Duadze, 2004; Braimoh and Vlek, 2005; Orekan, 2007) which threatens natural vegetation. Furthermore, West Africa's vegetation faces an increase in rainfall variability with recurrence of extreme events (IPCC, 2007) such as droughts (Kasei *et al.,* 2010) that affect vegetation density and growth (Bouriaud *et al.,* 2005). Vegetation dynamics are likely to respond to these disturbances (Gessner *et al.,* 2013a). However, there is still a gap in understanding vegetation response particularly in the West Africa's Sudan savannah where vegetation dynamics is poorly understood and needs further investigation (Compaore, 2006; Nacoulma *et al.,* 2011).

Previous studies on West Africa's vegetation dynamics targeted large scale monitoring of vegetation cover trend using coarse resolution satellite products like AVHRR 8-km NDVI (Normalised difference Vegetation Index) data (e.g. Anyamba and Tucker, 2005; Herrmann *et al.,* 2005a; Olsson *et al.,* 2005 Jamali *et al.,* 2014;) which did not provide detailed investigation. In addition, linear regression is the most popular methods applied to assess trend in vegetation dynamics in West Africa (e.g. Olsson *et al.,* 2005; Fensholt *et al.,* 2009; Fensholt and Rasmussen, 2011). However, the statistical assumptions of linear regression, which are independence of observations and normality of the data, are often violated (e.g. Herrmann *et al.,* 2005a; Hein *et al.,* 2011; Fensholt and Rasmussen, 2011), and this affects the reliability of the results (von Storch and Zwiers, 1999). Studies were also conducted at local scale and emphasized on change detection in Land Use/Cover (LULC) by classifying RS data such as Landsat images (e.g. Duadze, 2004; Braimoh and Vlek, 2005; Aduah and Aabeyir, 2012). Those studies applied the traditional mono-temporal classification which was found to be less accurate elsewhere (e.g. Lunetta and Balogh, 1999; Key *et al.,* 2001). This often leads to overestimation or underestimation of the change area, which injects bias into the LULC dynamics assessment.

These lacunas can be solved by multiplying local scale assessment of vegetation dynamics (Knauer *et al.*, 2014) with more accurate satellite data (Anyamba and Tucker, 2005) and more efficient methods, such as integrating approaches. The implementation of such solutions could aid to better understand vegetation dynamics in the Sudan savannah, and particularly in the southwest of Burkina Faso that falls within this zone. Indeed, few studies have focused attention on vegetation dynamics at local scale in the southwest of Burkina Faso. Yet, this region faces rainfall variability and population growth (INSD, 2011), which increase pressure on natural vegetation (Derbile, 2010). Thus, a spatiotemporal assessment of vegetation cover dynamics is needed in the southwest of Burkina Faso, and that will improve knowledge on vegetation resilience under human activities and natural stress (Gunderson, 2000).

Moreover, the Southwest of Burkina Faso and the entire West Africa in general need the development of approaches and applications based on the use of remote sensing technologies and geographic information systems to provide data and information related to appropriate land use management (WASCAL, 2015). This study focuses on current approach to better assess vegetation dynamics regarding Land Use/Land Cover Change (LULCC) and vegetation trends. Besides, this research provides information on deforestation and determines the potential vegetation dynamics drivers, which will be essential for policy makers to build effective vegetation monitoring strategies to reduce carbon emission and to ensure better environmental management. This research contributes to the United Nations programmes (e.g. Reducing Emissions from Deforestation and Forest Degradation, REDD and United Nations Convention to Combat Desertification, UNCCD) to help maintaining or restoring the environmental resilience in order to secure the availability of productive land to satisfy present and future generations.

1.3. Study objectives

The main objective of this study is to evaluate the response of vegetation dynamics to rainfall variability and land use in the southwest of Burkina Faso.

Specifically, the study aims to:

- ✓ Determine changes in land use/cover occurring in the southwest of Burkina Faso between 1999 and 2011;
- ✓ Determine the inter-annual variability of rainfall and its relationship with vegetation dynamics in the study area;
- ✓ Assess trends in vegetation dynamics in the savannah of southwest Burkina Faso.

1.4. Research questions

The present study has the following principal research question: What is the response of vegetation dynamics to rainfall variability and land use in the southwest of Burkina Faso?

Specifically it attempts to know:

- ✓ How did land use/cover change in the southwest of Burkina Faso between 1999 and 2011?
- ✓ What is the inter-annual variability of rainfall and its relationship with vegetation dynamics in this area?
- ✓ What are the trends of vegetation dynamics in the study area?

1.5. Dissertation outline

The PhD thesis has seven chapters. Chapter 1 focuses on the background of the study, problem statement and justification, objectives of the study and research questions. Chapter 2 presents the literature review; it provides the state of the art of science mainly on LULCC, vegetation dynamics assessment, rainfall variability and the relationship between rainfall and vegetation dynamics with more attention to the case of West Africa. In chapter 3, the description of the study area and the general methodology employed in this research are addressed. Chapters 4, 5 and 6 are clearly devoted to the first, second and third objectives of the study respectively.

They present in detail the methods used, the results achieved and their discussion. Chapter 4 and 5 represent the content of peer reviewed papers resulting from this study, while chapter 6 is a manuscript prepared for submission. The last chapter focuses on the conclusions and recommendations of the study.

.

Chapter 2: Literature Review

This chapter presents firstly a review of the state-of-the-art on Land Use/Cover Change (LULCC); it gives definitions and information related to Remote Sensing (RS) in the field of Land Use/Cover (LULC). In addition, it reviews the methods and approaches of LULC classification and changes assessment, and previous studies on LULC dynamics in West Africa. Furthermore, after defining some terms related to vegetation dynamics, it reviews the methods of vegetation trends assessment and discusses various studies on vegetation dynamics over West Africa. Finally, this review emphasizes on rainfall inter-annual variability and its relationship with vegetation in West Africa.

2.1. Land Use/Cover Change (LULCC)

2.1.1. Land cover, Land use and Land use/cover change

In this thesis, the term Land cover refers to the (bio) physical cover of the earth's surface (di Gregorio and Jansen, 2005). According to Lillesand *et al.* (2008), it describes the features that are found on the surface of the earth (e.g., forest, desert, water, ice, bare soil). In the case of Land use, it is linked to anthropogenic activity or economic function (e.g. forestry or residential areas) (Lillesand *et al.*, 2008). Land use is characterised by human arrangements and activities undertaken in some land cover types. In the southwest of Burkina Faso, land use is mainly characterised by agricultural land use. In literature, Land use/cover change is defined according to two groups: conversion and modification (Turner *et al.*, 1995; Lambin *et al.*, 2003). Conversion signifies a change from one cover type to another, while modification involves alterations of structure or function without a total change of the land cover type. In this study, the term "land use/cover" was adopted since it is a collective term, which means that the map consists of both land use and land cover types (Reese, 2011). This enables to monitor the

dynamics of the main land use type (e.g. cropland area) compared to change in natural vegetation.

2.1.2. Overview of remote sensing of LULC

Remote Sensing is defined as the science and art of obtaining information about an object, area, or phenomenon through the analysis of data acquired by a device that is not in contact with the object, area, or phenomenon under investigation (Lillesand *et al.*, 2008). Land surface objects, such as LULC types (e.g. Forest, water, grass, bare soil), have their unique spectral features (Xie *et al.*, 2010) that are captured by a sensor on board of a satellite (space borne) or aircrafts (airborne) by sensing and recording reflected or emitted electromagnetic energy from that object. Amongst the sensors, some produce their own source of energy (active sensors), while other depend on external sources of energy (passive sensors) such as the sun (Aggarwal, 2003a). Passive sensors are the most common in remote sensing (e.g. Landsat TM, ASTER and MODIS). The process of RS is illustrated by Figure 2.1 and can be summarised into six main stages according to Aggarwal (2003a).

- ✓ Electromagnetic Radiation (EMR) emission from source (sun/self- emission);
- ✓ Transmission of EMR from the source to the earth's surface, as well as absorption and scattering;
- ✓ Interaction of EMR with the earth's surface: reflection and emission ;
- ✓ Transmission of energy from the surface to the sensor;
- ✓ Sensor data output;
- ✓ Transmission, processing and analysis.

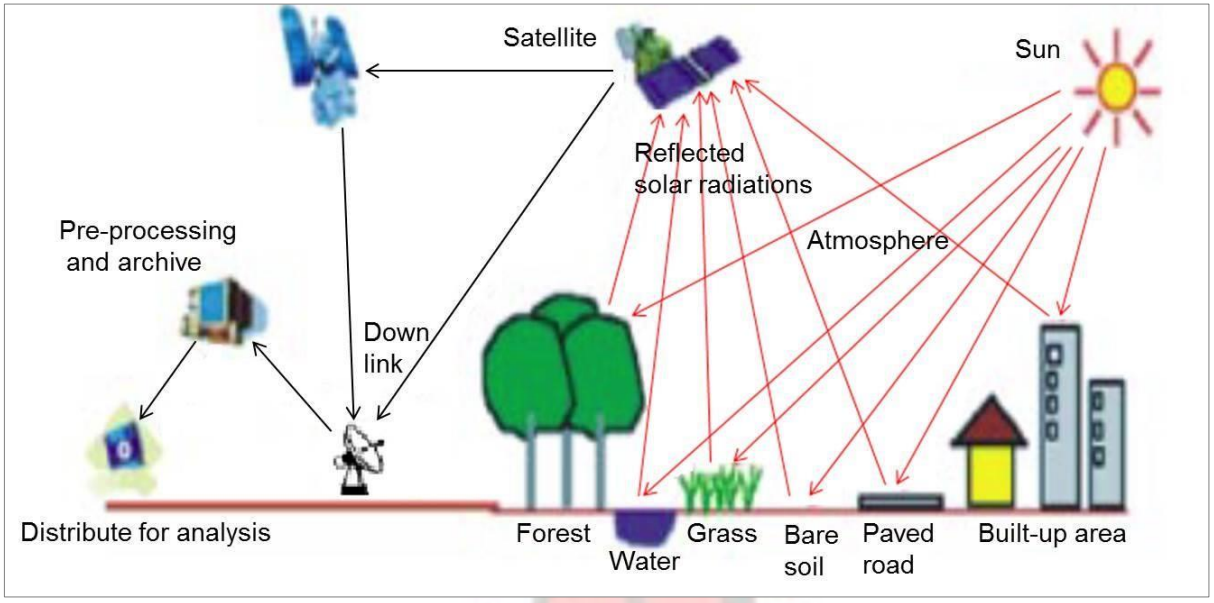

Figure 2. 1. Remote sensing process, adapted from Aggarwal (2003a)

Mapping LULC entailed acquisition of RS images (Xie *et al.*, 2010). The recording of image has been improved with time from balloons to airplanes, and today satellites are the most popular source of data collection. The advantages of using satellite to record image come from, among others, its ability to cover large area compared to aerial survey, and also it passes regularly over the same surface producing new images which is crucial for monitoring periodical changes in LULC (Aggarwal, 2003b). Most often, images used in literature for LULC mapping are from satellites such as Landsat (e.g. Mena, 2008; Jia *et al.*, 2014), TerraASTER (e.g. Yüksel *et al.*, 2008; Cord *et al.*, 2010) and SPOT (Lupo *et al.*, 2001; Carreiras *et al.*, 2006). Generally, researchers focus on spectral regions of the electromagnetic spectrum that range from visible bands (blue, green and red) to infrared bands (near infrared and middle infrared) (Figure 2.2) to produce multispectral images based on which LULC map is derived. Those multispectral images, which are digital images, are composed of picture elements (pixels) located at the intersection of each row and column in each bands of imagery. Each pixel has a Digital Number (DN) or brightness value that depicts the mean radiance of a relatively small area within a scene (Kumar, 2003).

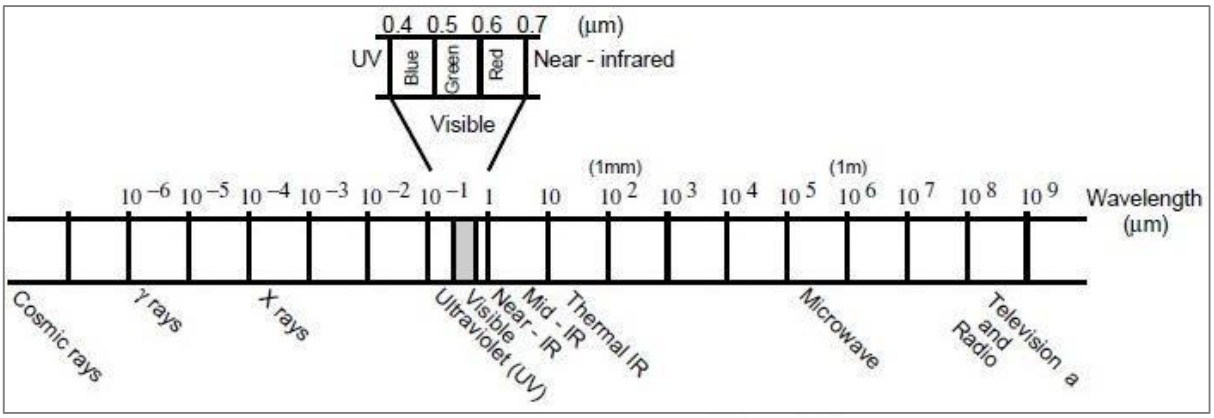

Figure 2. 2. The electromagnetic spectrum, from Lillesand and Kiefer (1987). The processing of satellite image involves corrections (geometric and radiometric) and information extraction. The latter refers to classification and consists of analysing multispectral image and applying statistics methods to identify the LULC of each pixel in the image (Kumar, 2003). In other words, it is to convert the DN values to significant LULC information at every pixel location in the image (Akar and Güngör, 2012). LULC classification can be performed with different combinations of spatial data, approaches and methods which are presented in the next section.

2.1.3. LULC classification

2.1.3.1. Images combination

Different combinations or integrations of spatial data are used to classify LULC types in literature. Mono-temporal satellite image is the most widely used among them (e.g. Dewan and Yamaguchi, 2009; Cord *et al.,* 2010; Kabba and Li, 2011). Mono-temporal classification deals with spectral bands from single date image to map LULC. Deficiencies were noticed with this procedure in terms of mapping errors (e.g. Lunetta and Balogh 1999.). Other authors (e.g. Key *et al.,* 2001; Lunetta *et al.,* 2006; Carrão *et al.,* 2008) found interest in combining bands of remotely sensed images from several periods to map LULC. According to these authors, this procedure, called multi-temporal classification, is a means for improving LULC classification. However, contradictory conclusions were noted in literature about the performances of mono-

temporal and multi-temporal classifications (e.g. Lunetta and Balogh 1999; Langley *et al.*, 2001), which indicates that the results may vary according to regions and LULC types under investigation.

Data fusion of multi-resolution image is another way of integrating spatial data, and it has been also applied as means of improving LULC classification (e.g. Zhou *et al.*, 1998; Garzelli and Nencini, 2007; Lu *et al.*, 2008). Remote sensing image fusion aims at integrating the information obtained with different spatial and spectral resolutions from sensors to produce fused image that contains more detailed information than each of the sources (Zhang, 2010). However, fusing remotely sensed images particularly multi-source images is challenging. This is because of the temporal and spectral variations within the input data set, landscape complexity and accurate co-registration issue (Zhang, 2010).

Remote sensing bands cannot always discriminate completely LULC classes (Franklin, 1995). This led researchers to include ancillary data into LULC classification process (Rogan *et al.*, 2003; Sesnie *et al.*, 2008; Mellor *et al.*, 2013). It refers to the combination of other spatial data (e.g. topographic and climatic data) with the remotely sensed bands to better classify LULC. For instance, Trietz and Howarth (2000) have noted an increase of classification accuracy from 5 to 10 percent with the inclusion of ancillary data in northern Ontario, Canada. Sesnie *et al.* (2008) also support the improving role of variables like elevation and slope in land cover classification in Nicaraguan tropical dry forest. Environmental ancillary data, such as topographic data, (ASTER GDEM, 30 m) are now downloadable free of charge and can help to implement this procedure.

2.1.3.2. Classification approaches

The most common LULC classification approaches found in literature are pixel-based, subpixel and object-oriented. The pixel-based approach analyses the spectral properties of every pixel

within the area of interest (Weih and Riggan, 2010). It is a pixel by pixel classification, and one pixel belongs only to one LULC class (Fisher, 1997). This approach is the most common in literature and widely applied by many traditional classifiers (e.g. Maximum Likelihood Classification and Minimum Distance).

Sub-pixel approach claims that the size of an object may be much smaller than the size of a pixel, that is to say, a pixel may not only contain a single LULC type, but a mixture of several LULC types (Li *et al.*, 2014). This fact is more obvious when considering medium (e.g. Landsat 30 m), or coarse satellite images (e.g. MODIS, 1 km). Several studies dealt with the LULC mixture issue by employing the spectral mixture analysis (e.g. Hostert *et al.*, 2003; Lu and Weng, 2004; Deng and Wu, 2013) and regression tree method (e.g. Liu and Wu, 2005; Huang and Townshend, 2003). With respect to the spectral mixture analysis, the mixed spectral signatures contained in a pixel are compared to "pure" reference data spectra, designed as endmembers, to enable the detection of multiple LULC types within the pixel (Lillesand *et al.*, 2004). For example, this algorithm was run by Kärdi (2007) based on Landsat data to classify impervious surface, vegetation and soil in Tartu (Estonia). Regression trees technique provides fractional land cover estimation based on multiresolution data (Tottrup *et al.*, 2007). Usually, high resolution images (e.g. Quickbird and RapidEye images) are used to derive training and validation data for mapping a medium or higher resolution image into fractional land cover. Gessner *et al.* (2013b) applied this method to derive fractional cover of bare surface, herbaceous and wood in the savannah of southern Africa.

Object-oriented approach takes into account spectral, textural and contextual information in order to discriminate LULC types in an image (Forkuor, 2014) based on segmentation technique. With this approach, image classification focuses on objects rather than pixels, that is, the basic unit for analysis are geographical objects, instead of individual pixels (Li *et al.*,

2014). Studies have found object-oriented approach giving satisfactory results in LULC classification (e.g. Myint *et al.,* 2011; Whiteside *et al.,* 2011).

Nevertheless, object-oriented approach has some challenges which are the overestimation or underestimation of the number of segment (Delves *et al.,* 1992), due to the variations of objects characteristics (e.g. colour and texture) and variations brought about by different environmental factors (Rao *et al.,* 2012). Object-based approach is more suitable when using high resolution satellite images since it assumes that multiple images pixels form a geographic object (Weih and Riggan, 2010; Li *et al.* 2014). However, over the Sudan savannah of West Africa, the acquisition of high resolution images is challenging (price and cloud cover) which constitutes a limit for an efficient implementation of object-oriented approach. Sub-pixel approach also have some challenges in the selection of pure endmembers (Deng and Wu, 2013), that is, pixels containing only one LULC type. This becomes more difficult in heterogeneous area like the Sudan savannah. For instance, in spectral mixture analysis implementation, the determination of endmembers strongly influences the accuracy of sub-pixel LULC (Weng et al., 2008). This is mainly caused by the within-class and between-class variations of endmember (Zhang et al., 2006). The within-class variation indicates the relative differences in spectral signature within the same LULC class, while the between-class variation means spectral variation between two or more different LULC classes (Deng and Wu, 2013). Therefore, because of the aforementioned limitations of objectoriented and sub-pixel approaches in the West African savannah area, this study will focus on pixel-based approach for LULC classification in the southwest of Burkina Faso.

2.1.3.3. Classification methods

Two classification methods are frequently considered in literature to map LULC: Supervised and unsupervised classifications.

Supervised classification requires that one selects representative sample sites with known class types (i.e. reference samples), and compares the spectral properties of each pixel in the image with those of the reference samples, then labels the pixel to the class type according to decision rules (Lillesand *et al.*, 2004). The reference sample is usually divided into training sample to train the classification, and test sample to assess the classification accuracy. The supervised classification includes classifiers such as Maximum Likelihood (e.g. Shalaby and Tateishi, 2007), Mahalanobis distance (e.g. Dwivedi *et al.*, 2004; Deer and Eklund, 2003), and Minimum Distance (e.g. Cord *et al.*, 2010) and machines learning techniques. These classifiers can be categorised into parametric and non-parametric classifiers.

Parametric classifiers are based on the assumption that the spectral signatures of elements within a spectral class are normally distributed (Kumar and Sahoo, 2012; Forkuor, 2014). Examples of parametric classifiers are MLC, Parallelepiped Classifier and Minimum Distance. However, among the parametric classification algorithms, MLC has been the most frequent classifier used for LULC mapping (e.g. Braimoh and Vlek, 2005; Ardli and Wolff, 2009; Dewan and Yamaguchi, 2009; Kabba and Li, 2011). Several works found this algorithm giving better results than the other parametric classifiers (e.g. Al-Ahmadi and Hames, 2009; Thakur, *et al.*, 2012). Non-parametric methods overcome the rule of statistical normal distribution. For example, artificial neural networks (e.g. Kavzoglu and Mather, 2003), support vector machines (e.g. Pal and Mather, 2005; Marconcini *et al.*, 2009) and decision trees classifiers (e.g. McIver and Friedl, 2002; Jiang *et al.*, 2012) are part of this category (Forkuor, 2014). Studies also found that non-parametric classifiers are better than the parametric ones (e.g. Murthy *et al.*, 2003; Waske and Braun, 2009; Mondal *et al.*, 2012).

Unsupervised classification consists in subgrouping a RS image into a number of classes based on natural grouping of the image values, without using training data or prior knowledge of the study area (Lillesand *et al.*, 2004; Puletti *et al.*, 2014). The K-mean (e.g.

Blanzieri and Melgani, 2008; Zhang, 2012) and the Iterative Self-Organizing Data Analysis (ISODATA) clustering algorithm (e.g. Dhodhi *et al.,* 1999) are the two unsupervised methods frequently used (Xie *et al*., 2008). However, unsupervised classification was found to be less efficient than the supervised one (Al-Ahmadi and Hames, 2009). Duadze (2004) run unsupervised classification and MLC to monitor LULC change in the Upper West region of Ghana for the periods of 1986 to 1991, 1991 to 2000 and 1986 to 2000. He noted that unsupervised classification could not discriminate between water bodies and shaded closed savannah woodland and wet or dark dry riverbeds. A combination of both unsupervised and supervised techniques (so-called the hybrid classification) has also been used as a means to yield more accurate LULC maps (e.g. Duadze, 2004; Alajlan *et al.,* 2012).

2.1.3.4. LULC classification schemes

Several LULC classification schemes have been suggested to the remote sensing community, for example, the classification schemes of USGS Anderson, UNESCO (United Nations Educational, Scientific and Cultural Organization) and FAO (Food and Agriculture Organization of the United Nations). Most often, researchers have modified those classification systems in their studies (e.g. Dewan and Yamaguchi, 2009; Forkuor *et al.,* 2013). The USGS Anderson scheme (Anderson *et al.,* 1976) is a multilevel LULC classification system. It has been originally developed for the USA (Dewan and Yamaguchi, 2009), but several studies have used it elsewhere for LULC mapping (Mundia and Aniya,
2006; Shalaby and Tateishi, 2007; Yuan *et al.,* 2005). The UNESCO classification scheme (UNESCO, 1973) has been produced to primarily map vegetation at a scale of 1:1 000 000, which includes only natural vegetation, while all other vegetated areas, such as cultivated areas and urban vegetated areas, are ignored (di Gregorio and Jansen, 2005). The need of an internationally accepted classification scheme and the weaknesses of the previous schemes (e.g. inconsistency, broad land cover classifications) have motivated the production of the

FAO classification system (di Gregorio and Jansen, 2005). The purpose of FAO Land Cover Classification System (LCCS) module is to define a land cover class according to two main phases:

- ✓ an initial Dichotomous Phase, where the user derives the main land cover types;
- ✓ a subsequent Modular-Hierarchical Phase, where a land cover class is defined by the combination of sets of pre-defined classifiers.

In this research, the FAO LCCS has been modified and adapted to the environment of the southwest of Burkina Faso.

2.1.4. LULCC detection

Change detection is the process of observing an object or phenomenon at different times to identify differences in its state (Singh, 1989). According to Bhagat (2012), change detection using satellite data is the measurement of difference between reflected/backscattered radiance from land object/phenomenon recorded in reference scene and target scene at different time. Timely and accurate LULCC detection is relevant for understanding relationships and interactions between human and natural phenomena in order to ensure efficient decision making (Lu *et al.*, 2004). LULCC is a subject of interest and has been widely studied using several methods (Lu *et al.*, 2004; Bhagat, 2012; Hussain *et al.*, 2013). Here, four broad categories are distinguished, and these are spectral-based, classification-based, subpixelbased and hybrid methods.

Spectral-based methods, also called thresholding or pre-classification methods, apply a threshold value to distinguish change from non-change areas (Hussain *et al.*, 2013) based on spectral bands and derived images using vegetation indices (Lu *et al.*, 2014). These methods require identifying suitable bands and thresholds in the changed areas histogram to separate change from non-change areas (Lu *et al.*, 2005). Examples of spectral-based methods include techniques like image differencing, vegetation index differencing (Hayes and Sader, 2001),

principal component analysis (Deng *et al.*, 2008), change-vector analysis (Chen *et al.*, 2003) and regression analysis (e.g. Dhakal *et al.*, 2002). However, the selection of the threshold value is subjective and remains a difficult task (Lu *et al.*, 2004; Xian *et al.*, 2009). Very low threshold value will exclude areas of change, while very high value will include many areas of change (Hussain *et al.*, 2013). The result of the change assessment is scene-dependent, under influence of external factors (e.g. phenology and soil moisture) and depends on the analyst's ability and familiarity with the study area (Lu *et al.*, 2004, 2005 and 2014). Besides, spectral-based methods do not provide detailed information on the nature of the LULCC (Yuan *et al.*, 2005) and change matrix as well.

Classification-based approaches are composed of post-classification comparison and direct multi-date classification method. Post-classification comparison is the most popular LULCC methods in literature (e.g. Braimoh and Vlek, 2005; Dewan and Yamaguchi, 2009; Xu *et al.*, 2010; Peng *et al.*, 2011; Lu *et al.*, 2012). It is the comparison of two LULC maps from different periods in order to determine changes. In fact, this method focuses on "from to" change detection technique. The advantages of Post-classification comparison are the production of change matrix information and the reduction of external effects due to atmospheric and environmental differences between the images (Lu *et al.*, 2004). Postclassification comparison depends mainly on the accuracy of each individual image (Lu *et al.*, 2014). Therefore, the development of more accurate classification technique remains a crucial point. Furthermore, the lack of reference point to validate historical classification often limits this method of change detection.

Direct multi-date classification method was less applied in LULCC assessment. This method is based on the analysis of a combined dataset of the two dates in order to identify areas that have changes (Singh, 1986). Practically, two date images are combined into one multitemporal image and then classified. Actually, classes where changes occurred are expected to present

statistics that are significantly different from where changes did not take place (Mas, 1999). The difficulty of this method is the collection of ground truth points especially for transition area.

However, in complex and heterogeneous area, mixed pixels affect the accuracy of LULCC assessment when applying pixel-based methods described earlier. This is exacerbated mainly when using coarse resolution satellite image, for change areas are small and scattered in different locations (Lu *et al.,* 2008).Thus, studies have considered subpixel-based change detection methods to solve this issue (e.g. Yang *et al.,* 2003; Haertel *et al.,* 2004, Zanotta and Haertel 2012). These methods produce multi-date fractional LULC images, and then apply a spectral-based method to assess the change. According to Lu *et al.* (2014), sub-pixel-based methods have two major limitations. Firstly, it is difficult to generate fractional LULC data from medium or coarse spatial resolution images. Secondly, there is no suitable algorithm, for instance, to produce 'from-to' change trajectories using multi-temporal sub-pixel images.

To improve the change detection accuracy, some authors opted for hybrid methods which combine different change detection techniques (e.g. Im and Jensen 2005; Liu *et al.,* 2008; Ghofrani *et al.,* 2014). According to Lu *et al.* (2014), hybrid methods may be applied either combining different methods into one change detection procedure (e.g. spectral-based and post-classification comparison methods) or combining change detection results from different methods into a new result using certain rules or fusion methods such as feature or decisionlevel fusion.

2.1.5. Change in LULC over West Africa

Over West Africa, population and climate change pressures on natural resources have led to many investigations on LULCC (e.g. Wardell *et al.,* 2003; Reenberg *et al*., 2003; Braimoh, 2004; Da *et al.,* 2009; Houessou *et al.,* 2013; Vittek *et al.,* 2014). Most often, two or more RS images (Satellite images or aerial photos) were classified independently into different LULC

types, and then post-classification comparison method was applied to assess change in LULC. The results from those studies highlighted a decrease in natural vegetation. For instance, Braimoh (2004) examined the impact of seasonal migration on LULCC in northern Ghana using three Landsat scenes collected from November 1984, December 1992 and November 1999. The MLC classification returned overall accuracies of 85%, 82% and 88% respectively for 1984, 1992 and 1999, and the results of the analysis revealed that the most important characteristics of LULCC are the conversion of woodland to agricultural land and a general transition to less vegetation cover. In Sissili province of southern Burkina Faso, Ouedraogo *et al.* (2010) performed MLC with satellite images (Landsat and ASTER) and found that forest land was progressively converted to croplands at an annualised rate of 0.96% from 1986 to 2006. The population size and distribution were found to play a key role in the LULCC. In the same country, Dipama (2005) analysed vegetation cover dynamics of the province of Kompienga based on LULCC assessment using aerial photos and Landsat images. He noticed a degradation of natural vegetation which was brought about by the scattering of human activities, such as agriculture, across the province. Orekan (2007) observed, between 1991 and 2000 in central Benin, a deforestation rate of 8% which was characterised by conversion of 20% of woodland savannah into shrub savannah and 5 % of shrub savannah into farmland. Other authors have also supported the general decline of natural vegetation (e.g. forest and woodland) in different spots of West Africa (e.g. Duadze, 2004; Oloukoi *et al.*, 2006; Zombre, 2006; Adjonou *et al.*, 2010; Efiong, 2011; Spiekermann *et al.*, 2015).

Nevertheless, some LULC studies have also observed patterns of natural or anthropogenicbased re-greening areas in West Africa. For example, Wardell *et al*. (2003) analyses LULC trajectories in savannah woodlands in the Central-West Region of Burkina Faso and the Upper East Region of Ghana. The study collected Landsat images from 1986 and 2011 to assess LULCC and found both deforested and regenerated areas. Sawadogo *et al*. (2008) monitor

LULC evolution in the Ziga locality in north-west Burkina Faso using aerial photos from 1952, 1984 and 1996. Their results showed that vegetation has regressed and bare soil became extensive between 1952 and 1984, meanwhile in 1996, a recovery of the vegetation was observed in areas treated with soil and water conservation techniques such as zaï and rock bunds. Anthropogenic activities (e.g. Agriculture, wood harvesting, bushfire, livestock grazing) were mentioned as drivers of LULCC in West Africa (e.g. Braimoh, 2004; Dipama, 2005; Akognongbe *et al.,* 2014; Spiekermann *et al.,* 2015) as well as rainfall variability (Ouedraogo *et al.* 2014).

Most of the previous studies applied mono-temporal classification procedure to map LULC across West Africa (e.g Braimoh, 2004; Dipama, 2005; Oloukoi *et al.*, 2006). Very rare studies have paid attention to multi-temporal data classification and the incorporation of ancillary data to classify LULC in this region (e.g. Forkuor, 2014). Furthermore, comparing studies of those combinations of spatial data are lacking across West Africa, whereas such studies will enable to come out with an efficient procedure to accurately map LULC. The MLC algorithm is largely used as classifier (e.g. Braimoh, 2004; Orekan, 2007; Ouedraogo *et al.*, 2010). Yet, it has been found to be less accurate than machine learning algorithms such as random forest classifier (e.g. Akar and Güngör, 2013) that has been applied by few studies in
West Africa (e.g. Forkuor, 2014). In addition, many authors (e.g. Dipama, 2005; Orekan, 2007; Sawadogo *et al*., 2008) derived LULC area directly from classified satellite images (e.g. pixel count). This practice is misleading since the area of LULC classes obtained directly from a map may be different from the true area because of classification errors (Olofsson *et al.,* 2013). For instance, a LULC class affected by omission error will have its area underestimated while the area of a LULC class affected by commission error will be overestimated in the map (Mas *et al.,* 2014). The use of statistics methods with area uncertainty estimate can increase the reliability of the computed LULC areas; however, such practices were also found very rare in

LULC mapping in West Africa. This thesis will contribute to fill these gaps observed in literature about LULC mapping and change assessment in West Africa with particular attention to the Sudan savannah of southwest Burkina Faso.

2.2. Vegetation dynamics

2.2.1. Definitions related to vegetation dynamics

The quantity of vegetation cover is related to its productivity which can be defined as the amount of mass a plant gains over some period of time, or better yet, how much the plant grows over a given time frame (Chesworth, 2008). Satellite-derived indices of photosynthetic activity, such as NDVI, are widely used as proxies of vegetation productivity (e.g. Fensholt *et al.*, 2009; Landmann *et al.*, 2014, Traore *et al.*, 2014). Those vegetation indices are the primary data source for studying vegetation dynamics (Guay *et al.*, 2014).

Hobbs (1990) has distinguished three main types of vegetation dynamics that are seasonal vegetation responses, inter-annual variability, and directional vegetation change. This research deals with the directional change of vegetation productivity, which is perceived as its response under anthropogenic and natural pressures. Therefore, in this study, vegetation trend refers to the trajectory (increasing or decreasing) detected in the directional change of vegetation productivity based on time series of satellite-derived indices. A time series is a collection of observations (e.g. NDVI values) made sequentially through time (Chatfield,
2003). It may be either based on annual step for vegetation trend and change assessment (e.g. Duadze, 2004; Fensholt and Rasmussen, 2011; Jamali et al., 2014) or monthly step to analyse vegetation seasonality or phenology dynamics (e.g. Zhang *et al.*, 2005; Zhang *et al.*, 2003; Vintrou *et al.*, 2014).

The significance of vegetation response to environmental perturbations can be linked to its dynamics persistence. Vegetation persistence indicates vegetation tendency to persist in

increasing or decreasing (Simoniello *et al.*, 2008), and it is related to the concept of resilience, that is, the ability of vegetation to recover from disturbances (Simoniello *et al.*, 2008). Spatiotemporal assessment of the persistence of vegetation trend can aid in understanding vegetation dynamics under human pressure or/and natural stresses (Gunderson, 2000).

2.2.2. Remote sensing methods for assessing trends in vegetation dynamics

In the context of climate change and carbon emission reduction, monitoring vegetation dynamics became crucial. From literature, this issue has drawn much attention (e.g. Bunn and Goetz, 2006; Li *et al.*, 2011; Zhao *et al.*, 2012; Wessels *et al.*, 2012; Forkel *et al.*, 2013). Different RS methods were applied in literature to assess vegetation trends with satellitederived indices as indicators of vegetation dynamics. Among those methods, linear regression is the most frequent method (e.g. Herrmann *et al.*, 2005a; Fensholt *et al.*, 2009; Fensholt and Rasmussen, 2011; Li *et al.*, 2014). It is a parametric method based on assumptions of independent observations and normally distributed error terms with constant variance (Muhlbauer *et al.*, 2009). The results of linear regression might not be reliable irrespective of those assumptions (von Storch and Zwiers, 1999). However, instead of testing these assumptions, many studies assumed normality in NDVI time series distribution before performing linear regression analysis (e.g. Tottrup and Rasmussen, 2004; Hein *et al.*, 2011; Fensholt and Rasmussen, 2011). When performing linear regression, the independent and dependent variables are time and vegetation index (e.g. NDVI) respectively, and the main outputs are slope and correlation coefficient, and their statistical significance (Jamali, 2014).

Another popular method is the non-parametric Mann-Kendall's trend test (e.g. Pouliot *et al.*, 2009; Neeti and Eastman, 2011; Sobrino and Julien, 2011; Traore *et al.*, 2014) which measures the monotonicity of a trend and is not dependent on the linear regression assumptions (Higginbottom and Symeonakis, 2014). Indeed, the Mann-Kendall's trend test is robust against non-normality, seasonality, missing values and serial dependence (AlcarazSegura *et al.*, 2010).

Besides, it has a low sensitivity to abrupt breaks due to inhomo-geneous time series (Jaagus, 2006). Non-parametric methods may avoid the problem associated with data skew (Smith, 2000).

However, the aforementioned trend methods can be influenced by the erratic inter-annual variabilities of vegetation (Simoniello *et al.*, 2008), which might affect the final trend result. Thus, in order to limit this issue, Lanfredi *et al.* (2004) initiated the temporal persistence analysis that deals with changes in NDVI trends (Harris *et al.,* 2014). This method should be implemented in other regions (e.g.West Africa) and with more accurate data (e.g. MODIS NDVI 250 m) to confirm its effectiveness.

2.2.3. Vegetation dynamics trend over West Africa

Vegetation trend is of paramount interest in West Africa, since it remains a matter of debate in the scientific community (e.g. Hein and de Ridder, 2006; Prince *et al.*, 2007). Through literature, divergent vegetation trends have been observed across this region. Studies claimed that there are dominant increasing trends over West Africa. For example, in the Bani river basin in Mali which covers portions of Sahelian, Soudanese and Soudano-Guinean ecoclimatic zones, Traore *et al.* (2014) applied Mann-Kendall's trend test to analyse long-term vegetation change in the period of 1982-2011. Their findings revealed that 49% of the total area showed significant increasing trend, while 8% were affected by significant decreasing trend. Focusing on vegetation dynamics in three climatic zones of West Africa (Sahelian, Sudanian and Guinean zones), Leroux *et al.* (2014) found that most of the significant vegetation trends were principally in the Sahel and Sudan zones and exhibited an increase in vegetation production. This greening trend of vegetation across the Sahel is also supported by Kaptué *et al.* (2015).

Other authors supported the idea that vegetation is decreasing over West Africa. For instance, in Niger, Hountondji *et al*. (2005) analysed vegetation dynamics using AVHRR NDVI and

rainfall data from 1981 to 1999, and they used the Rain Use Efficiency (RUE) to identify areas with apparent land degradation. The RUE was defined as the ratio between NDVI and Rainfall, and decreasing RUE over time indicates a degradation of the land. The authors noticed a negative widespread trend of the RUE and supported a progressive diminution of the vegetation productivity. According to the authors, this situation suggested a consistently environmental degradation during the observation period over most of the Sahel belt of Niger. Hountondji *et al*. (2006) analysed the state of the vegetation productivity in Burkina Faso from 1982 to 1999 using long-term time series of AVHRR NDVI data and compared it to rainfall data of 128 stations across the entire country. The study observed that 57.8% of the stations were affected by stable trend of the RUE, 39.8% had a weak to strong negative trend, while only 2.4% showed a weak positive trend. For the authors, these dominant negative trends (as compared to positive trends) may reflect ongoing land degradation processes in

Burkina Faso. According to several authors (e.g. Olsson *et al.*, 2005; Herrmann *et al.*, 2005a; Traore *et al.*, 2014), in addition to rainfall, anthropogenic factors (e.g. land use change and migration) contributed to the observed trends of vegetation over West Africa.

Several many studies have emphasized on the West African Sahel zone (e.g. Hein and de Ridder, 2006; Hein *et al.*, 2011; Dardel *et al.*, 2014), whereas studies targeting especially the Sudan zone, for instance, remain rare. Besides, the above studies used coarse resolution satellite data (NOAA/AVHRR NDVI) and considered large geographical study area which did not allow a detailed monitoring. Local investigation with the use of more accurate resolution data (e.g. Landsat and MODIS data) could be an asset for better evaluating vegetation dynamics (Anyamba and Tucker, 2005a; Knauer *et al.*, 2014). The current study therefore seeks to fill up the gap by investigating vegetation cover response under rainfall variability and LULCC in the southwest of Burkina Faso.

2.2.4. Local population perception of vegetation dynamics

Most of the previous studies on vegetation dynamics assessment have focused especially on remote sensing observations using vegetation indices (e.g. Olsson *et al.*, 2005; Herrmann *et al.*, 2005a; Hountondji *et al.*, 2006; Simoniello *et al.*, 2008; Washington-Allen *et al.*, 2008). However, according to Mbow *et al.* (2015), local indigenes perceptions and knowledge should be considered in the analysis of vegetation dynamics. Over West Africa, some studies have monitored change in vegetation cover based on local population perception (e.g. Arouna *et al.*, 2011; Sop and Oldeland, 2011; Ouaba, 2013). For example, Ouoba *et al.* (2014) analysed the perception of farmers about woody vegetation dynamics in three villages sites located in the sahelian zone of Burkina Faso. In general, the results showed that most of the household heads perceived a reduction in vegetation cover, while some of the respondents reported an increasing trend. Based on the results achieved, the authors suggested the consideration of local perceptions to support sustainable natural resources conservation and management. Sop and Oldeland (2011) assessed the local perceptions of the distribution of socio-economically important tree species in the Sub-Sahel of Burkina Faso using semistructured interviews performed with 87 groups of informants from 20 villages. The findings highlighted that, more than 80% of the 90 listed species were declining, and over 40% were identified as threatened, including several plants of great economic value. According to the authors, data collected from local knowledge were consistent with that of many ecological studies. In the Sudano-Guinean area of Benin, Arouna *et al.* (2011) analysed local population perceptions on the socio-economic determinants of vegetation degradation. Agriculture, logging, charcoal production and hunting have been recognised by local actors as key socioeconomic factors that determine vegetation degradation in the study area.

The conclusions of the previous works revealed that local knowledge and perceptions are reliable and can be associated to RS to assess changes in vegetation dynamics, and even to validate the results of RS observation. This approach will be used in the present study.

2.3. Rainfall: its variability and relationship with vegetation

2.3.1 Definition of climate change and rainfall variability

IPCC (2007) defines climate change as a change in the state of the climate that can be identified (e.g. using statistical tests) by changes in the mean and/or the variability of its properties, and that persists for an extended period, typically decades or longer. It refers to any change in climate over time, whether due to natural variability or as a result of human activity. According to IPCC (2007) changes in greenhouse gases and aerosols concentrations in the atmosphere, land cover and solar radiation affect the energy balance of the climate system and are drivers of climate change. Anthropogenic activities result in activities (e.g. industrialization, burning of fossil fuel and gas flaring) that emit greenhouse gases, such as methane (CH_4), carbon dioxide (CO_2), nitrous oxide (N_2O) and halocarbons (a group of gases containing fluorine, chlorine or bromine), into the atmosphere (IPCC, 2007; Odjugo, 2010). Human effects are also perceived through activities that reduce the amount of carbons absorbed from the atmosphere (e.g. deforestation, alterations in Land Use/Cover and agricultural practices) (Odjugo, 2010).

Climate through its parameters, such as rainfall and temperature, plays an important role in driving vegetation dynamics (e.g. Nezlin *et al.*, 2005; Zeng and Yang, 2009.). However, among both parameters, rainfall determines largely vegetation dynamics in West Africa (Knauer *et al.*, 2014). In this region, changes in climate have favoured the increase of rainfall variability (IPCC, 2007) which can be seen as the degree to which the amount of rainfall varies overtime (temporal variability) or over space (spatial variability). Intra-annual rainfall variability is the

distribution of rainfall within a year, while inter-annual variability is the annual distribution of rainfall amount over several years.

2.3.2. Assessing rainfall inter-annual variability and trend

Different way of measuring the variability of rainfall can be found in literature. The Coefficient of Variation (CV) has been used to analyse rainfall variability (e.g. Ishappa and Aruchamy, 2010; Bibi *et al.,* 2014). The CV is the ratio of the standard deviation to the mean, and it is a measure of the relative dispersion of the variable (Dodge, 2010). Some authors have used the variation in the mean annual rainfall and other statistics, such as maximum, minimum and standard deviation, as indicators of rainfall variability (e.g. Singh and Mulye, 1991; Kansiime *et al.,* 2013). Variability was also measured as rainfall deviations (anomalies) over a given period of time from a climate statistic (long term mean) average over a reference period (Vuille, 2011). In this sense, the Standardised Precipitation Index (SPI) or Standardised Anomaly Index (SAI) was the common rainfall variability measure applied in literature (e.g. Le Barbé *et al.,* 2002; Kasei *et al.,* 2010). It is calculated as the difference between the annual total of a given year and the long term average rainfall records divided by the standard deviation of the long term data (Kasei *et al.,* 2010; Hadgu *et al.,* 2013). The advantage of SPI is that it allows the determination of dry/wet years (Hadgu *et al.* 2013) and rainfall extreme events based on SPI intensity ranges defined by Mckee *et al.* (1993). A rainfall extreme event is the occurrence of a value of rainfall above (or below) a threshold value near the upper (or lower) ends of the range of observed values of rainfall (IPCC, 2012). Flood and drought are the two extreme events that characterise rainfall, and among them drought constitutes an important threat for vegetation (Bouriaud *et al.,* 2005). According to Raziei *et al.* (2013) drought originates from a deficiency of rainfall (less than normal) over an extended period of time.

A trend may be associated with the variability observed in rainfall time series data. Two major statistical tools are used in literature to detect trend in rainfall time series: parametric tests and

non-parametric tests. In parametric tests (e.g. student t-test, linear regression), data must be independent with a normal distribution, while non-parametric tests (e.g. MannWhitney test, Wilcoxon test, Mann-Kendall test) require only independent data (Chen *et al.* 2007). The non-parametric tests (e.g. Mann–Kendall test) were therefore commonly used for rainfall trend analysis (e.g. Gemmer *et al.* 2004; Obot *et al.* 2010; Rai *et al.* 2010; Capra *et al.* 2013).

2.3.3. Rainfall variability and its relation with vegetation over West Africa

Rainfall in West Africa is characterised by its spatial and temporal variability with occurrence of wet and dry periods, and has drawn attention in literature (e.g. Le Barbé *et al.*, 2002; Nicholson, 2005). The region has been experiencing severe drought events in the 1970s and 1980s (Nicholson, 2013), while a recovery of rainfall was observed since the end of the 1990s (Lebel and Ali, 2009) with flooding events such as in Ouagadougou and Niamey in 2009 and 2012 respectively (Panthou *et al.*, 2014). For instance, a study by Lucio *et al.* (2012) noted, between 1950 and 1980, a significant rainfall decrease in the West African Sahel with a deficit of about 70% over the whole region. They also observed that the three decades of the study period (1981-2010) showed some improvements. The decade 2001-2010 was observed as the most humid. In the Volta Basin, Owusu *et al.* (2008) found out a significant reduction of mean annual rainfall totals from 1,400 mm to 1,200 mm in the south and from 700 mm to 600 mm in the north during the period 1951-2000. Burkina Faso was one of the most affected by this decline in rainfall.

Others studies focused on the intra-annual fluctuation of rainfall (e.g. Odekunle, 2004; Laux *et al.*, 2008; Amekudzi *et al.*, 2015). There is a shift in the onset of the rainy season which occurs later in the year according to farmers (Van de Giesen *et al.*, 2010), and in Senegal the cessation dates tend to be earlier (Camberlin and Diop, 2003). Sarr (2012) noticed in a review that, in semi-arid Africa, the future projection revealed a late onset, early cessation dates of rainfall

and reduction of the growing period length. The variability of rainfall over West Africa is due to sea surface temperature changes, and this variability is exacerbated by local vegetation feedback mechanisms, surface albedo and soil moisture (Nicholson, 2001). Climate change also increases the variability of rainfall in this region (IPCC (2007).

Spatially, a north–south stratification of vegetation cover is observed in the West African region in line with rainfall (Knauer *et al.,* 2014). This relationship between rainfall and vegetation dynamics in West Africa has also been discussed in literature (e.g. Hermann *et al.,* 2005; Bobée *et al.,* 2012; Olusegun and Adeyewa, 2013). The response of vegetation to rainfall constituted a particular interest to several studies. Martiny *et al.* (2005) investigated on the response of vegetation activity to rainfall in semi-arid regions of Africa based on statistical approaches (simple and partial correlations, linear multiple regressions) and found out that annual vegetation dynamics highly depends on annual rainfall of the concurrent year and the previous year. Nicholson *et al.* (1990) noticed that in the West African Sahel, vegetation is best correlated with the rainfall total for the concurrent plus two antecedent months. Morten and Fensholt (1999) examined the link between rainfall and vegetation development in the Sudano-Sahelian Zone of Burkina Faso through the combined use of rainfall point measurements and vegetation index NDVI derived from NOAA/AVHRR. They found a significant strong relationship between rainfall and vegetation development especially within rainfall values between 650 and 850 mm/ year. Klein and Roehrig (2006) examined differences of the correlation between rainfall and NDVI of the main vegetation covers according to time lag and number of integrated days in semi-humid Benin. On the whole, for all vegetation covers, the study noted a high correlation between rainfall and

NDVI, and the maximum correlation was reached with a lag of 1.5 and a sum of 5 decades.

Many studies have considered the relationship between rainfall and vegetation to be linear

(e.g. Tottrup and Rasmussen, 2004; Herrmann *et al.,* 2005a; Fensholt and Rasmussen, 2011). However, Hein *et al.,* (2011) noticed a non-linearity of this relationship in the Sahel. Many of these previous studies have employed NDVI as indicator to express vegetation response to rainfall (e.g. Nicholson *et al.* 1990; Herrmann *et al.,* 2005a; Roehrig, 2006), while this index was found elsewhere limited to express vegetation dynamics (Liu and Huete, 1995). The use of other indices to analyse vegetation response to rainfall is rare in the West Africa's region (e.g. Bobee *et al.,* 2012). The present thesis will fill this gap.

Chapter 3: Study Area and General Methodology

3.1. Description of the study area

3.1.1. Geographical location

The study area is located in the Black Volta river basin of southwest Burkina Faso and lies approximately between latitudes 10º53´0´´N to 11º37´0´´N and longitudes 2º43´0´´W to 3º20´0´´W (Figure 3.1). It covers an area of 5120 km^2, and the main localities are Diebougou, Dano, Fara and Dissin that hold the four rain gauges stations with long time series data.

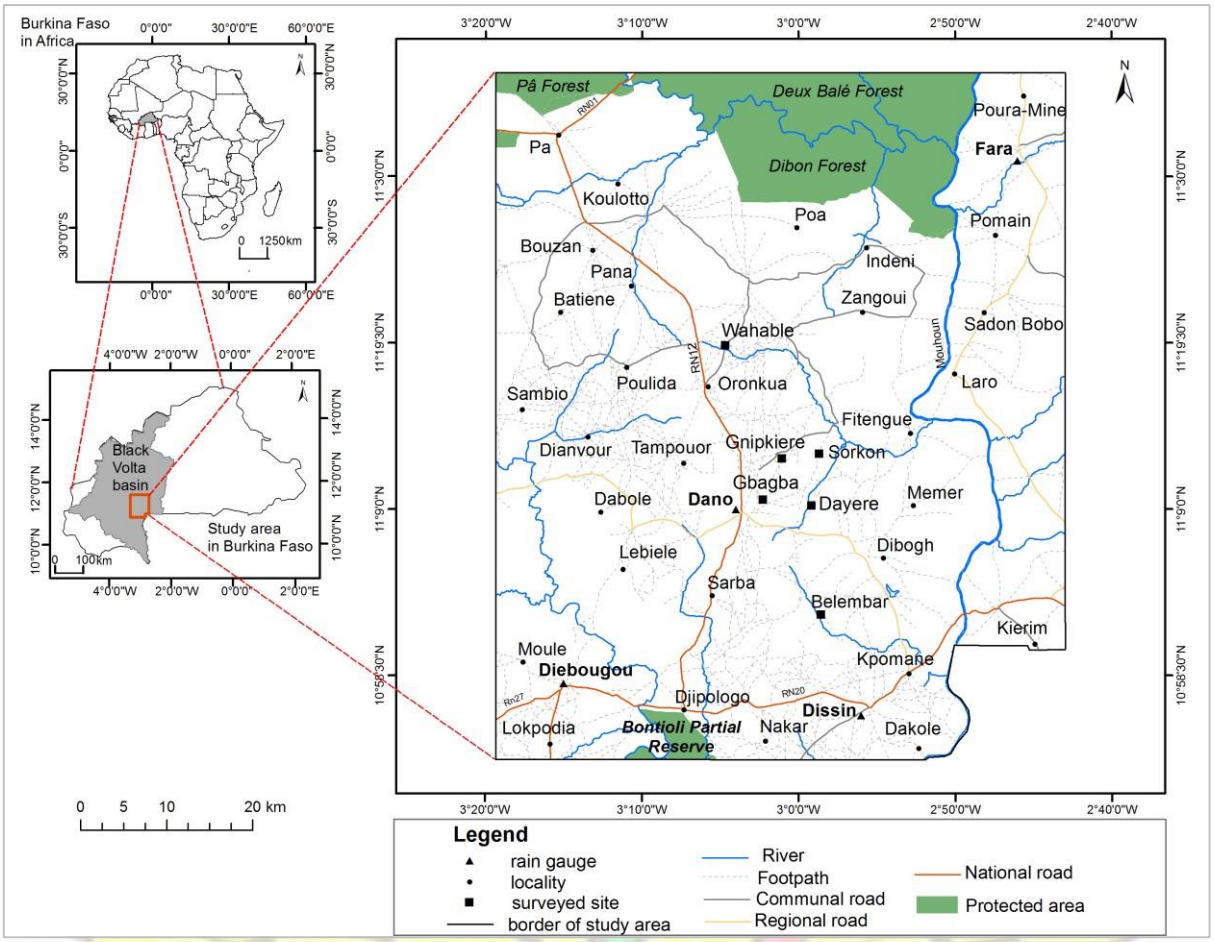

Figure 3. 1. Map highlighting the geographical location of the study area (source: BNDT, Burkina Faso)

3.1.2. Geology and geomorphology

The geology of the study region can be divided into two major formations. These are Precambrian D and Precambrian C. The Precambrian D or Ante-birimian represents more than half of the area of Burkina Faso, and it is essentially a compound of undifferentiated granitic and gneissic rocks (Boeglin, 1990). The Precambrian C, well known as birimian, is characterised by rocks of Paleoproterozoic age which is associated with the West African craton (Wright *et al.*, 1985). In the southwest Burkina Faso, the birimian is a compound of predominantly clastic formations (composed of fragments, or clasts, of pre-existing minerals and rock) and volcano-clastic formations; the clastic sequence consists of intensely deformed

pelitic (clay) and psammitic (sandy) metasediments (Schlüte, 2008). The main Birimian rocks are granites, gneiss, phyllite, schist, migmattite and quartzite (Gyau-Boakye and Tumbulto 2006).

The study area is a gently undulating peneplain located at about 200-576 m of altitude (Figure 3.2a). A peneplain is considered to have formed by the lowering of an entire region containing more than one watershed to a common base level, and later uplift may lead to a rejuvenation of erosional processes so that the area is cut by new valleys and interfluves to produce a dissected peneplain (Chesworth, 2008). The geomorphological data, collected from the Bureau National des Sols (BUNASOLS) in Burkina Faso at a scale of 1:500,000, show that the study area is dominated by a large glacis (with and without duricrusts cover) and lateritic duricrusts which are interrupted by crusted terraces, butte with duricrust cap, rock outcrops and residual reliefs (Figure 3.3). The latter occurs, for instance, around the areas of Dano and Diebougou, where elevations exceed 500 m (e.g. Ioba hill, 525 m of altitude, see Figure 3.2b). Alluvium/colluvium sediments are found in slight depressions (inland valleys) along rivers such as Mouhoun or Black Volta river and its tributaries. These wetlands are mostly used for irrigated agriculture during the dry season (due to proximity to water and high groundwater level), and for rice cultivation during the rainy season (Forkuor, 2014). Natural vegetation such as woodland dominates along river beds in those topographic depressions (Cord *et al.*, 2010).

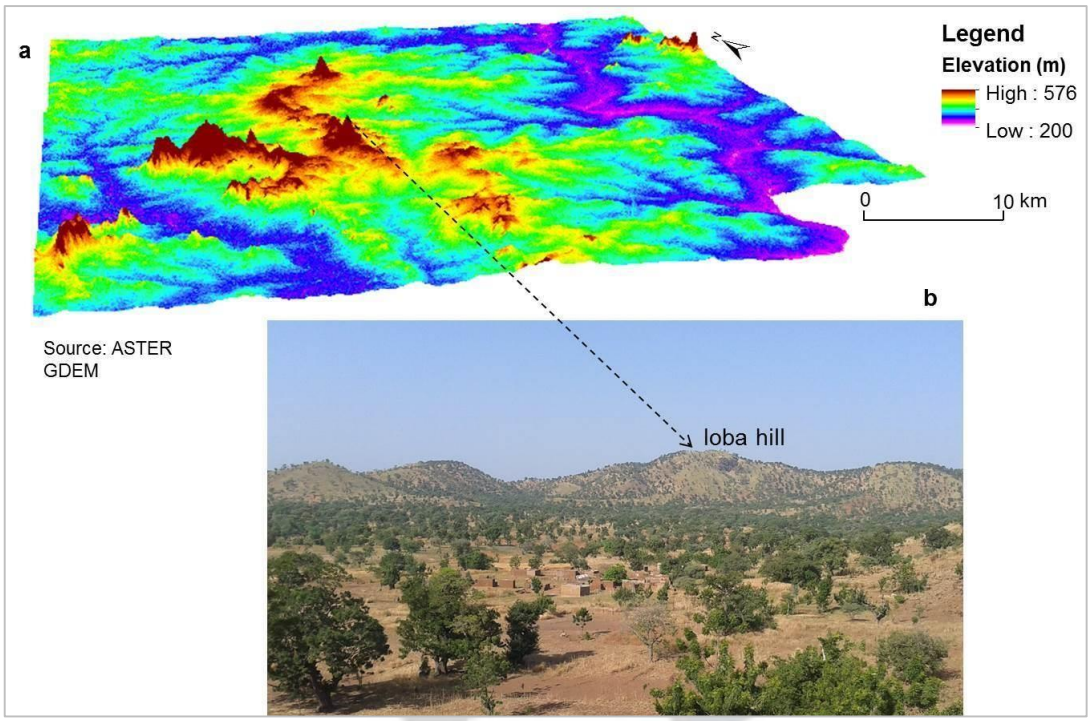

Figure 3. 2. a) Relief of the study area; and b) Picture showing the Ioba hill in Dano

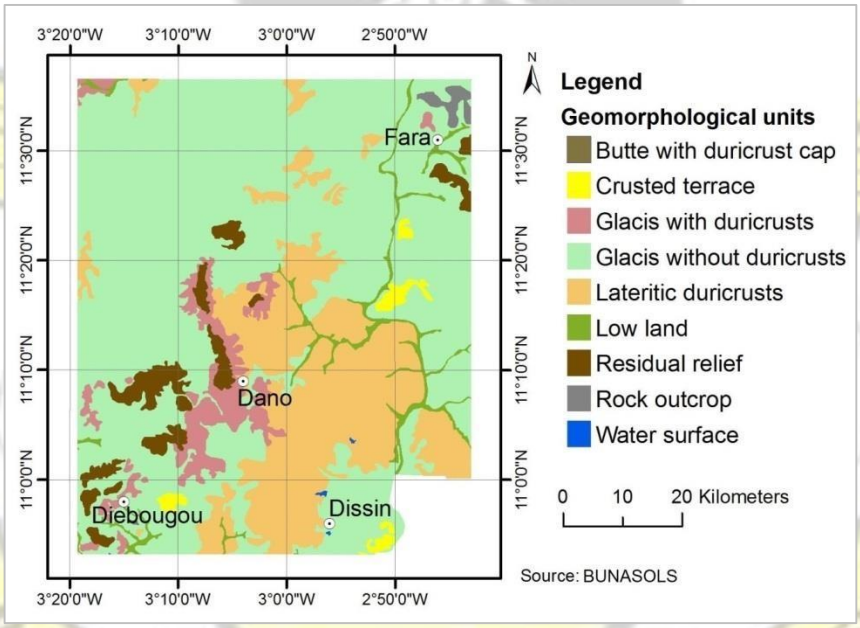

Figure 3. 3. Geomorphological units found in the study area, 1/500,000

3.1.3. Climate

The climate of West Africa is governed by the oscillations of the Inter-Tropical Discontinuity (ITD) from south to north and vice versa. The ITD is the demarcation line between two air masses that have different moistures conditions. These are the maritime southwest monsoon

flow (humid) that emanates from the Atlantic Ocean, and the continental north-eastern harmattan winds (dry) originating from the Sahara (Nicholson, 2013). As a result, there are two main seasons that characterise the climate of the study area. A rainy season that extends from May to October, and a dry season that occurs from November to April.

Rainfall is assumed to result from local thermal instability, facilitated by the low-level wind convergence within this zone (Nicholson, 2013). The months of August, July and September are particularly more humid (Figure 3.4). The amount of rainfall is characterised by interannual variability that influences the dynamics of vegetation (Compoaore, 2006). In general, this variability of rainfall over West Africa has been intensified by climate change (IPCC, 2007). For instance, rainfall data collected from the Direction Générale de la Météorologie (DGM) in Burkina Faso indicated that, in the period 1981-2012, rainfall varied from 560 to 1206 mm/year and from 634 to 1239 mm/year at the stations of Fara and Dissin respectively. The average annual amount of rainfall recorded in that period was 862.87 mm.

The mean monthly temperature spans from 26 ºC to 32 ºC. Figure 3.5 shows that highest daytime temperatures are observed during the months of March and April in dry season, while lowest day-time temperatures occur during the period July-September. On the other hand, the lowest night-time temperatures, associated with the Harmattan winds, are recorded between December and February (Forkuor, 2014).

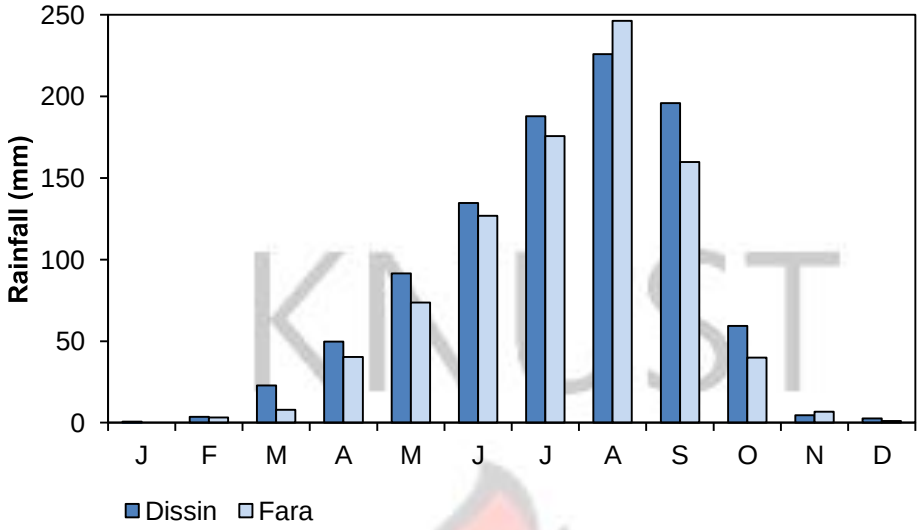

Figure 3. 4. Average monthly rainfall in Dissin and Fara, from 1981 to 2012 (Source: DGM, Burkina Faso)

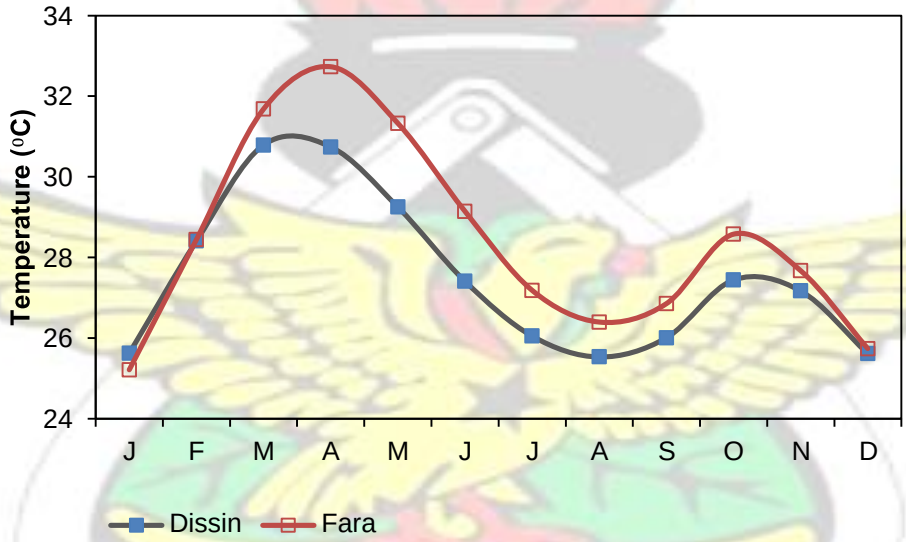

Figure 3. 5. Average monthly temperature in Dissin and Fara, from 1981 to 2012 (Source: DGM, Burkina Faso)

3.1.4. Soil types and vegetation

In the savannah region, soils are largely developed from acidic metamorphic rocks, hence they have low activity kaolinitic clay, but have coarse texture in the topsoil and, depending on the cultivation history, have low organic matter content (Callo-Concha *et al.*, 2012). In addition, the soils have low supply of nitrogen (N), phosphorus (P) and sometimes micronutrients. They are very susceptible to erosion and compaction (Callo-Concha *et al.*, 2013). Based on data

collected from BUNASOLS, the soils of the study area are made up of lixisols (64.4%), fluvisols (12.8%), cambisols (10.1 %), leptosols (9.2%) and arenosols (3.5%) (Table 3.1). Fluvisols are usually used for paddy rice cultivation (Forkuor, 2014), while the rest of crops are grown on the other soil types that require more fertiliser inputs (FAO, 2006).

Table 3. 1. Soil types distribution in the study area

Type of soil	Lixisols	Fluvisols	Cambrisols	Leptosols	Arenosols	Total
Percentage	64.4	12.8	10.1	9.2	3.5	100

Source: BUNASOLS

The study area is characterised by a savannah vegetation of the Sudan phytogeographic zone (Guinko, 1984). It is mainly composed of woody savannah of which the dominant species are *Vitellaria paradoxa sp., Parkia biglobosa, Lannea microcarpa, Adansonia digitata, Tamarindus indica, Bombax costatum, Berlinia grandifotia*, among other. The shrubby savannah is dominated by species such as *Combretum glutinosum, Combretum nigricans, Ximenia Americana, Entada Africana* and *Acacia gourmaensis*, whereas the main herbaceous are *Andropogon gayanus, Andropogon tectorium, Hyperthelia dissoluta, Hyparrhenia glabriuscula,* among other (Sandwidi, 2007). Natural vegetation is distributed according to edaphic conditions, topography (altitude, slope and aspect) and ground water availability (Cord *et al.*, 2010; Nacoulma *et al*., 2010).

The Sudan savannah vegetation is threatened by anthropogenic activities (e.g. agriculture, wood harvesting and mining) combined with the effects of rainfall variability that increased in this region (IPCC, 2007).

3.1.5. Demography and livelihood activities

The population of the study area is particularly dynamic like in the whole West African region which has experienced high population growth rate in recent years due to high fertility rates (Callo-Concha *et al.*, 2012). In the administrative region of Southwest of Burkina Faso, which covers the major part of the study area, population size increased from 441,525 inhabitants in

1985 to 620,767 inhabitants in 2006 and further to 708,336 inhabitants in 2011 (INSD, 2011) as shown in Table 3.2. The increase in population is also observed in the provinces of the Southwest region. For instance, in the Ioba province (Dano as main city), population increase was estimated to be 9% between 1985 and 1996 and 19% between 1996 and 2006 (INSD, 2007).

This increase in population size has been favoured, among others, by the high level of migration, mostly of Mossi farmers from the northern and central regions of Burkina Faso (Gray, 2005). In rural areas, such a population growth combined with shifting agriculture increased the need of more farmlands leading to excessive pressure on vegetation and the depletion of natural resource stock in general (Derbile, 2010). The population of the study area is essentially rural and made up of Dagara, Mossi, Lobi and Dioula as principal ethnic groups distributed in 170 localities. In 2011, population size and density were 273,940 inhabitants and 53.5 inhabitants / km^2 respectively (Table 3.3).

Table 3. 2. Evolution of the administrative region of Southwest of Burkina

Years	1985	1996	2006	2009	2011
Population size	441525	485313	620767	667737	708336

Source: INSD

Table 3. 3. Demographic statistics of the study area

Variables	Number of locality	Population (inhabitants)	Density (inhabitants/ km^2
Statistics	170	273940	53.5

Source: INSD

Agriculture, including crop farming and livestock, remains the principal source of livelihood for the rural populace of the study area as well as for the entire country where 86% of the workforce is primarily devoted to agriculture (Sanfo, 2010; Forkuor, 2014). Farming is characterised by the use of low quantity of fertilizers and slash and burn is the popular farming

practice (Duadze, 2004). Small-scale subsistence farming is the main agricultural practice in the study region (Reenberg *et al.,* 2003).

The main crop species are cotton, sorghum, millet, rice and maize. Rice is cultivated usually in low land or close to water surface (Cord *et al.*, 2010). The cultivation of sorghum, maize and millet is important for the provision of carbohydrates to the local diet, and also by generating by-products such as the straw for fuel and foliage to feed animals (Callo-Concha *et al.,* 2012). Livestock rearing is practised often as livelihood strategy in the face of crop failure and income losses (Barrett *et al.*, 2001). Sometimes, livestock is sold to provide income (e.g. cow, sheep and goat), and also used to feed the household (e.g. poultry) (Forkuor, 2014). It also contributes to farming by providing dung and manure, and also animal traction for ploughing. Small-scale artisanal mining is also observed in the study area; farmers are turning to this activity as also a complement to their principal livelihood activity.

3.2. General methodology

This research is divided into three main parts (Figure 3.6). The first part consists of classifying the study area into the main Land Use/Cover (LULC) classes and monitoring Land Use/Cover Change (LULCC). The second targets the analysis of rainfall variability and its relationship with vegetation dynamics based on the different LULC types. The last part emphasizes on the assessment of vegetation trends in the study area. Finally, vegetation response to rainfall variability and land use was analysed based on the results of these sections.

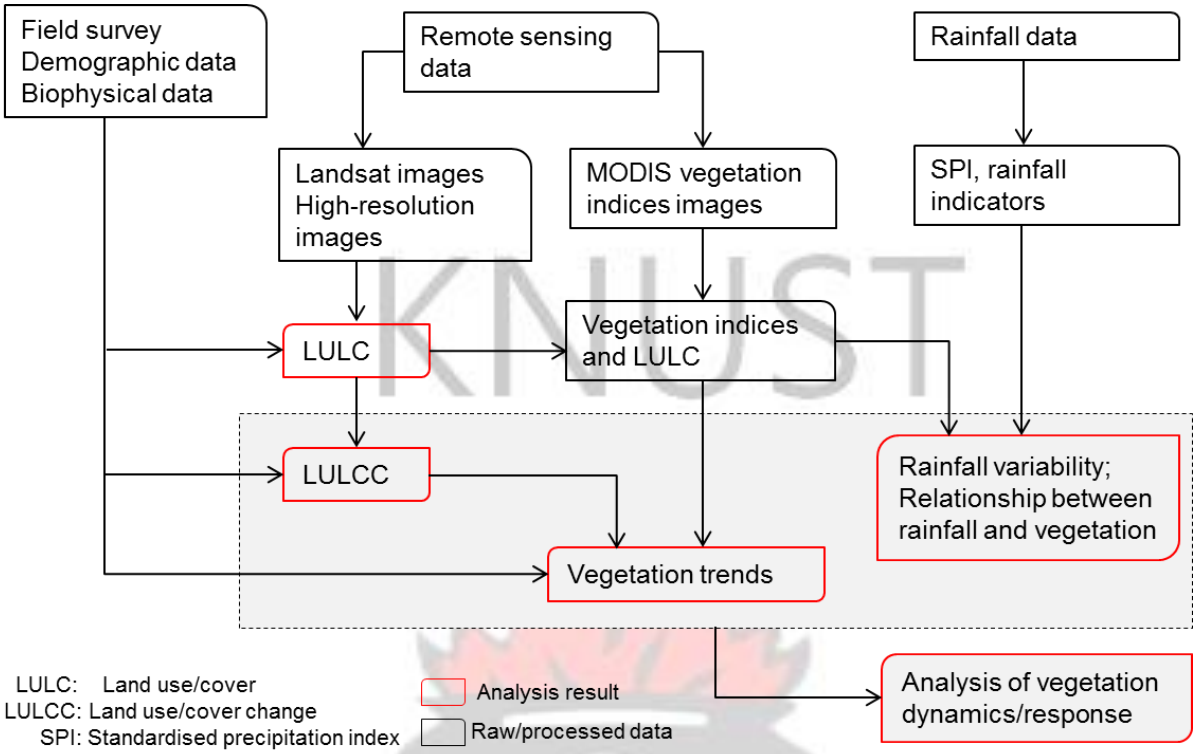

Figure 3. 6. General approach applied for vegetation dynamics/response assessment

3.2.1. LULC classification and change monitoring

LULC classification and LULCC monitoring entailed the use of Landsat TM (Thematic Mapper) images from 1999, 2006 and 2011 and environmental data (Elevation, slope, geomorphological units and soil types). The reference data for training and validating the different LULC and LULCC maps were collected from high-resolution images (Quickbird, RapidEye, Google Earth and aerial photo) and field data. A field survey was conducted in October 2013 for ground truth samples collection and to observe local population practices that cause changes in LULC.

The adopted approach consisted of two steps (Figure 3.7). Firstly, the most appropriate temporal window to classify mono-temporal satellite data was determined, and then the performance of mono-temporal data was compared with those of other combinations of spatial data. The results of mono-temporal (single date) and multi-temporal (multi-dates) data classifications as well as their integration with environmental ancillary data were assessed to

determine the most accurate and suitable classification type. This has been achieved based on accuracies comparison and by using the non-parametric McNemar's test that evaluates the difference between paired proportions. All the classifications were performed with the Random Forest (RF) algorithm which is a machine learning classifier. This classifier gives the importance of each variable in the classification using the Mean Decrease Accuracy (MDA) based on which the importance of satellite image bands and ancillary data were assessed. Secondly, the most accurate classification type was then applied to monitor LULCC by adopting a post-classification change detection method. Contrary to the other change detection techniques (e.g. spectral-based methods), post-classification change detection provides a change matrix.

The LULC and LULCC maps statistics were based on adjusted error matrix (Olofsson *et al.*, 2013) that enables computation of classification accuracies, area estimates and area uncertainty. This method adjusts the ordinary pixel count error matrix (Congalton, and Green, 2009) with the area of each LULC and LULCC categories on the classified maps. The adjusted error matrix reduces biases in area computation due to map classification errors by including the area of map omission error and removing the area of map commission error (Olofsson *et al.*, 2013). This reduces the overestimation and underestimation of the areas of the LULC and LULCC classes and increases the reliability of the statistics. However, the adjusted error matrix requires the use of probability sampling design (e.g. stratified random, simple random and systematic sampling) to collect the reference data (Olofsson *et al.*, 2013). The combination of accurate LULC classification type and more reliable statistics computing method (e.g. based on adjusted error matrix) could lead to efficient land change monitoring in region like West Africa where there is rapid change in LULC (Orekan, 2007). A detailed description of the method applied for LULC classification and LULCC monitoring is given in section 4.2 of chapter 4.

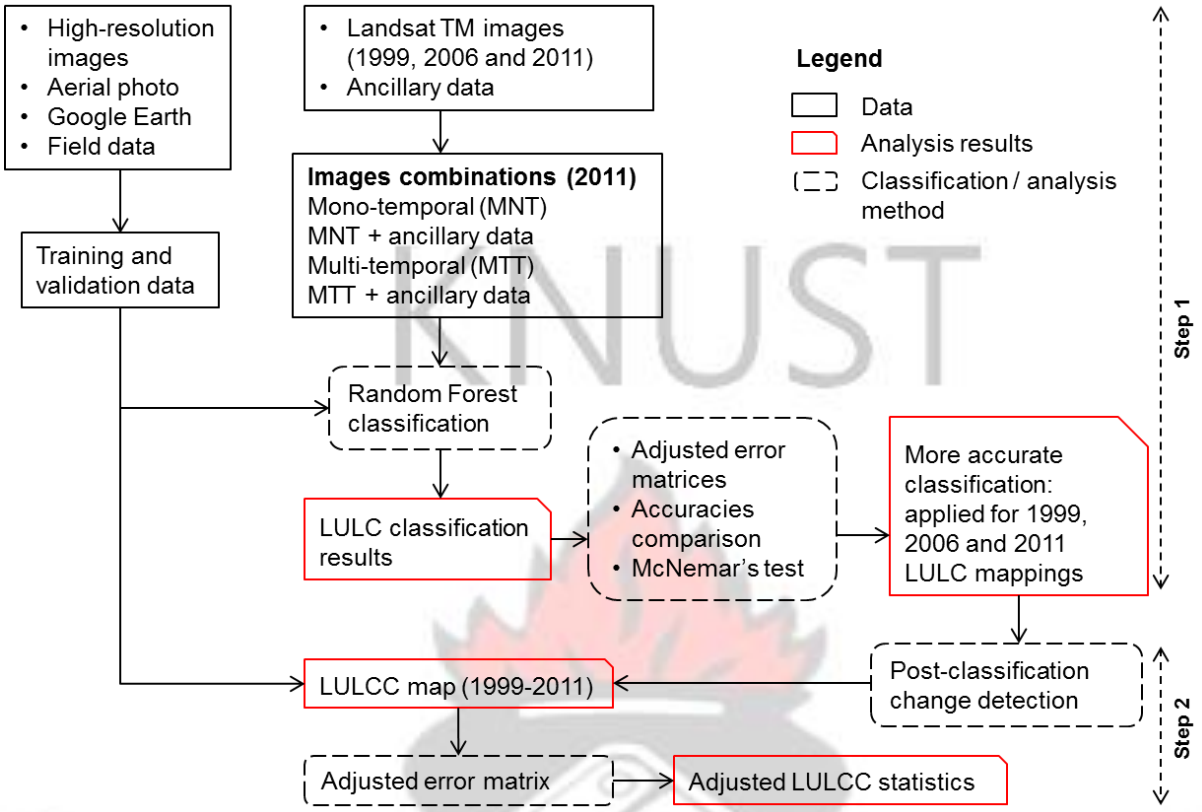

Figure 3. 7. Approach applied for LULC and LULCC mappings

3.2.2. Rainfall variability and its relationship with vegetation dynamics

Monthly rainfall data set (1981-2012), vegetation indices (MODIS, 2001-2011) and persistent LULC map (1999-2011) are the data used to determine rainfall inter-annual variability and analyse the relationship between rainfall variability and vegetation dynamics (Figure 3.8). A first step of this investigation targets the assessment of rainfall inter-annual variability and trend between 1981 and 2012. The Standardised Precipitation Index (SPI) was used to express annual rainfall departure. The computation of this index requires the arithmetic average and the standard deviation of the rainfall time series. SPI allows the evaluation of each year in terms of deficit or surplus of rainfall. In this sense, a classification of the range of SPI values produced by McKee *et al.* (1993) was adapted to this research to determine drought/wetness intensities for each year of the time series. The non-parametric Kendall's tau-b test was used to assess rainfall trend in the period 1981-2012 and for each decade within this period.

A second step emphasizes on the relationship of rainfall with vegetation dynamics. For this purpose, different rainfall indicators (annual amount of precipitation with one month lag, cumulated 2, 3 and 4 months precipitation) were derived, and time series of two vegetation indices were extracted for each vegetated LULC by focusing on persistent area that were obtained by change detection between the LULC maps of 1999, 2006 and 2011. The Normalized Difference Vegetation Index (NDVI) and the Enhanced Vegetation Index (EVI) were both selected as proxy for vegetation. This study found relevant to compare both indices in the study region in order to determine the most appropriate to express vegetation dynamics. Finally, linear correlation analysis was performed between each LULC indices (NDVI and EVI) and the different indicators of rainfall to assess their relationship. Section 5.2 of chapter 5 gives more details about this methodology.

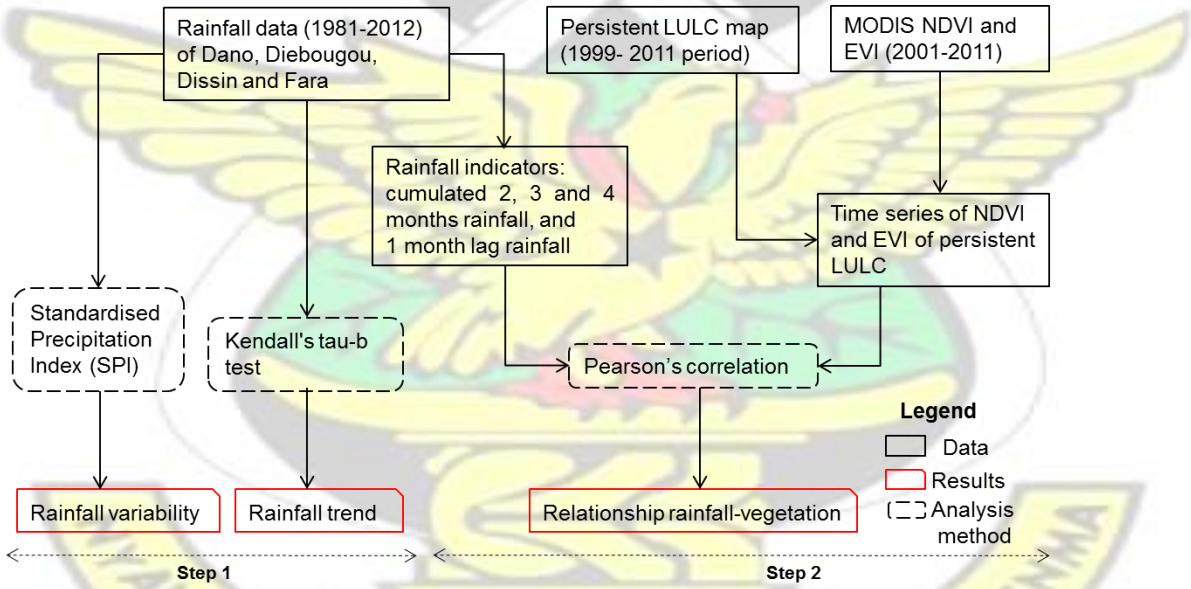

Figure 3. 8. Approach applied for assessing rainfall variability and its relationship with vegetation

3.2.3. Assessment of vegetation dynamics trends

This part of the study combined temporal persistence analysis and Mann-Kendall's trend test to assess vegetation trends using MODIS vegetation index (2000-2013) and ancillary data (Biophysical and anthropogenic variables).

Two major steps also compose this approach (Figure 3.9). Firstly, the combination of temporal persistence analysis and Mann-Kendall's trend test enabled the detection of trends categories in vegetation dynamics and their distribution according to LULC and LULCC classes. Temporal persistence analysis is a recent method developed by Lanfredi *et al.* (2004), and it enables reducing the effect of the year-to-year instabilities of vegetation on the trend analysis. Mann-Kendall's trend test computes the strength and the significance of the relationship between two variables (here, vegetation index and time). Furthermore, the significant consistent trends of vegetation were modelled using RF classification algorithm with biophysical and anthropogenic variables as predictors. Thus, the contribution of those variables to the occurrence of significant consistent trends was determined using RF variable importance measure.

The second step focused on local population survey which was conducted to determine their perception about vegetation trends during the period 2000-2013. Six villages, Gbagba, Balembar, Gnipkiere, Sorkon, Dayere and Wahable (Figure 3.1) were considered for the survey that focused on 360 household heads selected randomly. This enabled the comparison of remote sensing-based vegetation trend result with the perception of local population.

Details of this part are presented in section 6.2 of chapter 6.

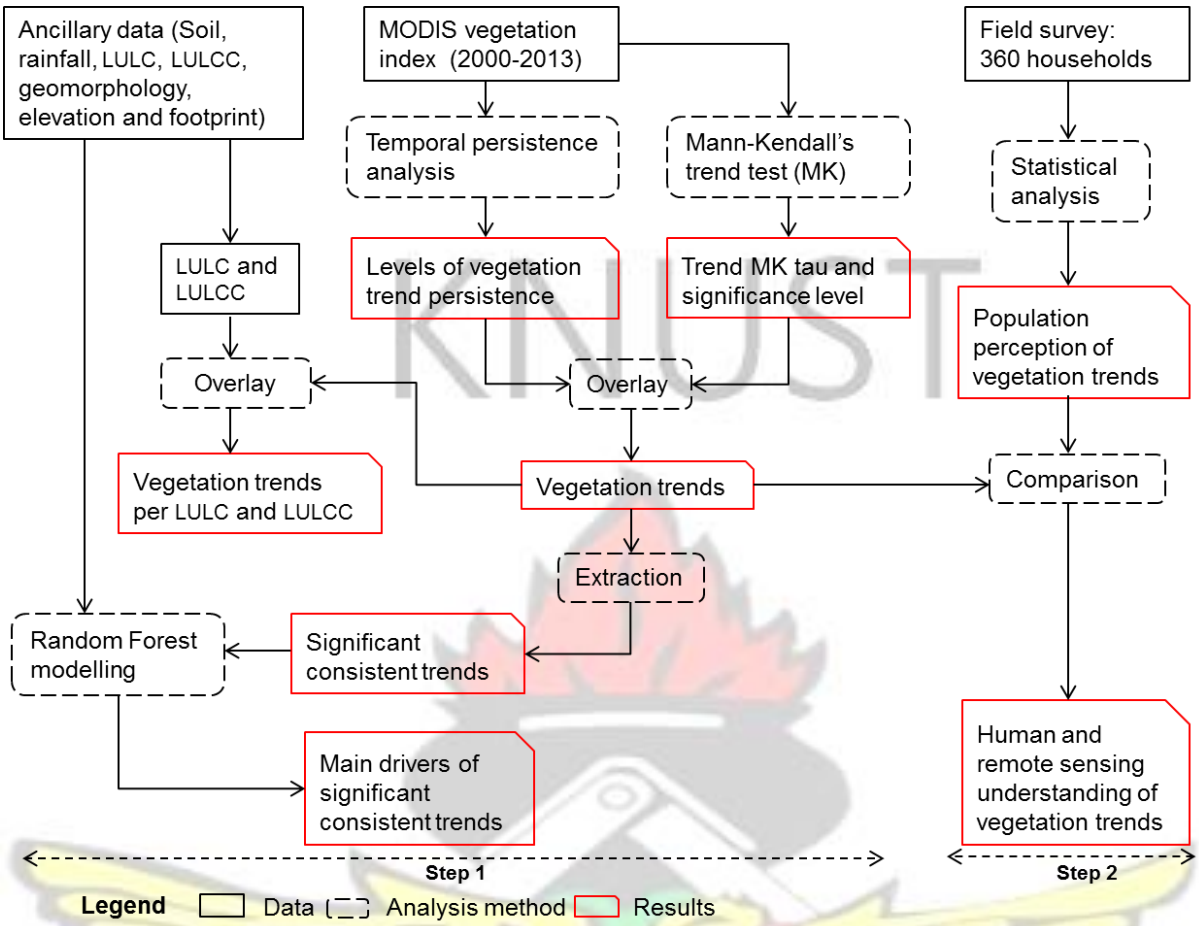

Figure 3. 9. Approach applied for assessing vegetation trends

Chapter 4: Land Use/Cover Change in the Southwest of Burkina Faso

This study is based on: Zoungrana, B. J-B., Conrad, C., Amekudzi, L.K., Thiel, M., Da, E.D., Forkuor, G. and Löw, F. 2015a. Multi-Temporal Landsat Images and Ancillary Data for Land Use/Cover Change (LULCC) Detection in the Southwest of Burkina Faso, West Africa. *Remote Sensing*, 7: 12076-12102.

Abstract

The present study was conducted in the Southwest Burkina Faso to determine a suitable period to map Land Use/Cover (LULC), compare mono-temporal and multi-temporal LULC classifications as well as their combination with ancillary data and to determine Land Use/Cover Change (LULCC) using accurate classification results. Landsat data (1999, 2006

and 2011) and ancillary data served as input features for the random forest classifier algorithm. A reference database was established using high-resolution images, aerial photo and field data. LULCC and LULC classification accuracies, area and area uncertainty were computed based on the method of adjusted error matrices. The results revealed that late rainy season image (e.g. October image) yielded more accurate LULC map than the other periods of the year for mono-temporal classification. Multi-temporal classification significantly outperformed those solely based on mono-temporal data. However, combining monotemporal imagery and ancillary data for LULC classification had the same accuracy level as multi-temporal classification indicating that this combination is an efficient alternative to multi-temporal classification in the study region, where cloud free images are rare. The study area experienced an increase in agricultural area and bare surface and a reduction in natural vegetation (woodland and mixed vegetation), which attests to the ongoing deforestation.

Natural vegetation loss was estimated to be 17.9% ± 2.5% between 1999 and 2011.

4.1. Introduction

Remote sensing plays an important role in the management of the earth's surface by providing spatiotemporal information on LULC (e.g. water, forest, bare area, and cropland).

Change in LULC affects the global environment (Lambin, 1997), its biodiversity (Sala *et al.*, 2000), local, regional and global climate (Chase *et al.*, 1999; Houghton *et al.*, 1999) and also can accelerate, among others land degradation, which reduces ecosystem services and functions (Vitousek *et al.*, 1997). Monitoring Land Use/Cover Change (LULCC) is, therefore, relevant for sustainable landscape and environmental management. For instance, in regions like West Africa, where LULC is known to change rapidly (Duadze, 2004; Orekan, 2007), regular map updates could lead to better estimation of deforestation and land degradation rates, which are key components of the UN REDD (Reducing Emissions from Deforestation and Forest

Degradation) programme and UNCCD (United Nation Convention to Combat Desertification) strategy "Zero Net Land Degradation", respectively.

Remote sensing provides an effective means for mapping LULC, especially over large areas (Di Gregorio and Jansen, 2005). Different types of classifications have been applied for LULC mapping (Lunetta and Balogh, 1999; Rogan *et al.,* 2003; Shalaby and Tateishi, 2007; Blanzieri and Melgani, 2008). Some of these classifications are based on mono-temporal image (e.g. Cord *et al.*, 2010; Ouedraogo *et al.*, 2014), multi-temporal images (e.g. Lunetta and Balogh, 1999; Key *et al.*, 2001), or in combination with ancillary data (e.g. Trietz and Howarth, 2000; Rogan *et al.,* 2003; Sesnie *et al.,* 2008) such as biophysical variables (e.g. elevation, slope and soil types). Mono-temporal classification is widely used in literature (e.g. Duadze, 2004; Ouedraogo *et al.*, 2010; Houessou *et al.*, 2013; Ouedraogo *et al.*, 2014); this analysis focuses on a single date image for LULC mapping. The processing of single date image is faster as compared to multi-temporal classification. In multi-temporal classification, bands from more than one date, season, or year are combined and classified (Langley *et al.*, 2001). This approach involves the use of more images, which increases processing time.

Multi-temporal classification has been used to classify the LULC of various landscapes (e.g. Mickelson *et al.*, 1998; Lunetta and Balogh, 1999; Key *et al.*, 2001).

A comparison of mono-temporal and multi-temporal classifications in different areas revealed contradictory results (Key *et al.*, 2001; Langley *et al.*, 2001). For instance, in two states in the United States of America (USA), Lunetta and Balogh (1999) used single date Landsat image against two dates of imagery and found that the latter increased wetlands identification accuracy from 69% to 88%. Key *et al.* (2001) also noticed a positive effect of multi-temporal classification for discriminating individual tree species in a temperate hardwood forest (West Virginia University forest). Contrary to the aforementioned studies, Langley *et al.* (2001)

compared single date and multi-temporal satellite image classifications in semi-arid grassland and found out that single date classification produced more satisfactory results than multi-temporal classification. The integration of ancillary data with monotemporal image has been found in some places suitable for improving LULC classification accuracy (e.g. Rogan *et al.*, 2003; Sesnie *et al.*, 2008).

Although mono-temporal and multi-temporal classifications as well as the addition of ancillary data have been compared in elsewhere, such investigations remain rare in West Africa, especially in the Sudan savannah zone. In addition, determining an efficient LULC mapping method is crucial for performing accurate post-classification change analysis and to monitor environmental degradation in this region, which is particularly exposed to effects of climate change and population growth. Furthermore, an accurate LULCC map could be an efficient decision-making support tool for mitigating carbon emission and for proper environmental change management, such as forest cover restoration through reforestation campaigns. LULCC assessment in West Africa is challenging, as the region lacks atmospherically undisturbed and cloud free satellite images, which is a limiting factor for LULC mapping. Beside, lack of ground truth information for past years limits assessments of historical LULC (e.g. Aduah and Aabeyir, 2012) as well as validation of LULCC map (e.g.

Braimoh, 2004; Duadze, 2004; Ruelland *et al.*, 2008).

The goal of this study is to determine changes in LULC in the southwest of Burkina Faso. Specifically, it aims at determining a suitable period to map LULC in the study area when using mono-temporal image, comparing mono-temporal and multi-temporal LULC

classifications as well as their combination with ancillary data, and determining LULCC in the study area using accurate classification results.

4.2. Methodology

4.2.1. Landsat images and pre-processing

Landsat TM data (30 m resolution, scene 196/052) were used for LULC classification. In total, ten monthly images were downloaded from United States Geological Survey (USGS) website for the years 1999, 2006 and 2011 (Table 4.1) using a criterion of cloud cover less than 10%. Five Landsat bands were considered in this study: blue (0.45–0.52 μm), green (0.52–0.60 μm), red (0.63–0.69 μm), near infrared (0.76–0.90 μm) and middle infrared (1.55–1.75 μm). The Landsat data were calibrated and corrected to remove atmospheric influences. Firstly, the Digital Numbers (DN) values of the TM images were calibrated into radiance based on information from the meta data files provided by USGS (e.g., sun elevation, acquisition date). Afterwards, the radiance data were converted to surface reflectance using the ENVI 5 FLAASH (Fast Line-of-sight Atmospheric Analysis of Spectral Hypercubes) module, which has shown to be efficient for satellite images atmospheric correction (e.g. Yuan, J. and Niu, 2008). This module requires information such as sensor altitude, initial visibility, atmospheric model, aerosol model, flight date, pixel size, and scene centre location (ENVI, 2009). Some of these parameters were obtained from meta data files, while others were already included in the module such as atmospheric and aerosol models which were set to tropical and rural, respectively, during the atmospheric correction process to match with the study area environment. Image-to-image co-registration was performed to ensure good alignment of pixels in the respective images. A root mean square error of less than one pixel was achieved for all the co-registrations. The images were already georeferenced to the Universal Transverse Mercator (UTM) projection WGS84 zone 30 north.

Table 4. 1. Monthly Landsat TM images of 2011, 2006 and 1999

2011	2006	1999
3 March	31 October	20 October
6 May	16 November	14 February

7 June	18 December	-
9 July	-	-
29 October	-	-

4.2.2. Ancillary data and pre-processing

Ancillary data were also included in the LULC classification process (Table 4.2): slope, elevation, soil types and geomorphology. Slope and elevation were derived from version 2 of Digital Elevation Model (DEM) of ASTER, which has a spatial resolution of 30 m × 30 m. The DEM was georeferenced to UTM WGS84 zone 30 north. Vector layers (shapefiles) for geomorphology and soil types were obtained from the National Soil Office of Burkina Faso (BUNASOLS) at a scale of 1:500,000. They highlighted different geomorphological units and soil types found in the study area. The shapefiles were projected to UTM WGS84 zone 30 north, then rasterized and resampled to 30 m × 30 m using ArcGIS 10.1.

Table 4. 2. Ancillary data used in LULC classification

Ancillary data	Source	Description	resolution
Elevation	ASTER	Height	30 m × 30 m
Slope	ASTER	degree	30 m × 30 m
Soil	BUNASOLS-BF	Soil types	30 m × 30 m
Geomorphology	BUNASOLS-BF	geomorphological units	30 m × 30 m

4.2.3. Reference data sources

High-resolution images (Table 4.3) and field data were used to collect LULC reference samples to train and validate the Landsat images classifications. The high-resolution images were acquired as close as possible to the acquisition dates of the Landsat TM images.

RapidEye image (from April 2011) was collected from the RapidEye Science Archive Team (RESA) of the German Aerospace Center (DLR) at level 3A (i.e., orthorectified with a spatial resolution of 5 m × 5 m and georeferenced to UTM projection). In addition, Quickbird image (2.4 m × 2.4 m) was acquired from October 2012, and scanned aerial photo (June 1999) was obtained from the National Geographic Institute of Burkina Faso (IGB) with a resolution of

2.3 m × 2.3 m. High-resolution images of Google Earth (from October 2006 and November 2007) were also used in this research. Apart from the RapidEye image that was already corrected, the other spatial data were geometrically adjusted (co-registration) to the Landsat images and georeferenced to UTM WGS84 zone 30 north.

A field campaign was conducted in October 2013 to collect LULC ground truth samples with a handheld Global Positioning Systems (GPS) using the projection system UTM WGS84 zone 30 north. LULC areas that remained stable since 2011 were sampled based on local population knowledge. Five broad LULC classes were identified (Table 4.4) using a modified LULC classification scheme of the FAO (di Gregorio and Jansen, 2005): Woodland, bare surface, agricultural area, water and mixed vegetation. Homogeneous areas of 30 × 30 m were surveyed for each LULC (to match Landsat pixel), and the coordinates of the centre recorded. In total, 150 samples were recorded across the study area.

Table 4. 3. High-resolution images used in the analysis

Images	Date	Resolution	Extent	% of study area covered
RapidEye	April 2011	5 m × 5 m	625 km^2	12.20
Quickbird	October 2012	2.4 m × 2.4 m	25.7 km^2	0.50
Aerial photo	June 1999	2.3 m × 2.3 m	188 km^2	3.70
Google Earth image 1	November 2007	2.4 m × 2.4 m	306.9 km^2	6.00
Google Earth image 2	October 2006	2.4 m × 2.4 m	309.8 km^2	6.05

Table 4. 4. Adapted LULC classification scheme, modified from FAO (di Gregorio and Jansen, 2005)

Non-Modified	Modified	
Level 1	Level 2	Adopted LULC classes
Vegetated	Woodland Mixture of grasses, shrubs and trees	Woodland Mixed vegetation

	Cultivated area	Agricultural area
Non-vegetated	Bare land Built up Tarred road Rock	Bare surface
	Rivers Artificial water bodies Lakes	Water

4.2.4. LULC classification

4.2.4.1. Image combinations

In order to assess the classification of mono-temporal and multi-temporal satellite data as well as their combination with ancillary data, four spatial data set combinations were produced using Landsat images and ancillary data (Table 4.5). These image combinations are: (1) mono-temporal image; (2) mono-temporal image plus ancillary data; (3) multitemporal images; and (4) multi-temporal images plus ancillary data. For the combination of mono-temporal image with ancillary data (Table 4.5, column 2), only the image that produced the highest overall accuracy amongst all mono-temporal classifications (Table 4.5, column 1) was selected.

Table 4. 5. Different approaches of image combinations used for the year 2011

	Mono-temporal image	**Mono-temporal image plus ancillary data**	**Multi-temporal images**	**Multi-temporal images plus ancillary data**
Landsat bands	Five images (October, July, June, May and March)	Image which achieved the highest accuracy in monotemporal classification	Five images (October, July, June, May and March)	Five images (October, July, June, May and March)
Ancillary data	-	Elevation Slope Geomorphology Soil types	-	Elevation Slope Geomorphology Soil types

4.2.4.2. Classification algorithm: Random Forest classification algorithm

Supervised classifications of the Landsat images were performed using Breiman's (2001) non-parametric Random Forest (RF) classifier. RF is a machine learning algorithm (Rodriguez-Galiano *et al.*, 2012a) that can incorporate diverse sources of data (Mellor *et al.*, 2013), such as biophysical and remotely sensed data, and it was found more accurate than other classifiers such as maximum likelihood classification (e.g. Waske and Braun, 2009; Akar and Güngör, 2013), support vector machine (e.g. Akar and Güngör, 2013) and neural networks (e.g. Löw *et al.*, 2015).

RF is an ensemble of classification trees in which each tree contributes with a single vote for the assignment of the most frequent class to the input vector (X), $\hat{C}_{rf}^{B} = majority\ vote\ \{\hat{C}_b(X)\}_1^B$ (Breiman, 2001; Rodriguez-Galiano *et al.*, 2012b), where $\hat{C}_b(X)$ is the class prediction of the bth random forest tree, and *B* the total number of trees. In fact, RF collects different subsets of training data to grow the trees (Ntree) using bagging (Breiman, 1996) which is a technique used for training data creation by randomly resampling the original dataset with replacement (i.e., with no deletion of the data selected from the input sample for generating the next subset) (Liaw and Wiener, 2002; Rodriguez-Galiano *et al.*, 2012b). A second random sampling is operated by RF to select a subset of predictive variables (Mtry) for the division of every node, which reduces the generalisation error (Horning, 2010; Rodriguez-Galiano *et al.*, 2012a). This randomness included in RF process decreases the correlation between trees in the forest and increases accuracy (Gislason *et al.*, 2006). RF also computes the contribution of each variable to the classification using Mean Decrease Gini (MDG) and Mean Decrease Accuracy (MDA). However, Nicodemus (2011) noticed that MDG is sensitive to within-predictors correlation and differences in category frequencies, while MDA is robust to these data characteristics.

Field data (only for 2011) and visual interpretation of the high-resolution images provide the possibility to collect a first set of LULC truth points (for each year) to train the RF classifier. Polygons of homogeneous pixels were drawn around each truth point for each LULC class and saved as vector layer of training areas. Landsat pixels that overlap the training areas were then used to train the RF classifier using R statistical software. The highest accuracies were achieved when using 800 as number of trees built, and when using the square root of the total number of variables in each image as number of variables at each node split. Therefore, those values were applied for all the classifications.

4.2.5. LULCC mapping: Post classification change detection

Pixel-based post-classification change detection was performed using the classified maps of 1999 and 2011. It is a "from to" change detection technique and enables tracking the trajectory of each pixel between the two time steps of observation. In the present study, the post-classification change detection was performed in ArcGIS 10.1 where the LULC maps of 1999 and 2011 were combined into one raster file using the function "combine". This enabled the detection of 25 LULC conversions or LULCC classes using the attribute table of the produced raster. However, four generalized categories of LULCC classes were considered: Stable Natural Vegetation (SNV), Natural Vegetation Loss (NVL), Stable Non-Natural Vegetation (SNNV), and Other Change (OC). Based on a new field created in the attribute table of the combined raster file, the four LULCC classes were assigned to each pixel following the rules shown in Table 4.6.

Table 4. 6. LULC conversions and LULCC classes between 1999 and 2011

Name	Stable Natural Vegetation	Natural Vegetation Loss	Stable non-Natural Vegetation	Other Change

Conversions	Stable woodland	Woodland to other LULC unless mixed vegetation	Stable agricultural area	Agricultural area to all other LULC
	Stable mixed vegetation	Mixed vegetation to other LULC unless woodland	Stable bare surface	Bare surface to all other LULC
	Woodland to mixed vegetation		Stable water area	Water to all other LULC
	Mixed vegetation to woodland			

4.2.6. Accuracy and area assessment

4.2.6.1. Sampling design

The sampling design is the protocol for selecting the subset of spatial units that will form the basis of the accuracy assessment (Stehman and Czaplewski, 1998; Olofsson *et al.,* 2014). In this study, pixels were used as spatial units (30 m × 30 m). Stratified random sampling was applied for collecting a second set of reference points to test RF classifications and validate the LULCC map; this is because the statistics computed in this study were based on the adjusted error matrix that requires a probability sampling for collecting reference data (Olofsson *et al.,* 2013). Stratified random sampling is a probability sampling design and a key element of a statistically rigorous assessment (Stehman and Czaplewski, 1998). It enables statistical inference for computing estimates with confidence intervals.

Here, the different LULC and LULCC classes were considered as strata. Stratification is conducted when the strata are of interest for reporting results (e.g. accuracy and LULC class area), and to improve the precision of the accuracy and area estimates (Olofsson *et al.,* 2014). The strata sample allocation can be done either by equal sample size (same sample size for each class) or by proportional sample size (sample proportional to the spatial extent of each class in the map). The first method favours user's accuracy against overall and producer's accuracies

(Stehman, 2012), while, in the second method, the standard errors of estimating producer's and overall accuracies become smaller as compared to equal allocation (Olofsson *et al.*, 2014). In order to take advantage of both sample allocation methods, the recommendation of Olofsson *et al.* (2014) to increase the sample size of the rarer classes was followed in this study.

4.2.6.2. Response design

The response design is the protocol for determining the reference LULC classification of a sampling unit (Stehman and Czaplewski, 1998). The high-resolution images were used as reference data sources (Table 4.3). For each year, the portions of the classified Landsat data that overlapped the high-resolution images were extracted and converted to polygon vector layer (in ArcGIS 10.1) from which the RF training areas were excluded. Each class was isolated as an individual vector layer based on which a set of randomly selected pixels were generated for each stratum (class). Each pixel received a LULC label by visual interpretation of the high-resolution images. The labels of each reference pixels on the maps and the highresolution images were then compared to produce error matrices. Altogether, 371, 328 and 345 pixels were selected as samples for the years 2011, 2006 and 1999, respectively. The samples allocated to each stratum are shown in Table 4.7.

For the LULCC of the period 1999–2011, the overlapping area between LULCC map, aerial photo of 1999 and high-resolution images of 2011 were considered for reference pixels collection following the same procedure as above. However, Landsat images (1999 and 2011) were included especially for LULCC classes that were underrepresented in the highresolution images. In all, 300 LULCC reference pixels were selected based on the classes established in Section 4.2.5 (Table 4.6). The numbers of samples are given in Table 4.8. Finally, the labels of the reference pixels on the change map and also on the reference images of 1999 and 2011 were compared to build an error matrix.

Table 4. 7. Sample size allocated to each LULC class in 1999, 2006 and 2011

	Sample Allocated		
LULC classes (strata)	2011	2006	1999
Water	42	40	42
Woodland	100	97	111
Bare surfaces	59	45	45
Mixed vegetation	75	78	89
Agric. Area	95	68	58
Total column	371	328	345

Table 4. 8. Sample size allocated to each LULCC class

LULCC Classes (strata)	Sample Allocated
Stable natural vegetation	125
Natural vegetation loss	56
Stable non-natural vegetation	42
Other change	77
Total	300

4.2.6.3. Analysis

✓ **Accuracy assessment**

In order to determine the accuracy of a classified map with q categories, an error matrix is constructed (Congalton and Green, 2009). Following the suggestions of Olofsson *et al.* (2013) for assessing the accuracy of LULCC maps based on stratified random sampling strategies and pixel-based classifications, the error matrices of both LULCC and LULC classification were adjusted by the area of each category on the maps, and error matrices based on area proportions ($\hat{P}_{ij}$) were produced:

$$\hat{P}_{ij} = W_i \frac{n_{ij}}{n_{i+}} \tag{4.1}$$

where W_i is the proportion of area of category i in the map, n_{ij} is the number of samples mapped as i and belonging to category j in the reference data, n_{i+} is the number of samples mapped as category i in the map. In the adjusted error matrix (Table 4.9), each cell element P_{ij} indicates

the probability that a randomly selected area is classified under category i in the image and under category j in the reference data (Mas *et al.*, 2014).

Table 4. 9. Adjusted error matrix of estimated area proportions

		Reference						
		1	**2**					… **j** … **q**
		P_{11}	P_{12}				P_{1+}	
	2	P_{21}	P_{22}	…		…	P_{2+}	
				Total				
	1			…	P_{1j}		P_{1q}	
	⋮	⋮	⋮	⋮	⋮	⋮	⋮	⋮
Map	***i***	$\hat{P}_{i1}$	$\hat{P}_{i2}$	…	P_{ij}	…	P_{iq}	$\hat{P}_{i+}$
	⋮	⋮	⋮	⋮		⋮	⋮	⋮
	q	$\hat{P}_{q1}$	$\hat{P}_{q2}$	…	P_{qj}	…	P_{qq}	$\hat{P}_{q+}$
	Total	$\hat{P}_{+1}$	$\hat{P}_{+2}$	…	P_{+j}	…	P_{+q}	*1*

Based on this new error matrix, accuracies (overall, user's and producer's) were calculated. The overall accuracy (O) indicates the overall proportion of area correctly classified. It is the sum of $\hat{p}_{ii}$ of the adjusted error matrix diagonal.

$$O = \sum_{i=1}^{q} P_{ii} \tag{4.2}$$

User's accuracy (U_i) of class i is the proportion of the area mapped as class i that has reference class i, and producer's accuracy (P_j) of class j is the proportion of the area of reference class j that is mapped as class j. Both accuracies were computed according to Equations (4.3) and (4.4), respectively.

$$\hat{U}_i = \frac{\hat{P}_{ii}}{\hat{P}_{i+}} \tag{4.3}$$

$$\hat{P}_j = \frac{\hat{P}_{jj}}{\hat{P}_{+j}} \tag{4.4}$$

The Kappa index of agreement (K) was also computed to assess LULC classification accuracy. This index is intended to give a quantitative measure of the magnitude of agreement between the observations and predictions (Viera and Garrett, 2005).

The Kappa index was found more robust than the overall accuracy since it takes into account the agreement occurring by chance (Foody, 2002). A Perfect agreement between the observations and the predictions produces a value of K equal to 1. It is mentioned that a K value below 0 indicates no agreement between the observations and predictions, and 0 –0.20 as slight, 0.21–0.40 as fair, 0.41–0.60 as moderate, 0.61–0.80 as substantial, and 0.81–1 as almost perfect agreement (Loosvelt *et al*., 2012).The computing of K is described in Equation 4.5.

$$K = \frac{N\sum_{i=1}^{r} X_{ii} - \sum_{i=1}^{r}(X_{i+}X_{+i})}{N^2 - \sum_{i=1}^{r}(X_{i+}X_{+i})} \tag{4.5}$$

where r is the number of row in cross classification table (confusion matrix). X_{ii} is the number of combinations along the diagonal of the confusion matrix. X_{i+} corresponds to the total observations in row i, and X_{+i} the total observations in column i. N is the total number of observation.

✓ **Classification types performance**

McNemar's test was used to evaluate the performance of multi-temporal and mono-temporal classification as well as their integration with ancillary data. It is a non-parametric test that is more precise and sensitive than the Kappa z-test (Manandhar *et al.,* 2009). McNemar's test evaluates the difference between paired proportions. Here, the test is based on a pair of confusion matrices of correctly and wrongly classified reference samples. It produces a

chisquare (χ^2) statistics that is computed by Equation (4.6). The difference between two classification approaches is significant when the *p*-value is less than 0.05.

$$\chi^2 = \frac{(f_{12} - f_{21})^2}{(f_{12} + f_{21})} \tag{4.6}$$

where f_{12} indicates the number of cases that are wrongly classified by approach 2, but correctly classified by approach 1, and f_{21} is the number of cases that are correctly classified by approach 2, but wrongly classified by approach 1.

✓ **Area estimates and uncertainty**

In accordance with the systematic approach suggested by Olofsson *et al.* (2013), the adjusted error matrix was used to compute an area estimator based on the proportion of the area of category *j*. Equation (4.7) gives the area of category j $(\hat{A}_j)$.

$$\hat{A}_j = A_{tot} \times \hat{P}_{+j} \tag{4.7}$$

where A_{tot} is the total area, and

$$\hat{P}_{+j} = \sum_{i=1}^{q} W_i \frac{n_{ij}}{n_{i+}} \tag{4.8}$$

This area estimator is an error-adjusted estimator of area that includes the area of map omission error of category *j* and removes the area of map commission error (Olofsson *et al.*, 2013). Its standard error $S(\hat{A}_j)$was computed as follows.

$$S(\hat{A}_j) = A_{tot} \times S(\hat{P}_{+j}) \tag{4.9}$$

where the standard error for the stratified estimator of proportion of area$S(\hat{P}_{+j})$ is computed as:

$$S(\hat{P}_{+j}) = \sqrt{\sum_{i=1}^{q} \frac{W_i \hat{P}_{ik-} \hat{P}_{ik}^2}{n_{i+} - 1}} \tag{4.10}$$

The use of $\hat{P}_{+j}$(estimated from the reference samples) instead of P_{i+}(map areas) is because it allows the assessment of uncertainty of the area estimates in the form of sampling variability that can be computed as confidence interval. For $\hat{A}_j$the approximate 95% confidence interval (*CI*) was derived as:

$$CI = \hat{A}_j \pm z \times S(\hat{A}_j) \tag{4.11}$$

where z corresponds to the percentile from the curve of the standard normal distribution, and for 95% confidence, z = 1.96.

4.3. Results

4.3.1. Suitable period for mono-temporal LULC classification

In order to detect the most adequate period to classify the observed LULC, the year 2011 was selected because it had images from dry season (March), early rainy season (May and June), mid rainy season (July) and late rainy season (October), which cover the entire vegetation period. The results of the mono-temporal RF classifications are shown in Figure 4.1, and it can be observed that there is an increase in overall, average user's and average producer's accuracies and kappa from March to October. Table 4.10 presents the pixels count error matrices obtained from the five mono-temporal classifications. Major confusions were recorded, for instance, between agricultural area and natural vegetation, agricultural area and bare surface and among natural vegetation types. The use of October image for classification outperformed all other mono-temporal attempts, because it reduced confusion between natural vegetation classes (Woodland and Mixed vegetation) and between agricultural area and natural vegetation, among others. The matrices clarify that at the end of the dry period (March) the class agriculture area seems to spectrally resemble other classes, which explains the aforementioned low accuracies obtained for that period. The main finding is that the LULC classification of the late rainy season images (e.g., October) performed better than those applied

to images of the mid rainy, early rainy and dry seasons. Therefore, the monotemporal image of October served as benchmark for assessing the effect of multi-temporal images and ancillary data on LULC classification.

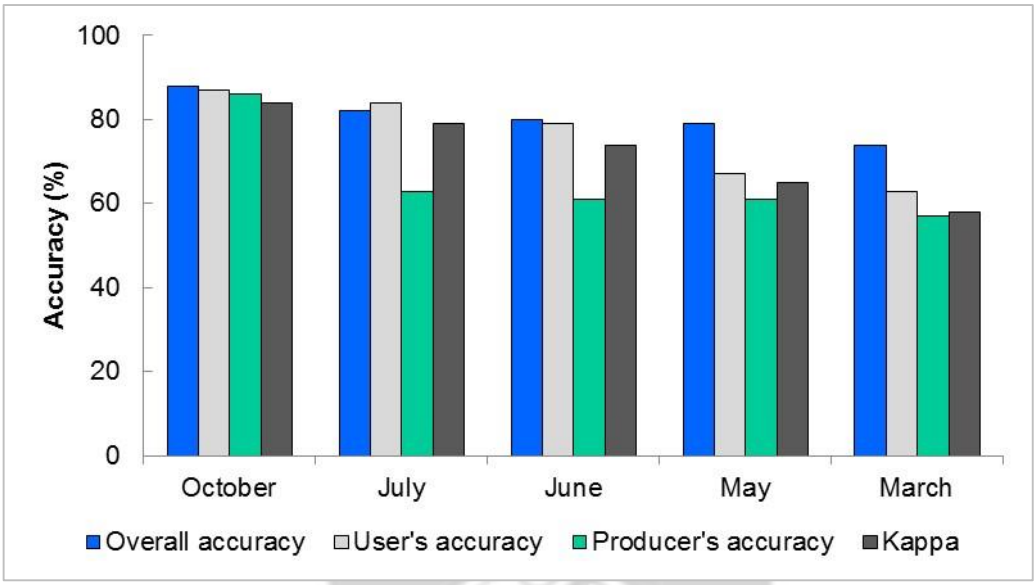

Figure 4. 1. Mono-temporal classification accuracies of different months

Table 4. 10. Error matrices of mono-temporal LULC classifications of 2011. The values in all the tables refer to the numbers of pixels. 1: Water; 2: Woodland; 3: Bare surface; 4: Mixed vegetation; 5: Agricultural area

				March					
				1	**2**	**3**	**4**	**5**	**Total**
1	15	0	2	0	25	42			
2	0	79	0	5	16	100			
3	0	4	35	9	11	59			
4	1	16	12	32	14	75			
5	0	0	0	5	90	95			
			Total	16	99	49	51	156	371

	1	2	May						
1	13	0	**3**	**4**	**5**	**Total**			
2	3	91	16	0	13	42			
3	0	2	0	3	3	100			
4	0	20	44	5	8	59			
5	1	4	4	39	12	75			
Total	17	117			2 5	83	95		
			66						

	1	2	June						
1	37	0			3 4	5	**Total**		
2	4	91	0	0	5	42			
3	0	5	2	1	2	100			
4	0	20	46	3	5	59			
5	0	3	9	36	10	75			
Total	41	119						1	5
			July					86	95
			58	45	108	371			

	1	2							
			3	**4**	**5**	**Total**			
1	42	0			0 0	0	42		
2	6	87			1 3	3	100		
3	0	6	46	2	5	59			
4	0	9	8	43	15	75			
5	0	2						1	0
Total	48	104	**October**					92	95
			56	48	115	371			

	1	2	3	4	5	Total
1	40	2	0	0	0	42
2	0	90	0	6	4	100
3	0	0	48	6	5	59
4	0	5	4	57	9	75
5	0	0	0	5	90	95
Total	40	97	52	74	108	371

4.3.2. LULC classification accuracies according to images combinations

The results presented in Table 4.11 show that mono-temporal classification (of the best performing data set, October) had the lowest accuracy among the four combinations of images. In contrast to the optimal mono-temporal approach, multi-temporal classification improved the overall accuracy from 88% to 94%, the average user's from 87% to 93%, the average

producer's from 86% to 91% and Kappa from 84% to 91%. The incorporation of ancillary data has also positively influenced the LULC discrimination. Indeed, their integration with mono-temporal image (October) yielded an overall accuracy comparable to the use of multi-temporal data (94%). There was also an improvement in average user's accuracy (87% to 93%), average producer's accuracy (86% to 91%) and Kappa (84% to 91%). However, the best performance in terms of the accuracy assessment was recorded by the combination of multi-temporal images and ancillary data, which produced the highest overall, average user's and average producer's accuracies and also Kappa with values of 95%, 95%, 92% and 93% respectively. This superiority of multi-temporal classification and the addition of ancillary data over mono-temporal classification is supported by the results of

McNemar's test (Table 4.12). The test showed significant difference ($p < 0.05$) in LULC classifications produced by multi-temporal, mono-temporal plus ancillary data and multitemporal plus ancillary data classifications over mono-temporal data. However, no significance difference was found between multi-temporal, mono-temporal plus ancillary data and multi-temporal plus ancillary data classifications.

Table 4. 11. Classification accuracy in 2011 (%) according to images combinations

Images Combinations	Overall accuracy	Av. User's acc.	Av. Producer's acc.	Kappa
Mono-temporal	88	87	86	84
Mono-temporal plus ancillary	94	93	91	91
Multi-temporal	94	93	91	91
Multi-temporal plus ancillary data	95	95	92	93

Table 4. 12. McNemar's test results between image combinations

	Mono-Temporal			
	f_{12}	f_{21}	Chi-square	*p*-value
Multi-temporal	4	22	12.5	0.0004
Mono-temporal plus ancillary data	6	23	10	0.001
Multi-temporal plus ancillary data	1	19	16.2	0.00005
	Mono-temporal plus ancillary			

	f_{12}	f_{21}	Chi-square	*p*-value	**Multi-temporal**	6	7	0.08
0.8								
Multi-temporal plus ancillary data		10	5	1.7	0.2			

	Multi-temporal			
Multi-temporal plus ancillary data	f_{12}	f_{21}	Chi-square	*p*-value
	8	3	2.3	0.1

The positive impact of multi-temporal images and ancillary data was also perceptible on each LULC class. The user's and producer's accuracies of each class, according to Tables 4.13 and 4.14, indicate that the discrimination of the individual LULC classes was improved with the use of multi-temporal images and the addition of ancillary data.

Table 4. 13. LULC user's accuracy (%) per image combination in 2011

Classification Approach	Water	Woodland	Bare surface	Mixed vegetation	Agricultural area
Mono-temporal	95	90	81	76	94
Mono-temporal plus ancillary	95	98	90	88	95
Multi-temporal	95	96	90	89	97
Multi-temporal plus ancillary	98	99	93	88	97

Table 4. 14. LULC producer's accuracy (%) per image combination in 2011

Classification Approach	Water	Woodland	Bare surface	Mixed vegetation	Agricultural. area
Mono-temporal	100	96	66	81	85
Mono-temporal plus ancillary	100	100	69	92	93
Multi-temporal	100	100	71	92	93
Multi-temporal plus ancillary	100	98	69	94	97

4.3.3. Contribution of remote sensing bands and ancillary data to LULC classification

The contribution of the remotely sensed bands and ancillary data to LULC classification in the study area is shown in Figure 4.2, which highlights the mean decrease accuracy (MDA) score of each variable. This was computed by RF algorithm based on the classification of mono-temporal image plus ancillary data. In general, near infrared, middle infrared and elevation

were the three most important variables for LULC classification. They are followed by geomorphological units, red, green and blue bands, whereas slope and soil types were the least important variables. Among the four environmental data used in this research, elevation and geomorphological units have more contributed to LULC discrimination compared to soil types and slope.

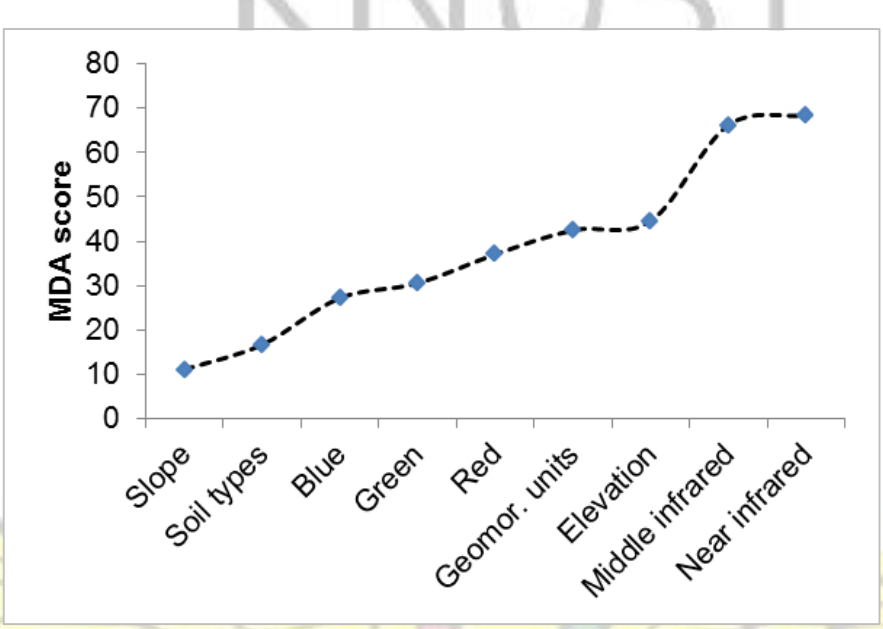

Figure 4. 2. Remotely sensed bands and ancillary data contributions to LULC classification based on mean decrease accuracy (MDA) score of RF mono-temporal image plus ancillary data classification

4.3.4. The dynamics of LULC in the study area over the years 1999, 2006 and 2011

In accordance with the results of the 2011 classifications, the combination of multi-temporal images and ancillary data was used to classify the images of 1999 and 2006. The monthly Landsat images of 1999 and 2006, specified in Table 4.1, were combined with ancillary data (Table 4.2), and the classification yielded 94% (93%) as overall accuracy and 85%(80%) as kappa index values for the LULC map of 1999 (2006). The distribution of each LULC area in 1999, 2006 and 2011 is presented in Tables 4.15–4.17, respectively. The mapped area is slightly different from the estimated area for all LULCs. In all cases, it could be found within the confidence interval (95%) around the estimated area indicating a high reliability of the produced maps (Olofsson *et al.*, 2013).

Table 4. 15. Proportion of LULC types in 1999

LULC	Mapped area %	Estimated area %	Confidence interval %
Water	1.7	1.7	± 0.1
Woodland	41.5	40.1	± 2.0
Bare surface	1.8	2.4	± 1.0
Mixed vegetation	33.2	33.2	± 2.3
Agricultural area	21.8	22.6	± 2.3
Total	100	100	

Table 4. 16. Proportion of LULC types in 2006

LULC	Mapped area %	Estimated area %	Confidence interval %
Water	0.7	0.7	± 0.04
Woodland	39	38.1	± 1.3
Bare surface	1.8	2.9	± 1.3
Mixed vegetation	32.5	32.3	± 1.7
Agricultural area	26	26	±2 .6
Total	100	100	

Table 4. 17. Proportion of LULC types in 2011

LULC	Mapped area%	Estimated area %	Confidence interval %
Water	0.2	0.2	± 0.01
Woodland	35.3	36.4	± 2.1
Bare surface	2.9	3.3	± 1.4
Mixed vegetation	31.6	30.4	± 1.3
Agricultural area	30	29.7	± 1.6
Total	100	100	

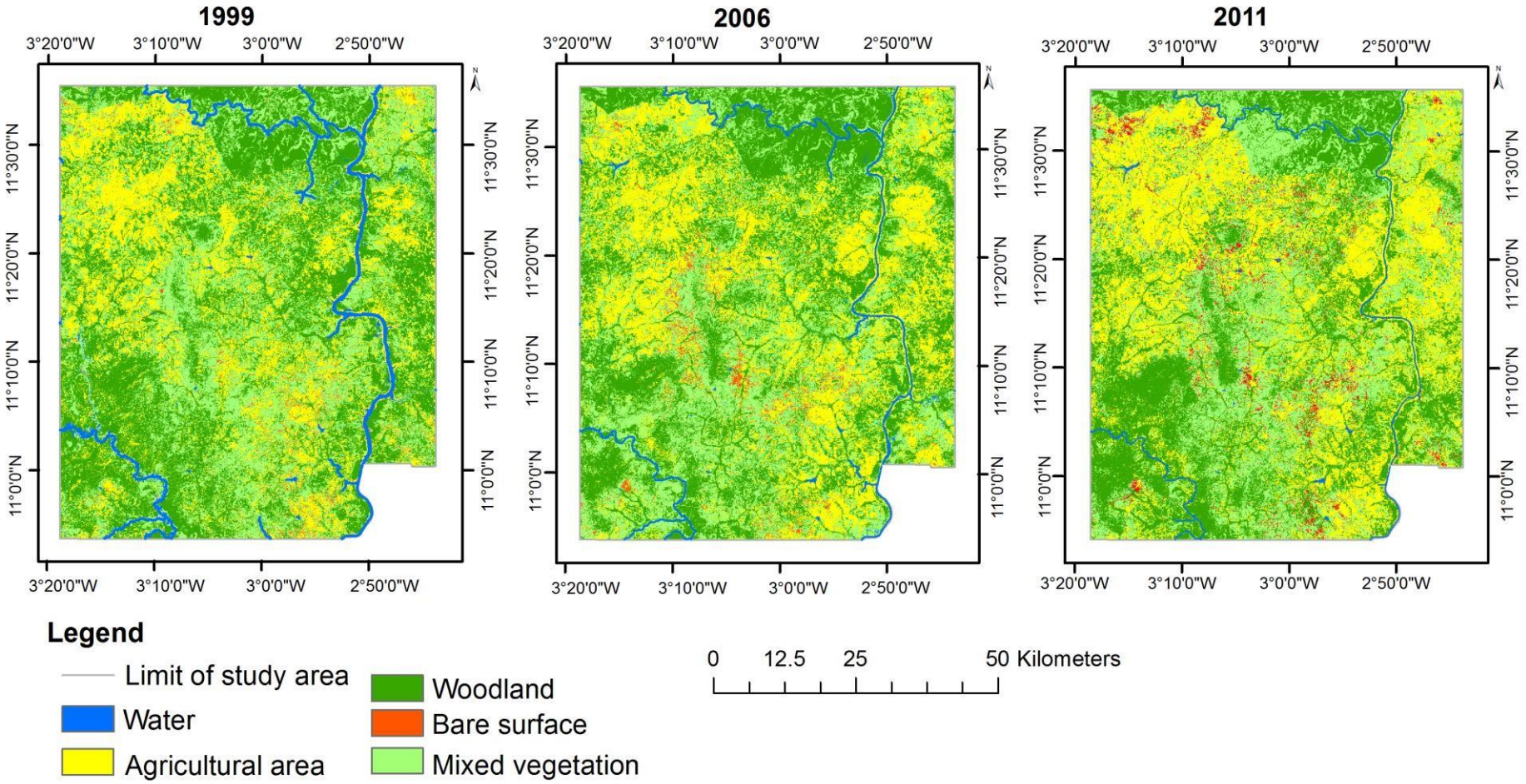

Figure 4. 3. LULC spatial distribution in the study area in 1999, 2006 and 2011

The results revealed that agricultural area and bare surface have increased in the study area at the expense of woodland and mixed vegetation, which decreased over the years. For instance, the proportion of agricultural area increased from 22.6% ± 2.3% in 1999 to 26% ± 2.6% in 2006 and further to 29.7% ± 1.6% in 2011. These dynamics are well captured in Figure 4.3, which highlights the expansion of agricultural area (in yellow) across the study area.

Contrary, the areas of woodland and mixed vegetation, as observed in 1999, decreased in 2006 and 2011 (Tables 4.15–4.17). A decreasing trend was also observed for water area.

4.3.5. LULCC in the study area between 1999 and 2011

The adjusted error matrix of the LULCC map derived between 1999 and 2011 is given by Table 4.18. The accuracy assessment returned kappa value of 86%, overall accuracy of 92%, while the user's accuracy ranged from 86% to 95% and the producer's accuracy from 84% to 95%.

Table 4. 18. Adjusted error matrix of LULCC map between 1999 and 2011. SNV: stable natural vegetation; NVL: natural vegetation loss; SNNV: stable non-natural vegetation; OC: other change

	SNV	**NVL**	**SNNV**	**OC**	**Total**	**User's (%)**
SNV	0.547	0.014	0	0.014	0.575	95
NVL	0.016	0.151	0.003	0.003	0.173	87
SNNV	0.004	0.01	0.129	0	0.143	90
OC	0.007	0.004	0.004	0.094	0.109	86
Total	0.574	0.179	0.136	0.111	1	
Producer's (%)	95	84	95	85		92

Table 4.19 presents the estimated and the mapped LULCC areas. In this case also, the map area of each LULCC class fell within the computed confidence interval (95%). Between 1999 and 2011, 57.4% ± 2.7% of the study area were dominated by stable natural vegetation. Area under loss of natural vegetation represented 17.9% ± 2.5%. Stable non-natural vegetation and other change covered 13.6% ± 1.5% and 11.1% ± 1.9% of the study area, respectively. The

distribution of the LULCC classes in the study area is shown in Figure 4.4 where most of the losses of natural vegetation are located in areas dominated by agriculture.

Table 4. 19. LULCC area between 1999 and 2011

	Map area	Estimated area	
LULCC classes	%	%	Conf. interval *(%)*
Stable natural vegetation	57.5	57.4	± 2.7
Natural vegetation loss	17.2	17.9	± 2.5
Stable non-natural vegetation	14.3	13.6	± 1.5
Other change	11	11.1	± 1.9
Total	100	100	

Figure 4. 4.

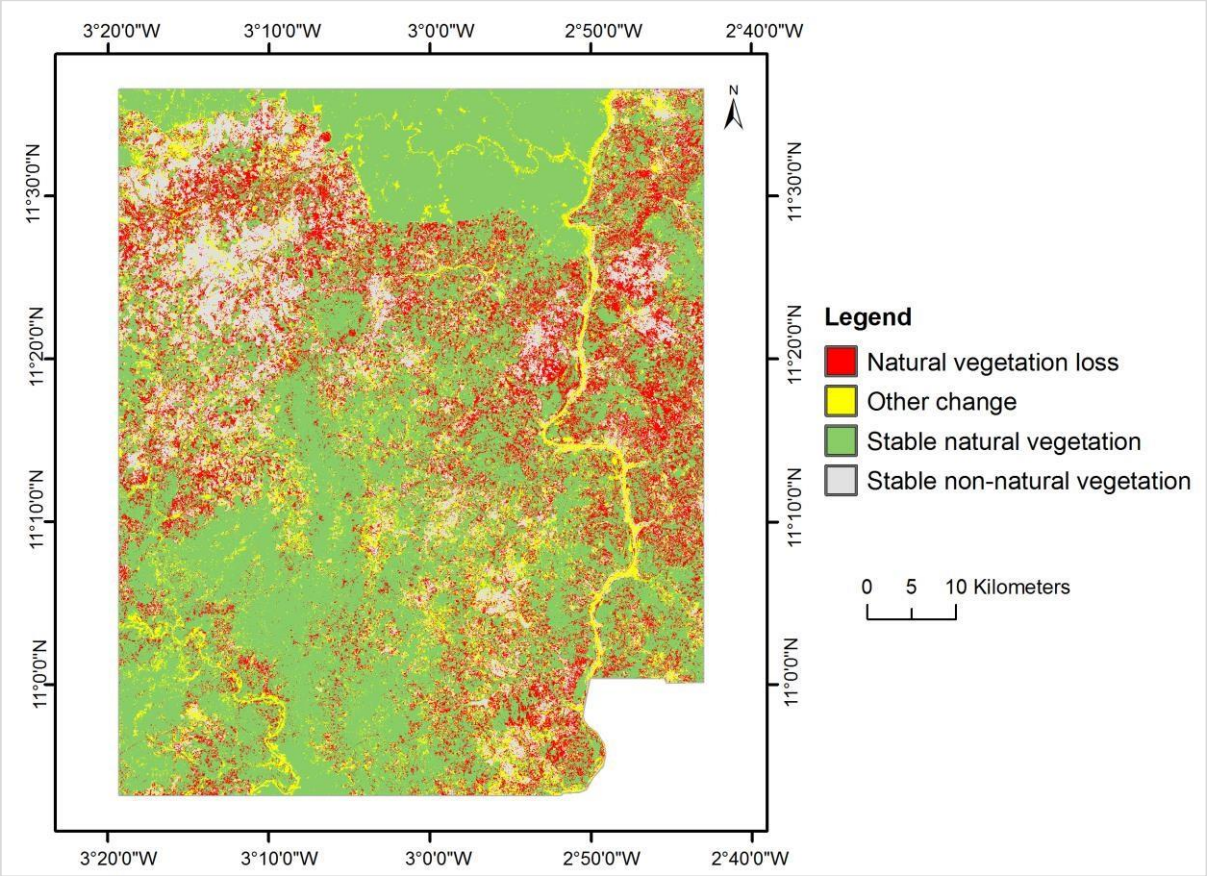

Distribution of LULCC in the study area between 1999 and 2011

The main LULC conversions observed between 1999 and 2011 (Table 4.20) consisted of changes from woodland to agricultural area (occurred on 8.6% of the study area), woodland to mixed vegetation (8.4%), mixed vegetation to woodland (7.2%) and mixed vegetation to

agricultural area (6.8%). Stable LULC are dominated by woodland, mixed vegetation and agricultural area, which covered 24.1%, 17.8% and 13.8% of the area, respectively. Although there was an important loss of natural vegetation (17.9% ± 2.5) in the study area, the transfer matrix highlighted that also regrowth of natural vegetation was recorded. As example, 2.7%, 4.5% and 0.8% of the study area were converted from agricultural area to woodland, agricultural area to mixed vegetation and bare surface to mixed vegetation, respectively. Those conversions could be cropland left under fallow, and potentially the result of reforestation and afforestation campaigns that are frequent in this area.

Table 4. 20. LULC transfer matrix between 1999 and 2011 expressed in percentage

		2011					
		Water	Woodland	Bare Surfaces	Mixed Veg.	Agric. Area	Area 1999
1999	Water	0.2	1.1	0	0.1	0.3	1.7
	Woodland	0	24.1	0.4	8.4	8.6	41.5
	Bare surfaces	0	0.2	0.3	0.8	0.5	1.8
	Mixed veg.	0.01	7.2	1.4	17.8	6.8	33.2
	Agric. Area	0	2.7	0.8	4.5	13.8	21.8
	Area 2011	0.2	35.3	2.9	31.6	30	100

4.4. Discussion

4.4.1. LULC classification

The use of late rainy season image (e.g., October image) was found more suitable than single image from other seasons (mid rainy, early rainy and dry seasons) for LULC classification in the Sudan savannah of southwest Burkina Faso. This is due the fact that late rainy season image provides better spectral information to separate confusing LULC classes such as agricultural area and natural vegetation. Medicinal, sacred, and fruit trees maintained in croplands creating intermixed areas (Figure 4.5) can be seen as one major reason for this spectral confusion between these two classes in the study region.

The result obtained for the Sudan savannah are in agreement with the study by Lunetta and

Balogh (1999) and Key *et al.* (2001), who noticed an improvement in LULC classification accuracy when they used multi-temporal images as compared to mono-temporal image. However, findings in this study are in contrast with those reported in Langley *et al.* (2001). This is because the study by Langley *et al.* (2001) focused on areas dominated by grassland located in the Jornada del Muerto plain of southern New Mexico, while the present work investigated an area dominated by woodland and mixed vegetation with many patterns of agricultural areas. These findings therefore highlight that differences in environment and LULC types might play a critical role.

Multi-temporal classification enables the analysis of images acquired at different phenological stages, which adds useful information for the classification, and in turn permits a better class discrimination. It has to be noted that this research did not assess different multi-temporal image compositions, like various combinations of months, which could be helpful for the choice of adequate temporal images (Förster *et al.*, 2012; Conrad *et al.*, 2014). However, the mono-temporal results strongly indicate that for multi-temporal mapping, the inclusion of late rainy season images is of relevance for accurate LULC mapping in southwest Burkina Faso. The remaining challenge is that frequent cloud cover in the region may reduce the availability of data in such important temporal windows suitable for classification (Forkuor *et al.*, 2014).

In the face of frequently disturbed atmospheric conditions and poor availability of cloud-free satellite data in the study region, it is of high interest that ancillary data can significantly improve LULC classification to almost the same accuracy level as multi-temporal classifications. In the study area for instance, natural vegetation distribution (e.g., Woodland) is influenced by topography (Cord *et al.*, 2010). This explains the usefulness of including environmental variables into LULC discrimination especially elevation and

geomorphological units that added most inputs to the classification after the remotely sensed infrared bands. These results confirm similar conclusions of previous studies, which utilized the environmental settings as add-on for an improved classification. Sesnie *et al.* (2008) found the overall accuracy increasing from 82.4% to 87.4% with the addition of terrain variables (e.g., elevation and slope) in the classification of nine land cover types in Nicaraguan tropical dry forest. For monitoring of land-cover change in San Diego County, Rogan *et al.* (2003) noted that ancillary variables (elevation, fire history, and Slope) contributed 15% to the overall accuracy of land-cover change mapping. The most accurate classification was achieved when multi-temporal images and ancillary data were combined. The accuracy of this approach significantly differed from mono-temporal classification (as shown by the McNemar tests at the 95% confidence level), but not from classification results using a combination of specific mono-temporal image with ancillary data. This again shows that combining mono-temporal satellite data with information about environmental settings can be assessed to be a suitable alternative even in the savannah of southwest Burkina Faso.

The ancillary data showed positive impact on the classification results, but it needs to be stated that geomorphology and soil data, were produced at a scale of 1:500,000, which is at a coarse spatial resolution in comparison to 30 m Landsat pixels. The use of higher spatial resolution data matching the satellite data pixel could possibly improve the accuracy of LULC classifications. In general, LULC/LULCC maps presented in this study can be seen as a valuable input for training and validating global or regional LULC maps, which in turn will be used for regional assessments e.g. of the carbon budget (Machwitz *et al.*, 2015). Local maps are of particular value within the very complex landscape of West Africa, which extremely challenges the accurateness of existing regional to global maps (Herold *et al.*, 2008). Assessing the accuracy of regional maps requires an estimation of error propagation and hence documented quality information about the local input maps. The maps presented here, have

such quality attributes even though it must be stated that validation was carried out on only 28.5% of the study area. For applying the validation throughout the study area, the availability of more high-resolution data sets would be desirable. With the increasing number of high-resolution data sources (e.g., QuickBird, RapidEye and Ikonos), future studies will potentially consider larger portions of their study area for accuracy assessment, which may give more confidence to the results. However, for instance validation activities of other LULC mapping studies relying on field observations can usually cover only those parts of the study areas which can be accessed either by car or by bike (e.g. Cord *et al.,* 2010), which also questions the spatial distribution of the samples and hence the overall validity of the accuracy assessment. However, a validated LULC map based on some portions of the study area remains more reliable than a non-validated LULC map as observed in previous studies conducted in West Africa (e.g. Aduah and Aabeyir, 2012).

Figure 4. 5. Harvested crop intermixed with trees in the study area (Source: field work, November 2014)

4.4.2. LULCC in the study area

Availability of adequate reference data provided a unique baseline for conducting LULCC map accuracy assessment in southwestern Burkina Faso. The observed changes of LULC in the study area were characterised by the increase in agricultural area and bare surface at the expense of natural vegetation (mixed vegetation and woodland). These dynamics attest to the ongoing deforestation in the southwest of Burkina Faso. Human activities are the main drivers of these changes in LULC, because in this region, where farming is characterised by low inputs such as fertilizers, farms are usually expanded and scattered across the landscape to increase yield (Boateng, 2013). Such a practice combined with population growth could explain the conversion of relatively huge areas of natural vegetation to agricultural area, as was observed in the period from 1999 to 2011. This conversion was also noticed elsewhere in the Sudan savannah (e.g. Braimoh, 2004; Ouedraogo *et al.*, 2010; Houessou *et al.*, 2013). Besides, in this region, fallowing practice has been reduced (Bado *et al.*, 2012) leading to excessive cultivation of the same land cover many years resulting in soil fertility loss, which favours the augmentation of bare surface. Furthermore, expansion of human settlement across the study area, as in Diebougou, Dano, Fara and Dissin, could also be a contributory factor to increasing bare surface at the expense of natural vegetation. Apart from agriculture and urban growth, other anthropogenic activities, such as wood harvesting, bushfire and mining, contribute to deforestation in the study area (Figure 4.6).

The loss of natural vegetation could have also been exacerbated by climate variability, which acts as a catalyst to the anthropogenic pressure. Indeed, in West Africa, IPCC (2007) reported that climate change has increased rainfall variability and the recurrence of extreme events such as droughts. The year 1999 was more humid in the southwest of Burkina Faso than 2006 and 2011, and it was characterised by floods in this part of the country (FAO, 1999). This further

buttress the observed increase in bare surface in 2011 compared to 2006 and 1999. In this region, a decrease in rainfall leads to an increase in barren land area (Ouedraogo *et al.*, 2014).

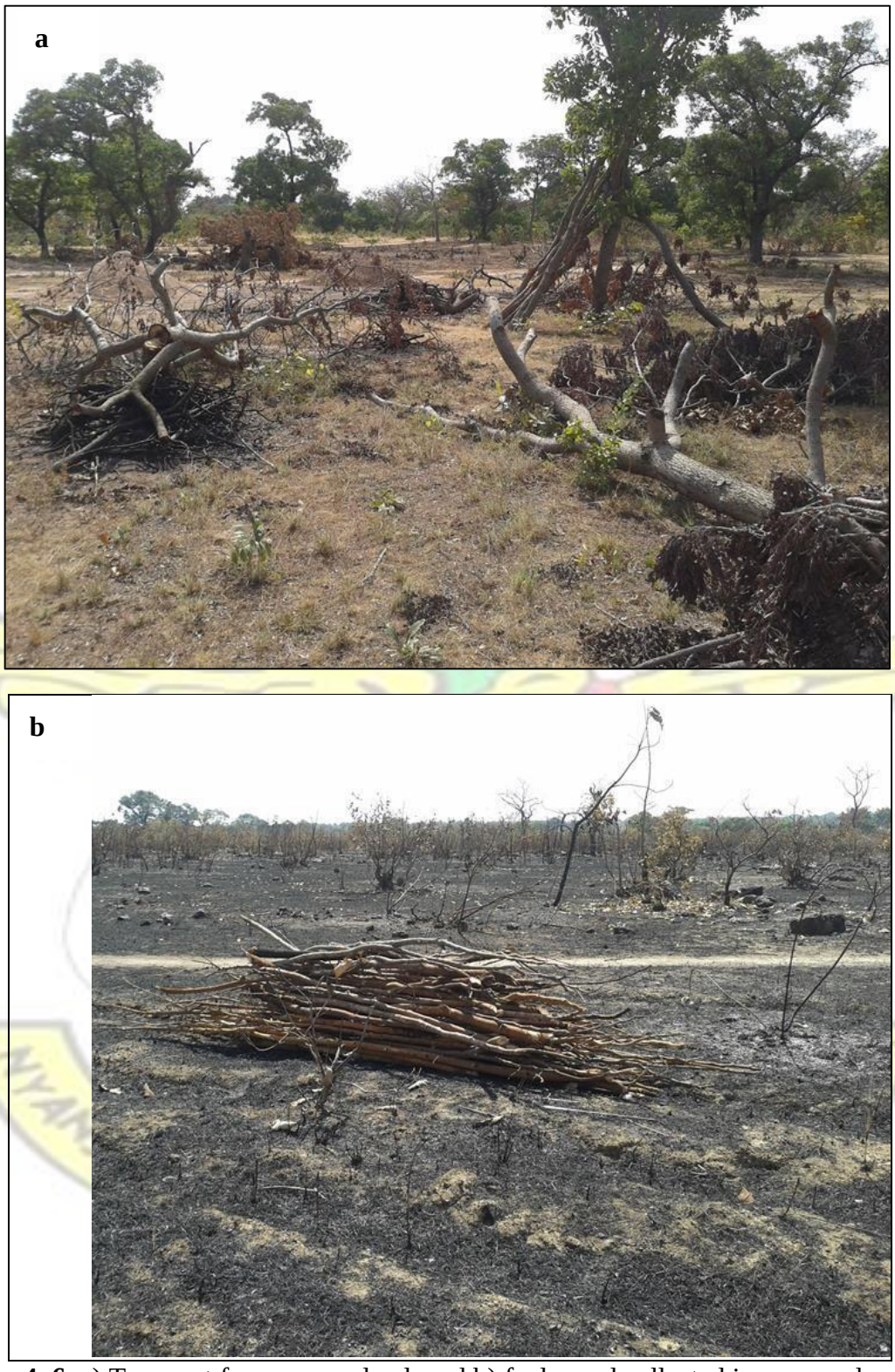

Figure 4. 6. a) Trees cut for new cropland; and b) fuel wood collected in an area devastated by bushfire (Source: field work, November 2014)

4.5. Conclusions

In the southwest of Burkina Faso, late rainy season image, used as input to a random forest classifier algorithm, produced higher overall accuracy than images from other periods. Multitemporal classification significantly improved mono-temporal classification of LULC in terms of overall and class-wise accuracies. The inclusion of ancillary data (e.g. elevation and geomorphology) was found beneficial for multi-temporal classifications and also enhances mono-temporal classification accuracies to the level of multi-temporal classifications. The results suggest that, at least for the heterogeneous Sudan savannah of southwest Burkina Faso, the inclusion of ancillary data reduces the data requirements for accurate LULC/LULCC maps, where atmospheric conditions are the limiting factors for the availability of multi-temporal data. However, at least a cloud-free satellite data set from late rainy season period should be available for successful mapping. This method needs to be tested in other regions not only within the Sudan savannah for a more generalised assessment of its performance and spatial transferability to LULC/LULCC maps in West Africa and beyond.

The study also found unsustainable LULC dynamics within the savannah of southwest Burkina Faso, which is mainly characterised by increasing agricultural area and bare surface and decreasing woodland and mixed vegetation. Human activities are supposed to be the main drivers of the observed changes in LULC, but rainfall variability probably also contributed to the observed LULCC. The loss of natural vegetation increases carbon emission into the atmosphere and could accelerate the process of land degradation in the study area.

Chapter 5: Rainfall Variability and its Relationship with Vegetation

This chapter is largely based on: Zoungrana, B. J-B., Conrad, C., Amekudzi, L.K., Thiel, M. and Da, E.D. 2015b. Land Use/Cover Response to Rainfall Variability: A Comparing Analysis between NDVI and EVI in the Southwest of Burkina Faso, *Climate*, 3: 63-77.

Abstract

A study was conducted in the southwest Burkina to determine the variability of rainfall and its relationship with vegetation dynamics. Monthly rainfall data (1981-2012) were collected from four rain gauges as well as three classified LULC maps for 1999, 2006 and 2011 which enabled the location of persistent LULC areas. Thereafter, MODIS 250 m monthly NDVI and EVI of plots of 750 × 750 m were extracted from 2001 to 2011 for persistent woodland, mixed vegetation, and agricultural area within 5 km radius around the rain gauges. Furthermore, Standardised Precipitation Index and correlation analysis were used to assess rainfall variability and the relationship between vegetation indices and rainfall indicators respectively. The results showed that in all the decades of the period 1981-2012, the study area was frequently under mild dry and mild wet rainfall events with intermittent occurrence of extreme events. A non-significant rising rainfall trend was predominant in the study area mainly in the periods 1981-2012 and 2001-2012. NDVI and EVI of all LULCs showed significant and strong positive correlation with the rainfall indicators. In general, NDVI was slightly more sensitive to rainfall than EVI, and constitutes a better proxy for vegetation. This finding agrees with some previous studies, but contrasting conclusions were also noted in literature.

5.1. Introduction

Climate change is intensifying rainfall variability over West Africa causing extreme events, such as droughts and floods (IPCC, 2007). This may have consequences on land surface vegetation in this zone since rainfall plays a key role in vegetation condition (Knauer *et al.*,

2014). Therefore, it is essential to assess and quantify the response of vegetation to rainfall variability.

Land Use/Covers (LULC) are of particular interest in assessing the relationship between vegetation and rainfall because their modification is a key factor in global environmental change (Lambin, 1997). For instance, Nightingale and Phinn (2003) found out strong relationship between rainfall and NDVI (Normalized Difference Vegetation Index) of five land cover types within South Australia and also noted significant positive correlation between rainfall and NDVI for cumulative rainfall over two to four months. Nicholson *et al.* (1990) also found the NDVI of different land cover types to be well correlated to rainfall in the Sahel and East Africa, and this correlation was better in the Sahel than in East Africa. In Central Asia, Gessner *et al.* (2013a) assessed vegetation sensitivity to rainfall anomalies based on time-series of NDVI and gridded rainfall datasets (GPCP) during the period 1982– 2006. The study found that the response of vegetation was strong for rainfall anomalies integrated over periods of two to four months, and there is a temporal lag between rainfall anomalies and vegetation activity for one to three months. Concerning the response timing of NDVI to rainfall, maximum correlation for lag of one month and three months cumulative rainfall have been reported by other researchers (e.g. Eklund, 1998; Richard and Poccard, 1998).

However, all these studies generally used long time series of NDVI and rainfall against LULC data derived for a single year (e.g. Gessner *et al.*, 2013a). These researches assumed no change in LULC during the time of observation. Applying this method in an area like West Africa's savannah where LULC change rapidly (Orekan, 2007) could cause bias in the analysis. Another common point of the previous studies (e.g. Nightingale and Phinn, 2003; Gaughan *et al.*, 2012; Gessner *et al.*, 2013) is the choice of NDVI as indicator of vegetation dynamics. Very few studies, like Bobee *et al.* (2012), tried other indices like leaf area index to study the response of vegetation to rainfall in northwest Senegal.

In savannah regions, NDVI signals were found to be limited to express vegetation response to rainfall (e.g. Farrar *et al.*, 1994; Liu and Huete, 1995). Huete *et al.* (1992) supported that this is due to spectral variability of background material, such as soil albedo, which causes nonlinearity between NDVI and vegetation cover. The Enhanced Vegetation Index (EVI) has been proposed by the MODIS Land Discipline Group to improve the quality of NDVI, by solving the problem of distortions in the reflected light due to atmospheric particles and the ground cover below the vegetation. In addition, EVI does not saturate rapidly as NDVI (Huete *et al.*, 2002).

However, in literature, comparison studies carried out between NDVI and EVI showed contrasting results. Son *et al.* (2014) noted that EVI-based models were slightly more accurate than those from NDVI-based models in rice crop yields estimation in the Mekong River Delta of Vietnam. On the other hand, Li *et al.* (2010) in a study carried out in Northern Hebei Province of China indicate that NDVI has a stronger correlation with field data of vegetation covers than EVI and so has obvious advantages for predicting natural vegetation coverage better than EVI. Wardlow *et al.* (2010) in turn found that for crop mapping EVI and NDVI produced equivalent results in Southwest Kansas. These contrasting conclusions raise the need for more investigation on the performance of NDVI and EVI especially relating to the relationship between vegetation and rainfall variability in West Africa's savannah where comparative studies are limited, and researches on both indices behaviour for different LULC types are still rare.

The present research will fill the above mentioned lacunas. The major goal of this study is to determine the inter-annual variability of rainfall and its relationship with vegetation dynamics in the southwest Burkina Faso. Specifically, the study aims to 1) assess rainfall inter-annual variability between 1981 and 2012 in the study area, 2) determine the relationship between

rainfall and vegetation dynamics for different LULC types in the study area, and 3) compare the sensitivity of NDVI and EVI to rainfall variability in the Southwest of Burkina Faso.

5.2. Methodology

5.2.1. Rainfall and LULC data collection and pre-processing

Rainfall data were collected from the Direction Générale de la Météorologie in Burkina Faso at monthly scale, from 1981 to 2012 and for the rain gauge stations of Dano, Diebougou, Dissin and Fara within the study area (see Figure 1). Time series of four indicators of rainfall (1 month lag rainfall, cumulated 2, 3 and 4 months rainfall) which were found to have better relation with vegetation dynamics (e.g. Nightingale and Phinn, 2003; Nicholson *et al.*,1990; Gessner *et al.,* 2013) were computed (Table 5.1). The four rainfall indicators data were test for normality distribution using Ryan-Joiner test with significance level of 0.05. The null hypothesis states that normality of the variable distribution in the population holds. The test produced p values of 0.10, 0.23, 0.12 and 0.18 for 1 month lag rainfall, cumulated 2, 3 and 4 months rainfall respectively. These values are greater than 0.05 meaning that the null hypothesis is accepted, and the data are normally distributed.

In addition, LULC maps of 1999, 2006 and 2011 were collected from chapter 4 and resampled to 250 m to match with the vegetation indices images using majority rules (i.e. the dominant LULC among the gathered 30 m x30 m pixels is assigned to the new 250 m x 250 m pixel). Change detection, performed in ArcGIS 10.1, enabled deriving persistent LULC areas according to the three dates. The aim was to focus the analysis on stable LULC areas that remained the same in 1999, 2006 and 2011. The vegetated LULC types, which are woodland, mixed vegetation and agricultural area, were considered in the analysis.

Table 5. 1. Indicators characterising rainfall variability in the study

Indicators	Description
Amount of rainfall (lag 1 month)	1 month lag rainfall

Cumulated 2 months rainfall	Sum of rainfall of current and previous 1 month
Cumulated 3 months rainfall	Sum of rainfall of current and previous 2months
Cumulated 4 months rainfall	Sum of rainfall of current and previous 3months

5.2.2. Vegetation indices acquisition and pre-processing

MODIS Terra MOD13Q1 product (2001-2011) was collected. In addition to the spectral bands, it has two vegetation indices which are EVI and NDVI. Both indices had a spatial resolution of 250 m. MODIS is on aboard of Terra and Aqua satellites (Xie *et al.,* 2008). The MODIS Terra MOD13Q1 product was downloaded from the United States Geological Survey (USGS) MRTWeb interface (USGS, 2014) and reprojected to WGS 84 zone 30. The software TiSeG (Time-Series Generator) developed by Colditz *et al.* (2008) was used firstly to assess the quality of the MODIS product and, secondly to correct invalid data and fill gaps by linear interpolation. Among other settings of TiSeG, the quality setting UI5-CS (PerfectIntermediate, no Cloud and no Shadow) was found giving results close to undisturbed situation and, therefore, was applied in this analysis.

Mean monthly NDVI and EVI time series were extracted for areas dominated by persistent LULC (for each type) and within plots of 750 x 750 m^2 (3 x 3 window). For each of the four rain gauges of the study area (Figure 3.1), three plots of woodland, mixed vegetation and agricultural area were drawn inside a radius of 5 km around each rain gauge. In all, 12 plots were located in the study area.

The distributions of the extracted indices data were assessed for normality using Ryan-Joiner test with significance level of 0.05. The test produced p-values greater than 0.05 for all NDVI and EVI samples, which indicates that the null hypothesis is accepted, and NDVI and EVI data were normally distributed.

The computation of NDVI and EVI is described in Equations 5.1 and 5.2 respectively.

$$NDVI = \frac{NIR - RED}{NIR + RED} \quad (5.1)$$

where, *NIR* and *RED* are respectively the near infrared and the red reflectance. NDVI generally is chlorophyll sensitive (Pettorelli *et al.*, 2005).

$$EVI = G * \frac{(NIR - RED)}{(NIR + C_1 * RED - C_2 * BLUE + L)} \quad (5.2)$$

where *NIR*, *RED* and *BLUE* are respectively near infrared, red and blue reflectance. L is the canopy background or soil adjustment factor. G is the gain factor. C1 and C2 are the coefficients of the aerosol resistance. In the selected Terra MOD13Q1 product the coefficient values are; L=1, C_1= 6, C_2 = 7.5, and G = 2.5. The EVI products are expected to improve sensitivity in high biomass area and reduce atmospheric and canopy background effect on vegetation signal. Therefore EVI is more responsive to canopy structural variations, including leaf area index, canopy type and architecture (Gao *et al.*, 2000; Pettorelli *et al.*, 2005).

5.2.3. Rainfall variability analysis

The Standardised Precipitation Index (SPI) was applied to assess rainfall variability. It is a simple and straightforward method since precipitation is the only meteorological variable used (Kasei, *et al.*, 2010). SPI in this research was calculated using the arithmetic average and the standard deviation of precipitation series of the period 1981-2012. For a given rainfall time series data, SPI was computed from Equation 5.3.

$$\text{SPI} = \frac{(\text{X} - \overline{\text{X}})}{S_X} \quad (5.3)$$

Where $\overline{X}$ is the average and S_X the standard deviation of the precipitation series. Negative values of SPI indicate rainfall deficits (dry events), while positive values stand for surplus of rainfall (wet events). McKee *et al.* (1993) produced a classification of the range of SPI values (Table 5.2) that has been adopted in this study.

Table 5. 2. SPI categories used in this study, modified from McKee *et al.* (1993)

SPI values	Category of intensity	Rainfall events
2 and more	Extremely wet	Extreme wet event
1.50 to 1.99	Very wet	
1 to 1.49	Moderately wet	Other event
0 to 0.99	Mildly wet	
0 to -0.99	Mildly dry	
-1 to -1.49	Moderately dry	
-1.5 to -1.99	Severely dry	Extreme dry event
-2 and less	Extremely dry	

5.2.4. Rainfall trend assessment

The non-parametric Kendall's tau-b test was performed for four periods of observation: 19812012, 1981-1991, 1991-2001 and 2001-2012. The Kendall's tau-b test does not require data to be normally distributed. Additionaly, it overcomes problem due to data skew (Smith, 2000) and is less sensitive to outliers (Hadgu *et al.*, 2013). It measures the strength of the relationship between two variables X and Y. A negative correlation indicates that when X is increasing then Y is decreasing. The Kendall's tau-b (τ_B) is computed by Equation 5.4.

$$\tau_B = \frac{(Number\ of\ concordant\ pairs) - (Number\ of\ discordant\ pairs)}{\sqrt{N_1}\ X\ \sqrt{N_2}} \qquad (5.4)$$

Where, N_1 is the number of data pairs not tied in a target feature, and N_2 the number of data pairs not tied in another target feature.

5.2.5. Analysis of LULC relationship with rainfall

Linear correlation analysis, focusing on the period 2001-2011, was performed between each LULC indices (NDVI and EVI) and the different indicators of rainfall (1 month lag rainfall, cumulated 2, 3 and 4 months rainfall) to assess their relationship. The coefficient of Pearson enabled measuring the magnitude of each correlation. In total 48 correlations have been

computed and the performance of each vegetation index was then investigated. The formula of coefficient of Pearson (r) is described by Equation 5.5.

$$r = \frac{\sum_{i=1}^{n}(X_i - \bar{X})(Y_i - \bar{Y})}{\sqrt{\sum_{i}^{n}(X_i - \bar{X})^2}\sqrt{\sum_{i}^{n}(Y_i - \bar{Y})^2}} \quad (5.5)$$

Where X_i and Y_i are individual observations of variables X and Y respectively. $\bar{X}$ and $\bar{Y}$ are the mean of X and Y. The values of r range from -1 to +1, and values of +1 and -1 indicate that the variables are perfectly linear related by an increasing relationship and a decreasing relationship respectively. However, Pearson's correlation coefficient requires a bivariate normal distribution of the two variables; this condition was met in this study as showed in section 5.2.2.

5.3. Results

5.3.1. Rainfall variability and trend between 1981 and 2011

The variability of rainfall is expressed by the SPI values in Figure 5.1. The red bars indicate deficit of water, and the blue ones surplus of water. Rainfall fluctuations in the four stations highlight patterns of dry and wet periods with different intensities as mentioned in Table 5.2 in section 5.2.3. Table 5.3 indicates that in the period 1981-2012 and during all the decades, mild dry and mild wet years were more frequent in all the stations. Extreme rainfall events have occurred by intermittence during the period 1981-2012 and were characterised by extremely or very wet years and extremely or severely dry years. Extreme dry rainfall event was observed in the stations of Dano (1983, 1984 and 2005), Dissin (1990 and 1992), Diebougou (1993 and 2001) and Fara (1983, 1992 and 2002). Extreme wet rainfall events have been recorded in Dano (1986, 2012), Dissin (1982, 2008 and 2010), Diebougou (1991 and 1994) and Fara (1994, 1999 and 2010).

2.5 3

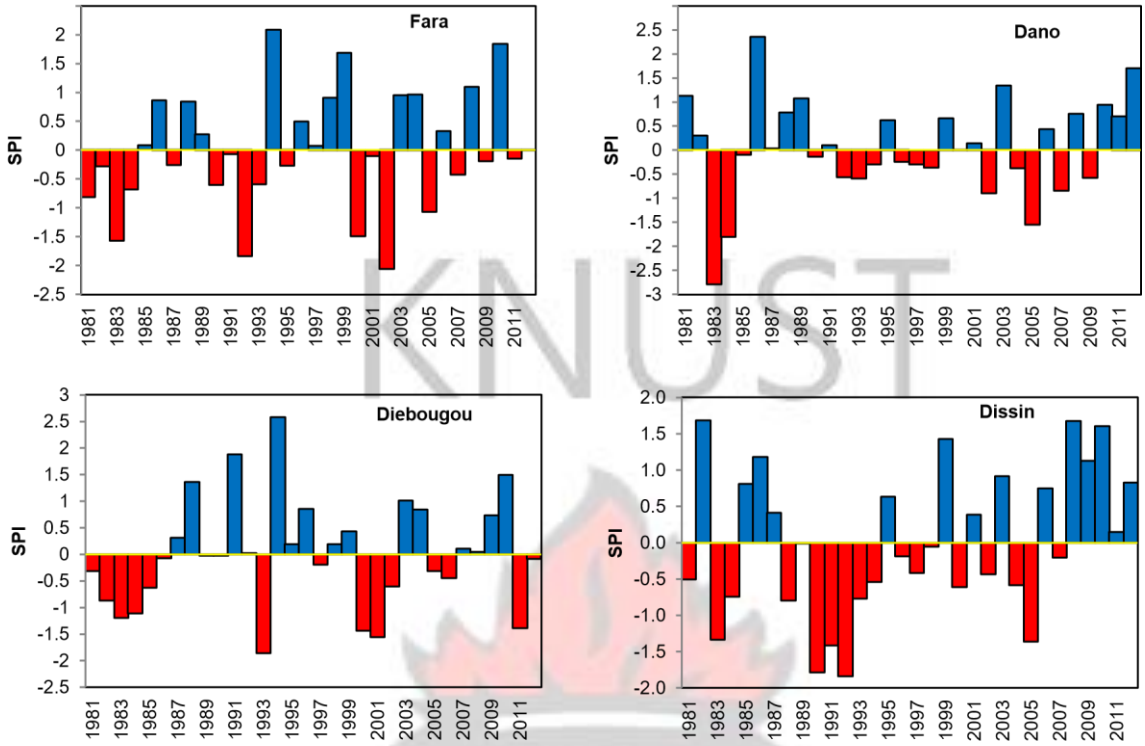

Figure 5. 1. Rainfall variability expressed by SPI values in the study area (1981-2012) The results of the Kendall tau-b test highlight particularly a non-significant rising trend of rainfall in all the stations in the period 1981-2012 and 2001-2012 (p value of 0.05) (Table 5.4). A non-significant increasing trend was also dominating in the periods 1981-1991 and 1991-2001 unless in Dissin and Diebougou respectively where both decades recorded a nonsignificant decreasing trend of rainfall.

Table 5. 3. . Frequency of dry and wet years per period in the four stations

	Dano				Fara				Diebougou				Dissin			
	1981-1991	1991-2001	2001-2012	1981-2012	1981-1991	1991-2001	2001-2012	1981-2012	1981-1991	1991-2001	2001-2012	1981-2012	1981-1991	1991-2001	2001-2012	1981-2012
Extremely wet	1	0	0	1	0	1	0	1	0	1	0	1	0	0	0	0
Very wet	0	0	1	1	0	1	1	2	0	1	0	1	1	0	2	3
Moderately wet	2	0	1	3	0	0	1	1	1	0	1	2	1	1	1	3
Mildly wet	**3**	**4**	**5**	**12**	**4**	**3**	**3**	**10**	**1**	**5**	**5**	**11**	**2**	**1**	**5**	**8**
Mildly dry	**2**	**6**	**4**	**12**	**5**	**3**	**5**	**13**	**6**	**1**	**4**	**11**	**4**	**6**	**3**	**13**
Moderately dry	0	0	0	0	0	1	1	2	2	1	1	4	1	1	1	3
Severely dry	1	0	1	2	1	1	0	2	0	1	1	2	1	1	0	2
Extremely dry	1	0	0	1	0	0	1	1	0	0	0	0	0	0	0	0

Table 5. 4. Rainfall trend in the four stations

Dano	Correlation Sig. (2-tailed)	0.815	0.186	0.131	0.795
Dissin	Correlation Sig. (2-tailed)	-0.345 0.139	0.527 0.024	0.273 0.217	0.214 0.086
Diebougou	Correlation Sig. (2-tailed)	0.636 0.006	-0.273 0.243	0.152 0.493	0.129 0.299
Fara	Correlation Sig. (2-tailed)	0.345 0.139	0.164 0.484	0.212 0.337	0.198 0.112
	Kendall tau-b test	**1981-1991**	**1991-2001**	**2001-2012**	**1981-2012**
		0.055	0.309	0.333	0.032

5.3.2. Correlation analysis between LULC and the indicators of rainfall

5.3.2.1. NDVI as LULC indicator

The NDVI of the LULC types and the rainfall indicators have strong positive correlation with Pearson's coefficient ranges from 0.798 to 0.945 (Table 5.5) and p value of 0.01. Table 5.5 revealed that most often NDVI was more sensitive to the variability of three months cumulated rainfall and less to one month lag rainfall. Table 5.5 also shows the response magnitude between and within LULC types. In the four stations, none LULC type has shown a noticeable domination over others. Furthermore, the comparisons of the four stations show a difference in coefficient of Pearson within the same LULC class.

Table 5. 5. Correlation between NDVI of LULC types and rainfall variability indicators

Station	**LULC**	**1 month Lag rainfall**	**Cum. 2 Months rainfall**	**Cum. 3 Months rainfall**	**Cum. 4 Months rainfall**
Dano	Agricultural area	0.861 0.849	0.848 **0.937**	0.934 0.917	**0.943**
	Mixed vegetation				0.825
	Woodland	0.864	0.893	**0.945**	0.917
Fara	Agricultural area	0.896	0.921	**0.944**	0.880
	Mixed vegetation	0.860	0.911	**0.918**	0.846
	Woodland	0.849	0.903	**0.919**	0.850
Diebougou	Agricultural area	0.843	0.873	**0.929**	0.899
	Mixed vegetation	0.829	**0.909**	0.898	0.798

	Woodland	0.824	0.869	**0.913**	0.871
Dissin	Agricultural area	0.855	0.873	**0.911**	0.878
	Mixed vegetation	0.859	0.896	**0.912**	0.858
	Woodland	0.875	0.891	**0.924**	0.877

Correlation is significant at the 0.01 level.

5.3.2.2. EVI as LULC indicator and comparative analysis with NDVI

The analysis with EVI showed significant and strong positive correlations with rainfall indicators (Table 5.6). The Pearson's coefficient for EVI is in the range of 0.768–0.946. This finding supports the good relationship noted in literature between the four rainfall indicators and vegetation indices. In this case also, none LULC type significantly dominated in the relation with rainfall indicators. Similar to the NDVI results, the strength of correlations between EVI and rainfall indicators is different within each LULC type.

There are also discrepancies in the results. Unlike NDVI, the EVI of LULC has stronger correlation with cumulated two months rainfall or cumulated three months rainfall, while lag of one month rainfall as well as four months cumulated rainfall had the lowest influence on EVI.The difference between NDVI and EVI was also noticed in the magnitude of their response to the rainfall indicators. Table 5.7 shows that the EVI often responded stronger to 2 months cumulated precipitation than NDVI. For the three other rainfall indicators, NDVI has better results. Generally, the magnitude of the correlations with EVI is often low compared to NDVI. This is illustrated by Figure 5.2 where 66.7% of the correlations were stronger with NDVI against 29.2% with EVI, and 4.1% of the correlations had the same coefficient of Pearson with both indices. For all the LULC types NDVI was found performing better than EVI mostly for mixed vegetation and woodland (Figure 5.3). The difference between the Pearson's coefficient values of both vegetation indices was insignificant in the four stations, which means that their performances with rainfall are not so much different.

It is also observed that the two indices showed opposite reaction to the number of cumulated month rainfall (from two to four months). NDVI performs better when the number of cumulated month of rainfall increases, whereas the performance of EVI rather decreases (Table 5.7). The difference noted with EVI and NDVI shows that the LULC reaction to rainfall in savannah areas varies according to the type of vegetation index and to the rainfall indicators.

Table 5. 6. Correlation between EVI of LULC types and rainfall variability indicators

Station	LULC	1 month Lag rainfall	Cum. 2 Months rainfall	Cum. 3 Months rainfall	Cum. 4 Months rainfall
figureDano	Agricultural area	0.872	0.887	**0.946** 0.893	0.922
	Mixed vegetation	0.830	**0.939**		0.783
	Woodland	0.859	0.904	**0.942**	0.890
Fara	Agricultural area	0.856	**0.907**	**0.907**	0.832
	Mixed vegetation	0.836	**0.910**	0.897	0.812
	Woodland	0.796	**0.904**	0.876	0.778
Diebougou	Agricultural area	0.859	0.897	**0.932**	0.877
	Mixed vegetation	0.828	**0.927**	0.889	0.768
	Woodland	0.844	0.903	**0.925**	0.857
Dissin	Agricultural area	0.844	0.881	**0.901**	0.844
	Mixed vegetation	0.831	**0.896**	0.890	0.811
	Woodland	0.860	0.908	**0.916**	0.840

Correlation is significant at the 0.01 level

Table 5. 7. Best performing index according to LULCs and rainfall indicators

Station	LULC	1 month Lag rainfall	Cum. 2 Months rainfall	Cum. 3 Months rainfall	Cum. 4 Months rainfall
Dano	Agricultural area	EVI	EVI	EVI NDVI	NDVI
	Mixed vegetation	NDVI	EVI		NDVI
	Woodland	NDVI	EVI	NDVI	NDVI
Fara	Agricultural area	NDVI	NDVI	NDVI	NDVI
	Mixed vegetation	NDVI	NDVI	NDVI	NDVI
	Woodland	NDVI	Equal	NDVI	NDVI
Diebougou	Agricultural area	EVI	EVI	EVI NDVI	NDVI
	Mixed vegetation	NDVI	EVI		NDVI
	Woodland	EVI	EVI	EVI	NDVI

Dissin	Agricultural area	NDVI	EVI Equal	NDVI	NDVI
	Mixed vegetation	NDVI		NDVI	NDVI
	Woodland	NDVI	EVI	NDVI	NDVI

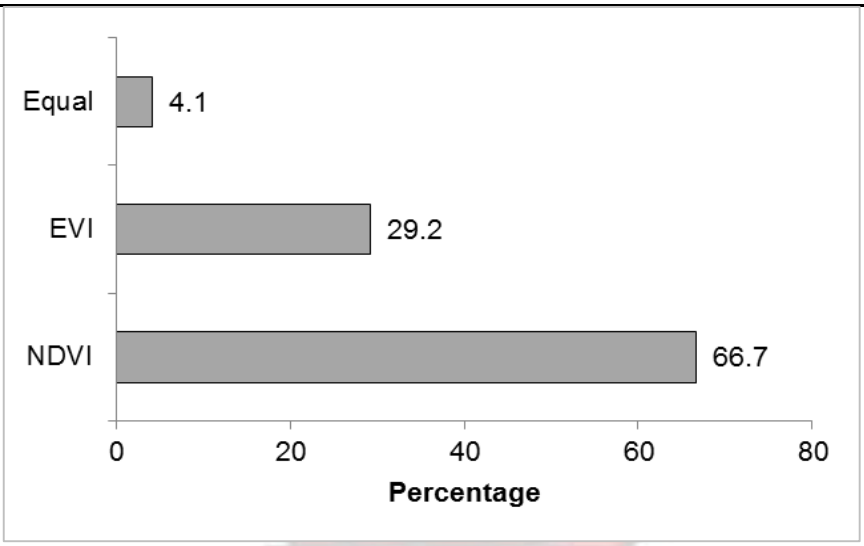

Figure 5. 2. Global best performance between NDVI and EVI

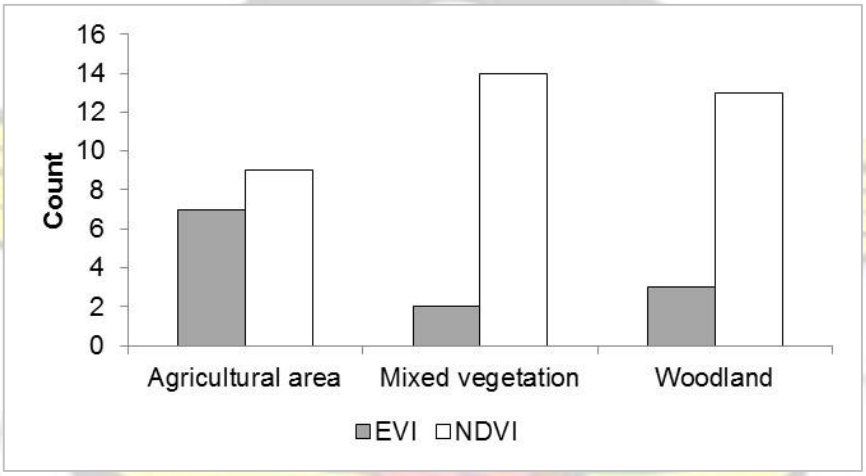

Figure 5. 3. NDVI and EVI performance according to LULC

5.4. Discussion

5.4.1. Rainfall variability

The results showed that between 1981 and 2012 the study area faced variabilities of rainfall standing from extreme deficit to extreme surplus of rainfall. However, during the period 1981-2012, the study area was frequently under near normal rainfall conditions highlighted by the predominance of mild dry and mild wet years. The non-significant rising rainfall trend observed in the study area in the periods 1981-2012 and 2001-2012 is in agreement with the

work of Lucio *et al.* (2012). They noticed an increase in rainfall during the three decades of the period 1981-2010 in West Africa and found the decade 2001-2010 to be the most humid.

This wet condition of the decade 2001-2010 is also supported by Bamba *et al.* (2015). In addition, SP/CONEDD (2011) also observed a non-significant rising trend of rainfall in the study region between 1980 and 2010.

5.4.2. Relationship between rainfall and vegetation dynamics

The present study found a high correlation between rainfall and both vegetation indices (NDVI and EVI) for each LULC. This indicates a strong relationship between rainfall and vegetation dynamics in the study area. Such a result confirms previous studies that found the relationship between rainfall and vegetation dynamics to be strong in West Africa (e.g. Nicholson *et al.*, 1990; Morten and Fensholt, 1999; Klein and Roehrig, 2006; Bamba *et al.* 2015) and in elsewhere (e.g. Davenport and Nicholson, 1993; Nightingale and Phinn, 2003; Gessner *et al.*, 2013a). For both vegetation indices, the observed difference of correlations strength within each LULC type is likely due to several factors, such as difference in soil moisture (Farrar *et al.*, 1994), plant community (Méndez-Barroso *et al.*, 2009), anthropogenic activities and vegetation phenology (Sims *et al.*, 2006; Zhao et *al.*, 2009; Jamali *et al.*, 2011). In the case of EVI, in addition to the aforementioned factors, topography may also cause difference in the response, for elevation controls EVI dynamics (Méndez-Barroso *et al.*, 2009). Although NDVI and EVI agreed on some aspects of the relation rainfall-vegetation dynamics (e.g. Positive strong relationship), opposite behaviour was noted. While NDVI performs better with the increasing number of cumulated month of rainfall, the performance of EVI rather decreases (Table 5.7). This situation might be due to the time lag of response of each vegetation index; indeed, NDVI has longer time lag of response to rainfall than EVI in the sub-Saharan savannah area (Jamali *et al.*, 2011). However, more investigations are necessary for better

clarification. In general, NDVI was more sensitive to rainfall than EVI, although the difference between the Pearson's coefficient values of both indices was insignificant. This finding disagrees with studies by Farrar *et al*. (1994) and Liu and Huete (1995), which found that NDVI signals were limited in savannah zone due to the effects of soil background material and exposure. The present work has demonstrated that those disturbances do not so much influence the performance of the signals of NDVI to express the response of vegetation to rainfall variability in the Sudan savannah of the southwest Burkina Faso. This result confirms the work by Li *et al.* (2010), which found that NDVI is a better proxy for vegetation cover than EVI in Northern Hebei Province of China.

Some possible factors that could explain the performance of NDVI have been discussed elsewhere. As mentioned by Li *et al.* (2010), estimating vegetation dynamics from NDVI or EVI is not a straightforward achievement. Although in this work quality assessment was done on the MOD13Q1 product to eliminate noises, other factors, such as plant community (Méndez-Barroso *et al.*, 2009), anthropogenic perturbation, vegetation phenology and sensor conditions (Lu *et al.*, 2003; Sims *et al.*, 2006; Zhao et *al.*, 2009), may influence the temporal dynamics of the two indices and their response to rainfall. NDVI and EVI are strongly correlated for all LULC types in the study area (Figure 5.4). This confirms that the problem of NDVI saturation is not quite pertinent in the study area and thus does not influence the reaction of the index, which can explain its performance. In addition, the sensitivity of NDVI and EVI to soil moisture, which was not investigated here, may also explain the discrepancies between them.

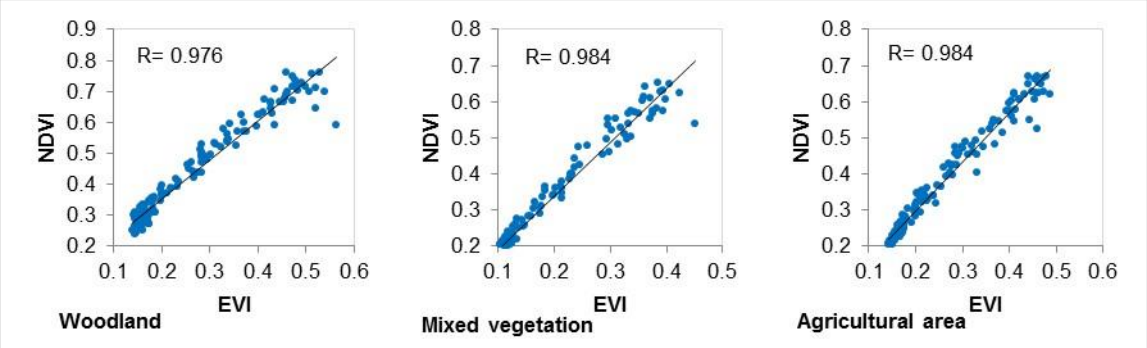

Figure 5. 4. Correlation between NDVI and EVI for different LULC

5.5. Conclusion

A study to determine rainfall variability and the relationship rainfall-vegetation dynamics has been carried out in the savannah biome of the Southwest Burkina Faso. The study revealed that in all the decades of the period 1981-2012, the study area was dominated by near normal rainfall conditions with intermittent occurrence of extreme events. A non-significant rising rainfall trend characterised the study area mainly in the periods 1981-2012 and 2001-2012. LULC vegetation dynamics were found strongly correlated with rainfall. Some similarities were noticed in the response of NDVI and EVI to rainfall, but discrepancies were also found and mainly seen on the response magnitude and the influence of the rainfall indicators. Between both indices, and for all LULCs, NDVI was more sensitive to rainfall variability than EVI, but the difference between the Pearson's coefficient values of both indices was insignificant. As this study focused on only a selected area on a local scale, further analyses should target regional scale in order to confirm the results obtained. Nevertheless, the study reveals important findings that will trigger further investigations on EVI and NDVI with respect to their accuracy in estimating vegetation temporal dynamics. For example, a study need to be conducted to understand the difference in response magnitude between both indices by determining the contributing factors.

Chapter 6: Trends in Vegetation Dynamics in the Study Area

This chapter is based on objective 3, and it is a manuscript prepared for submission.

Abstract

A study was conducted in the savannah of the southwest of Burkina Faso firstly to assess trends in vegetation dynamics at local scale and determine their distribution into LULC classes as well as the association between vegetation trends and changes in LULC. Secondly the study aimed to find out the main drivers of the detected trends and determine local population perception. An approach integrating temporal persistence analysis and MannKendall trend test was applied to detect trends in MODIS NDVI data (2000-2013) used as indicator of vegetation productivity. The detected trends were overlaid with LULC and LULCC maps to determine their distribution. Random forest modelling enabled to find out the main drivers of vegetation trends among anthropogenic and biophysical variables. Household chiefs were surveyed to determine their perception of vegetation dynamics in the period 2000-2013. The results revealed that the study area was dominated by inconsistent trends of vegetation in the period 2000-2013. Decreasing trajectory was prominent among the detected trends and was particularly found in agriculture areas and also in areas with high and medium human impacts, while greening trend was observed mainly in woodland and areas less affected by human pressure making human footprint to be the main driver as confirmed by random forest modelling. Association was found between increasing vegetation trend and stable natural vegetation and between decreasing trend and natural vegetation loss. Local population perception of vegetation dynamics agreed with the results of the remote sensing (RS) processing, which gives confidence to the RS method employed in this research.

6.1. Introduction

Vegetation is a key element in the interaction of the geosphere, biosphere and atmosphere (Mennis, 2001), and any change in vegetation cover can have an impact on the environment at any scale (Amri *et al.,* 2011). Assessing vegetation dynamics is therefore crucial for a better understanding of the environmental dynamics and for ensuring bases of a sustainable development particularly in regions where natural vegetation is confronted with anthropogenic pressures and climate change impacts like West Africa. Studies have been carried out on West Africa's vegetation dynamics based on remote sensing data (e.g. Herrmann *et al.,* 2005a; Fensholt and Rasmussen, 2011; Traore *et al.*, 2014). However, the direction of vegetation trend in this region is subjected to debate (Knauer *et al.,* 2014).

Contradictory trend directions were found in literature across West Africa. Although studies (e.g. Olsson *et al.*, 2005; Leroux *et al.*, 2014; Traore *et al.*, 2014) observed dominant increasing trend of vegetation, others supported the theory that shows a dynamics toward degradation (e.g. Hountondji *et al*., 2005 and 2006).

Many of the previous studies (e.g. Herrmann *et al.,* 2005a; Olsson *et al.,* 2005; Jamali *et al.,* 2014) were conducted at large geographical scale using coarse satellite images (e.g. NOAA/AVHRR NDVI of 8 km) and applying methods (e.g. Linear regression) that are affected by vegetation inter-annual fluctuation. Indeed, vegetation year-to-year variations have high content of erratic fluctuations (Simoniello *et al.,* 2008). In addition, vegetation dynamics in areas like the Sudan savannah is still poorly understood (Compaore, 2006) and need further researches (Nacoulma *et al.,* 2011). For this purpose, multiplication of local studies is needed to come out with reliable results on vegetation trend in this part of West Africa (Knauer *et al.,* 2014).

The use of 250 m MODIS data may contribute to better analyse vegetation dynamics in this region. In West Africa, MODIS vegetation indices were found to be better correlated to in situ

measured vegetation indices as compared to AVHRR NDVI (Fensholt and Sandholt, 2005) and SPOT VGT (Fensholt *et al.,* 2006). In this study, one recent methodological improvement of time series analysis, the so-called temporal persistence analysis (Lanfredi *et al.,* 2004), is implemented in the savannah of southwest Burkina Faso. This method focuses on the analysis of the persistence of vegetation trends that is essential for understanding vegetation dynamics face to human activities and/or natural stresses (Gunderson, 2000). In contrast to conventional time series analysis, the temporal persistence analysis focuses on identifying changes in NDVI trends as opposed to absolute values (Harris et al., 2014). This limits the effect of the erratic inter-annual variations of vegetation and also reduces the influence of the data initial period on the trend assessment, as noticed for instance in linear trend (Wessels *et al.*, 2012; Harris *et al.,* 2014). The temporal persistence analysis was successfully implemented in elsewhere with AVHRR NDVI (e.g. Simoniello *et al.*, 2008; Harris *et al.*, 2014), but not yet in West Africa, and also not with MODIS data. However, this method does not measure the significance of trends. To overcome that, the non-parametric Mann Kendall's trend test, which has been already applied in West Africa (e.g. Traore *et al.,* 2014), can be associated to detect significant trends.

The main objective of this study is to assess trends in vegetation dynamics at local scale in the Sudan savannah of southwest Burkina Faso. Particularly, it aims to 1) integrate temporal persistence analysis and Mann-Kendall's test to detect trends in MODIS vegetation index (2000-2013) used as indicator of vegetation productivity, 2) determine the distribution of vegetation trends into LULC types as well as the associations between vegetation trends and LULCC classes, 3) find out the main drivers of the detected trends of vegetation among anthropogenic and biophysical variables using Random Forest modelling approach, and 4) determine local population perception of vegetation trend.

6.2. Methodology

6.2.1. Remotely sensed vegetation data collection and pre-processing

MODIS Terra MOD13Q1 product (2000 to 2013) was downloaded from the United States Geological Survey (USGS) MRTWeb interface (USGS, 2014). The data were reprojected to UTM WGS 84 zone 30 by using MRT (Modis reprojection Tools) and resized to the outline of the study area. Among the vegetation indices of MODIS, 16-days composite NDVI was selected as proxy of vegetation productivity, since it performs better with rainfall than EVI in the study area (see chapter 5), and it is well correlated with in situ measured vegetation cover in savannah zones (Fensholt and Sandholt, 2005; Li *et al.*, 2010). Besides, NDVI is strongly related to biophysical variables that control vegetation productivity, such as the Leaf Area Index (LAI), the fraction of photo-synthetically-active radiation absorbed by vegetation and Net Primary Productivity (NPP) (Traore *et al.*, 2014). The advantage of using MODIS data is that it provides pixel-level data quality indicators which can be employed to filter time series and interpolate invalid data with statistical or contextual methodologies (Colditz *et al.*, 2011). The software TiSeG deals with those data quality indicators (Colditz *et al.*, 2008) and, therefore, it was used to assess NDVI data quality, correct invalid data and fill gaps based on linear interpolation. Interpolation does not modify the data and simply calculates the intermediate values required to fill gaps (Garza-Gisholt, 2014). As in chapter 5, the data quality setting UI5-CS of TiSeG was applied because of the closeness of its results with undisturbed situation. The NDVI data of the year 2000 were available since mid-February. Therefore, to be consistent and include the year 2000 in the trend assessment, time series of annual NDVI average (mid-February-December) was produced from 2000 to 2013 to assess per-pixel vegetation dynamics trends.

6.2.2. Biophysical data

LULC map of 2011 and LULCC map of the period 1999-2011 were collected from chapter 4. Elevation data were obtained from ASTER Digital Elevation Model (DEM) version 2 at a spatial resolution of 30 m. Mean annual rainfall was obtained from WorldClim at about 1 km spatial resolution. Vector layers for geomorphological units and soil types (1:500,000) were collected from BUNASOLS and rasterised. All those data were projected to UTM WGS 84 zone 30 and resampled to 250 m in ArcGIS 10.1 to match the pixels of MODIS NDVI. Table 6.1 gives further details on the data set.

Table 6. 1. Biophysical data used in this study

Ancillary data	Source	Description	Resolution/scale	Resampling resolution
Elevation	ASTER	Height	30 m	250 m
LULC	Landsat	LULC classes	30 m	250 m
LULCC	Landsat	LULCC classes	30 m	250 m
Soil	BUNASOLS-BF	Soil types	1/500,000	250 m
Geomorphology	BUNASOLS-BF	Geomorphological units	1/500,000	250 m
Rainfall	WorldClim	Mean annual rainfall	1 km	250 m

6.2.3. Human footprint map

Human footprint map (Sanderson *et al.,* 2002) was derived to estimate spatially human influence on vegetation in the study area. For that purpose, and due to the limitation of data, three types of data were considered as proxies for human pressures: population density, land transformation and accessibility. Based on localities population size, an isodensity map was produced with Kernel density method to estimate the distribution of population density in the study area. Kernel density estimation is a non-parametric interpolation technique, and therefore, it does not request normality in data distribution (Zheng and Xue, 2009), and it is appropriate for individual point locations (Bowman and Azzalini, 1997). Agricultural area density was used as land transformation activity, since agriculture is the principal livelihood activity in the study region. Its computation required fractional cover estimation by

aggregating the pixels of the 2011 LULC map from 30 m to 250 m. That is, for each 250 m x 250 m pixel, the percentage of agricultural area was derived. Accessibility consisted of distance to locality, distance to road and distance to river which were derived based on vector layers obtained from the Geographical Institute of Burkina Faso. In total, five data (population isodensity, agricultural area density, distance to locality, distance to road and distance to river) were gathered for mapping human footprint. All the maps were classified into the same range of category using natural grouping of the data. Based on literature (e.g. Sanderson *et al.*, 2002) and the reality of the study region, a weight was attributed to each map (Table 6.2) and their sum yielded the human footprint map (Figure 6.1).

Table 6. 2. Data used for human footprint mapping

Type of Data	Data	weight	Resolution
Population density	Isodensity map	5	250 m
Land transformation	Agricultural area density	4	250 m
Accessibility	Distance to locality	3	250 m
	Distance to road	2	250 m
	Distance to river	1	250 m

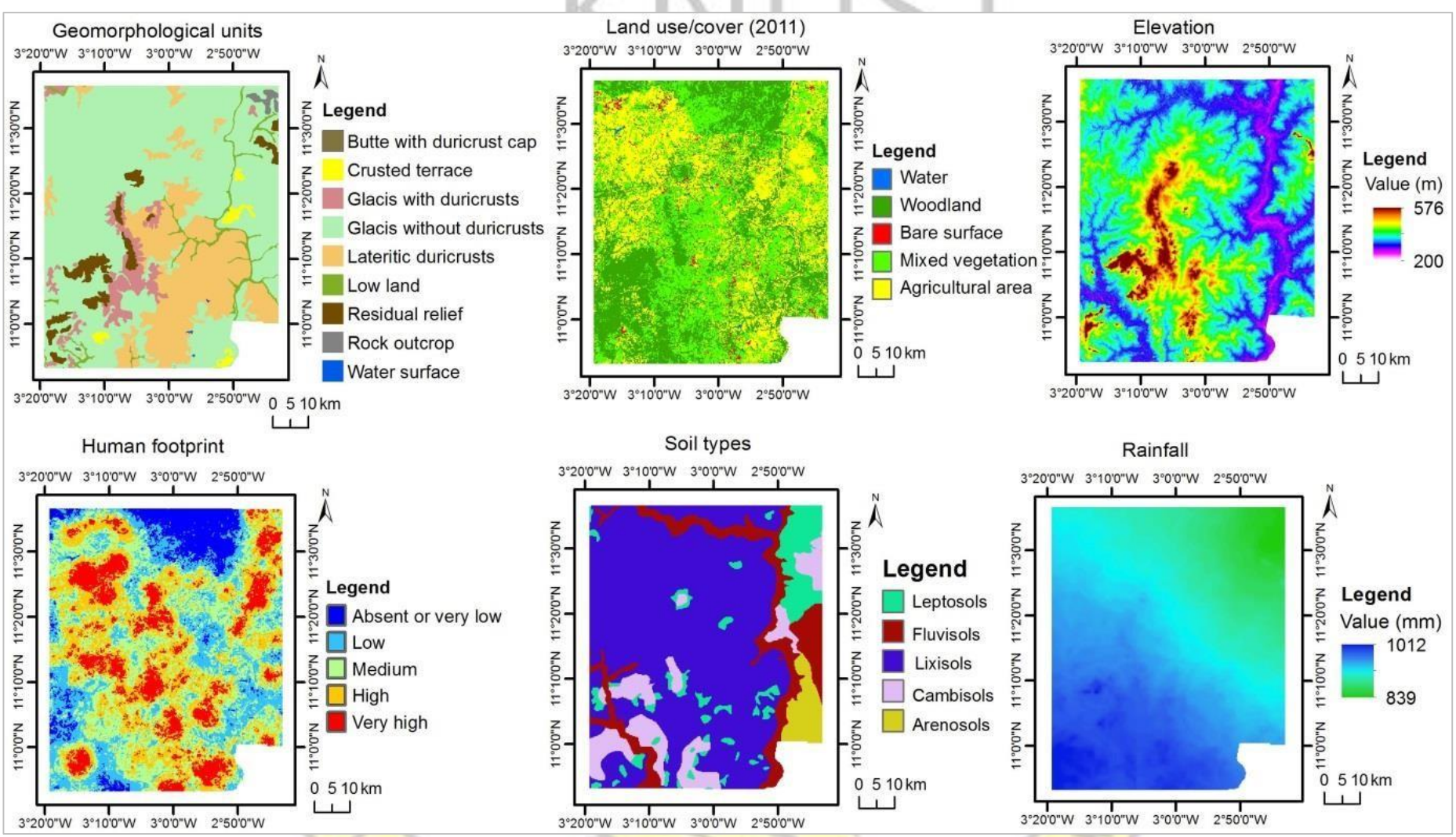

Figure 6. 1. Predictors used in Random Forest modelling

6.2.4. Vegetation trends analysis

6.2.4.1. Temporal persistent analysis

The first step of the trend assessment was to perform a temporal persistent analysis of NDVI trends. This method actually evaluates the tendency of vegetation to persist in increasing or decreasing since a reference period so as to characterise its response to disturbances (Simoniello *et al.*, 2008). The description of the method is based on Lanfredi *et al.* (2004) and is as follow. An initial reference map is produced by constructing a linear NDVI trend surface *s(x,y,t)* over the reference period [0,t] defined here as the period 2000–2008. The choice of this period was based on the constraint of the NDVI time series length (2000-2013) and in order to include a wide range of rainfall variability and also changes in LULC. Thus, pixels *(x, y)* for which the trend sign was positive over this initial period (t = t_i) were assigned a value of +1, otherwise a value of −1 was assigned. At the initial time t=t_i, a surface $s(x, y, t_i)$ is constructed. Then, using a yearly time step, new years are progressively added and persistent sites are tracked in persistence maps *P(x,y,t)* (Lanfredi *et al.*, 2004; Harris *et al.*, 2014). The trend persists if the additional years do not change the sign of the persistence map of the reference period, otherwise the trend stops. That is to say, those pixels where the additional years do not clear the trend previously detected at the reference period or to change its sign are classified as persistent (Simoniello *et al.*, 2008). Persistence maps are constructed according to the rule below (Lanfredi *et al.*, 2004):

$$P(x, y, t_i) = s(x, y, t_i) \qquad t = t_i \tag{6.1}$$

$$P(x,y,t) = \begin{cases} 0 & if\ s(x,y,t) \neq P(x,y,t-1) \\ P(x,y,t-1) & if\ s(x,y,t) = P(x,y,t-1) \end{cases} \qquad t > t_i \tag{6.2}$$

At the observational time T, a cumulative field is obtained by adding all the persistence maps. Here, persistence maps were calculated for 2008, 2009, 2010, 2011, 2012 and 2013, and then summed up to achieve the overall persistence map. For any pixel (x, y), the magnitude of such

a field indicates the number of years during which the trend was observed, and its sign indicates whether the trend was increasing or decreasing (Simoniello *et al.* 2008). Figure 6.2 shows the procedure for estimating temporal persistence.

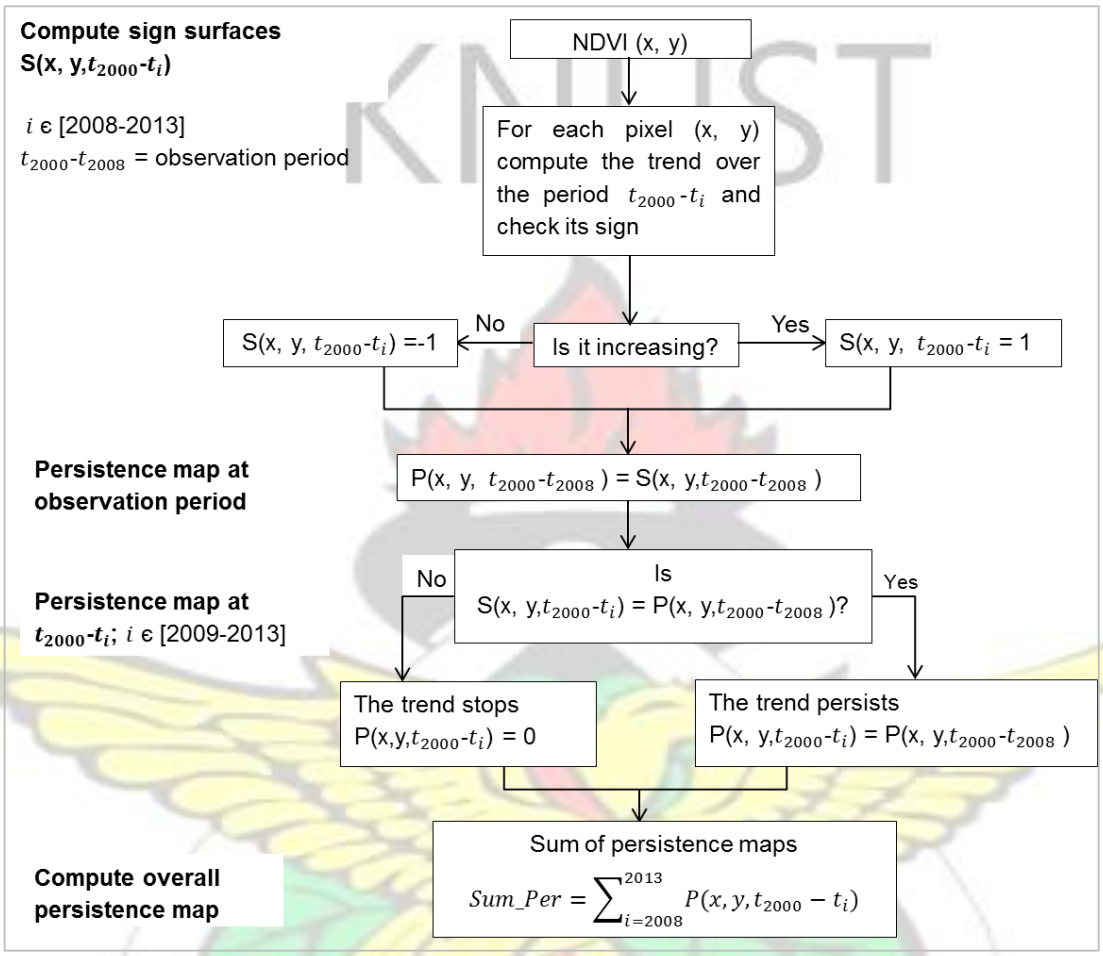

Figure 6. 2. Estimation of temporal persistence, modified from Lanfredi *et al.* (2004)

6.2.4.2. Mann-Kendall's monotonic trend test

The second step was to perform the Mann-Kendall monotonic trend test which is a nonparametric method. Contrary to other methods (e.g. linear trend), Mann-Kendall's trend test does not require the data to meet specific criteria (e.g. Normal distribution), and it can avoid the problem roused by data skew (Smith, 2000). Two parameters were considered: correlation coefficient and significance test. The correlation coefficient, ranging from -1 to +1, measures the degree to which a trend is increasing or decreasing (Wessels *et al.*, 2012), while

the significance test highlights the significance of the trend slope. A trend with p value less than

0.05 was qualified as significant. The Mann-Kendall correlation coefficient (S) is calculated by Equation 6.3.

$$S = \sum_{i=1}^{n-1} \sum_{j=i+1}^{n} \text{sign}(x_j - x_i) \quad (6.3)$$

and

$$\text{Sign}(x_j - x_i) = \begin{cases} 1 \text{ if } (x_j - x_i) > 0 \\ 0 \text{ if } (x_j - x_i) = 0 \\ -1 \text{ if } (x_j - x_i) < 0 \end{cases} \quad (6.4)$$

where n is the length of time series data, x_i and x_j are the observation at time i and j respectively. The computation of Mann Kendall significance produces a standardized Z (Equation 6.5) and corresponding probability p (Equation 6.6). Z here follows a standard normal distribution, and a positive Z value indicates an increasing trend, whereas a negative value of Z signifies a decreasing trend.

$$Z = \begin{cases} \frac{S-1}{\sqrt{\text{Var}(S)}} \\ 0, S = 0 \\ \frac{S+1}{\sqrt{\text{Var}(S)}} \end{cases} \quad (6.5)$$

and

$$p = 2[1 - \phi(|Z|)] \quad (6.6) \quad \text{Where } \phi(|Z|) = \frac{2}{\sqrt{\pi}} \int_0^{|Z|} e^{-t^2} dt \quad (6.7)$$

6.2.4.3. Detection of vegetation trends categories

The combination of the temporal persistence analysis and Mann Kendall monotonic trend test results enabled the detection of three categories of vegetation dynamics (Table 6.3). Pixels affected by the highest persistent decrease and with Mann-Kendall's correlation coefficient less or equal to -0.5 and P-value less than 0.05 were classified as under significant consistent

decreasing trend of vegetation. In the same time, pixels that exhibited the highest persistent increase persistence with Mann-Kendall's correlation coefficient higher or equal to 0.5 and Pvalue less than 0.05 were under significant consistent increasing vegetation trend. The other trajectories were qualified as inconsistent.

Table 6. 3. Scheme used to categorise vegetation trends in the study area

Vegetation trends	Trend persistence	correlation coefficient	Significance (p)
Significant consistent decreasing	Highest persistent decrease (6 years)	Correlation coef. =< -0.5	p < 0.05
Significant consistent increasing	Highest persistent increase (6 years)	Correlation coef. >= 0.5	p < 0.05
Inconsistent		Other trajectories	

6.2.5. Determining drivers of significant trend: Random Forest modelling

Random Forest (RF) classification algorithm was used to model vegetation significant consistent trends in order to determine potential drivers; this by assessing the contribution of each variable to the RF modelling. The description of RF classifier is detailed in section 4.2.4.2 of chapter 4. In this study, MDA (Mean Decrease in Accuracy) was used as proxy to determine main drivers of vegetation trends among anthropogenic and biophysical variables. MDA quantifies the importance of a variable by measuring the change in prediction accuracy when the values of the variable are randomly permuted compared to the original observations (Calle and Urrea, 2010). Human footprint, rainfall, elevation, geomorphological units, LULC and soil types were used as model predictors, while significant consistent vegetation trends were set as response variable. Ten reference samples collected based on random sampling were considered in the modelling process. For that purpose, the areas of significant consistent trends were extracted and converted to polygon vector layers based on which reference pixels were selected (ArcGis 10.1). Each reference sample contained 2000 pixels shared between training and testing samples. RF was run using R software with 800 as number of trees. At each node split, the number of variables was the square root of their total number. A confusion matrix enabled

the computation of each sample error rate, and the general error rate of the modelling over all the sample was given by Equation 6.8.

$$ME = \frac{\sum_{i=1}^{n} E_i}{n} \qquad (6.8)$$

Where ME is the mean error, E_i is the error rate of sample i, and n the number of sample.

6.2.6. Local population perception

A survey was carried out in November 2013 to determine local population perception of vegetation trend between 2000 and 2013. In total six villages, selected randomly, (Gbagba, Balembar, Gnipkiere, Sorkon, Dayere and Wahable) were considered in this investigation. The household heads were the target population. The software survey system was used to compute the sample size based on the total of household heads (1777), the confidence level (95%) and the margin of error (less than 5%). In all, 360 heads of household were surveyed randomly. The survey focused mainly on vegetation trend, the causes of the observed trend, and the affected vegetation species.

6.3. Results

6.3.1. Vegetation trends in the study area

Figure 6.3 shows the persistence map of vegetation trends during the period 2000-2013 with 2000-2008 as reference period. The green colour gradients indicate areas with persistent increasing trends, and the yellow to red colours characterise areas where decreasing trends persist. Table 6.4 indicates that the study area was dominated by decreasing trends (80.3%) with the longest persistent decreasing trend (6 years) covering 22.6 % of the study area. Only 19.7% of the study area exhibited increasing trends, and 11% knew 6 years of persistent increasing trends.

Figure 6.4a and 6.4b presents respectively the corelation coefficient and the trends significance maps resulted from Mann-kendall's monotonic trend test. The combination of the correlation coefficient, significance and persistence maps enabled the categorisation of vegetation dynamics into different types of trends which are highlighted by Figure 6.5. It came out that, in the period 2000-2013, 83.8% of the study area had inconsistent vegetation trend against 14% for significant consistent decreasing trend and 2.2% for significant consistent increasing trend (Table 6.5). Of the significant consistent trends, 86.4% were decreasing and 13.6% increasing.

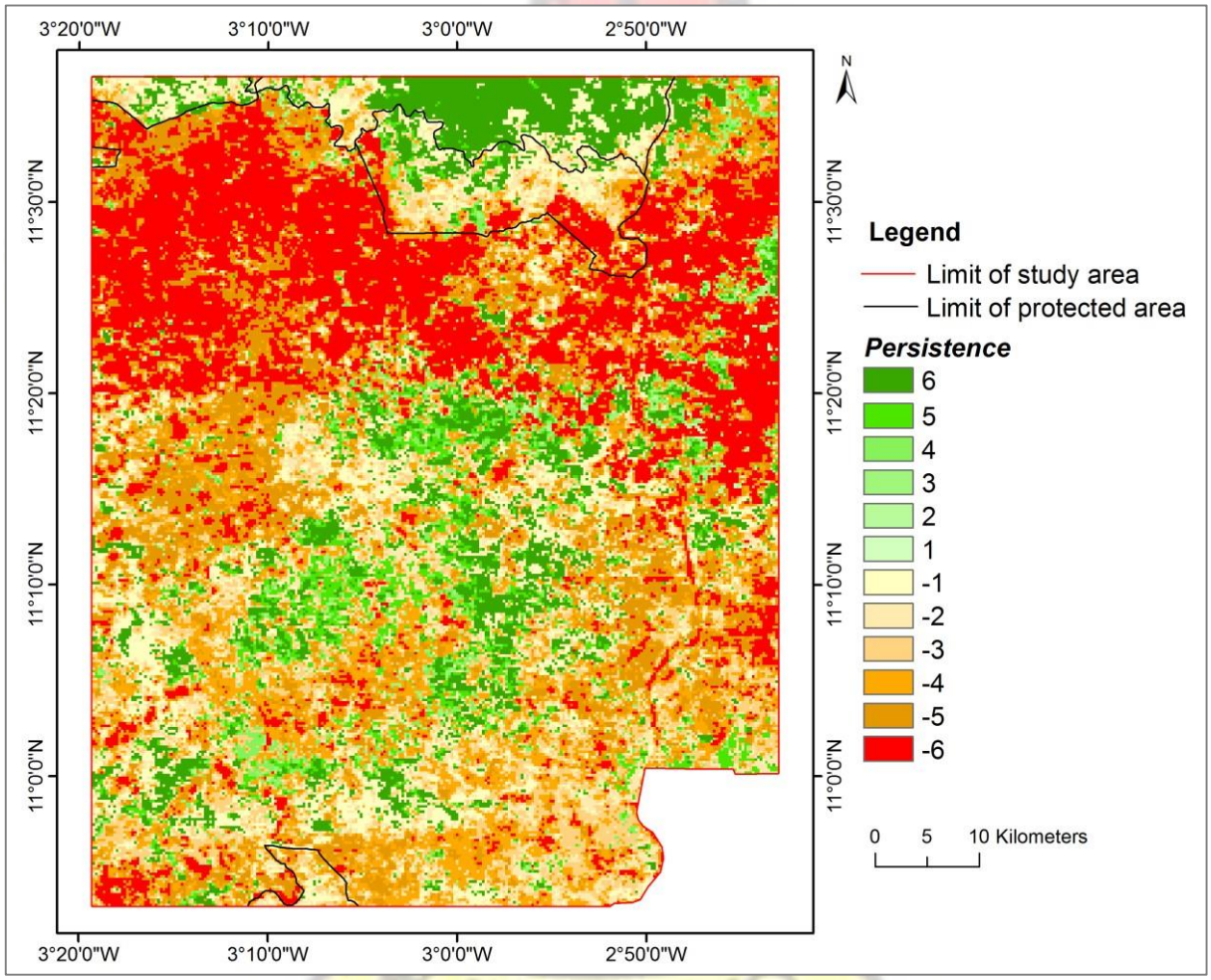

Figure 6. 3. Patterns of vegetation trends persistence in the study area (2000-2013) **Table 6. 4.** Proportion of vegetation persistence types in the study area

	Decreasing persistence							Increasing persistence
Persistence levels	-	-1	1	2	3	4	5	6	Total

Percentage (%)	22.6	16.1	13.4	7.4	0.1	0	1	2.2	5	100
	11.7	9.1				11				
	80.3					19.7				100

.

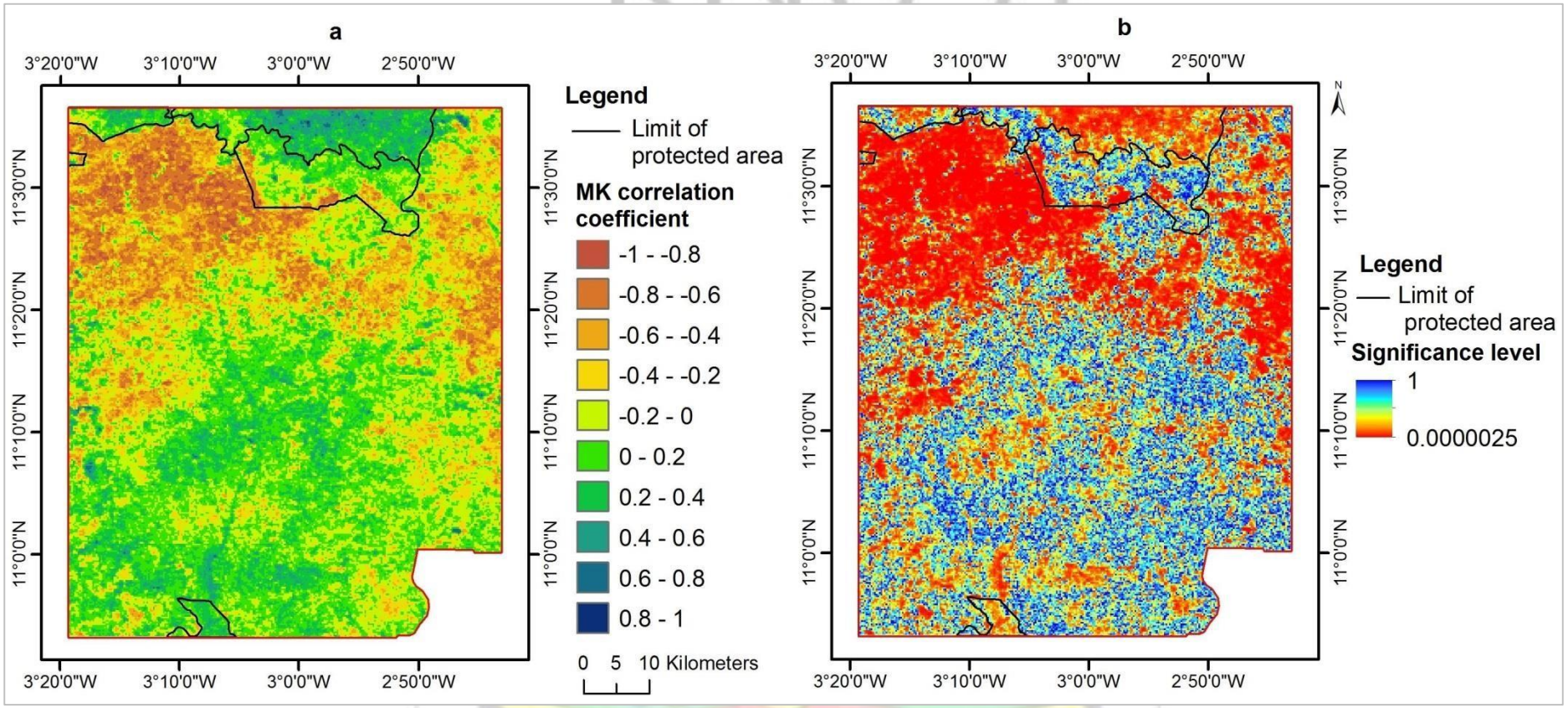

Figure 6. 4. Mann Kendall's trend test results over the period 2000-2013, a) Distribution of Mann-Kendall correleation coefficient, b) Distribution of significance level (p value)

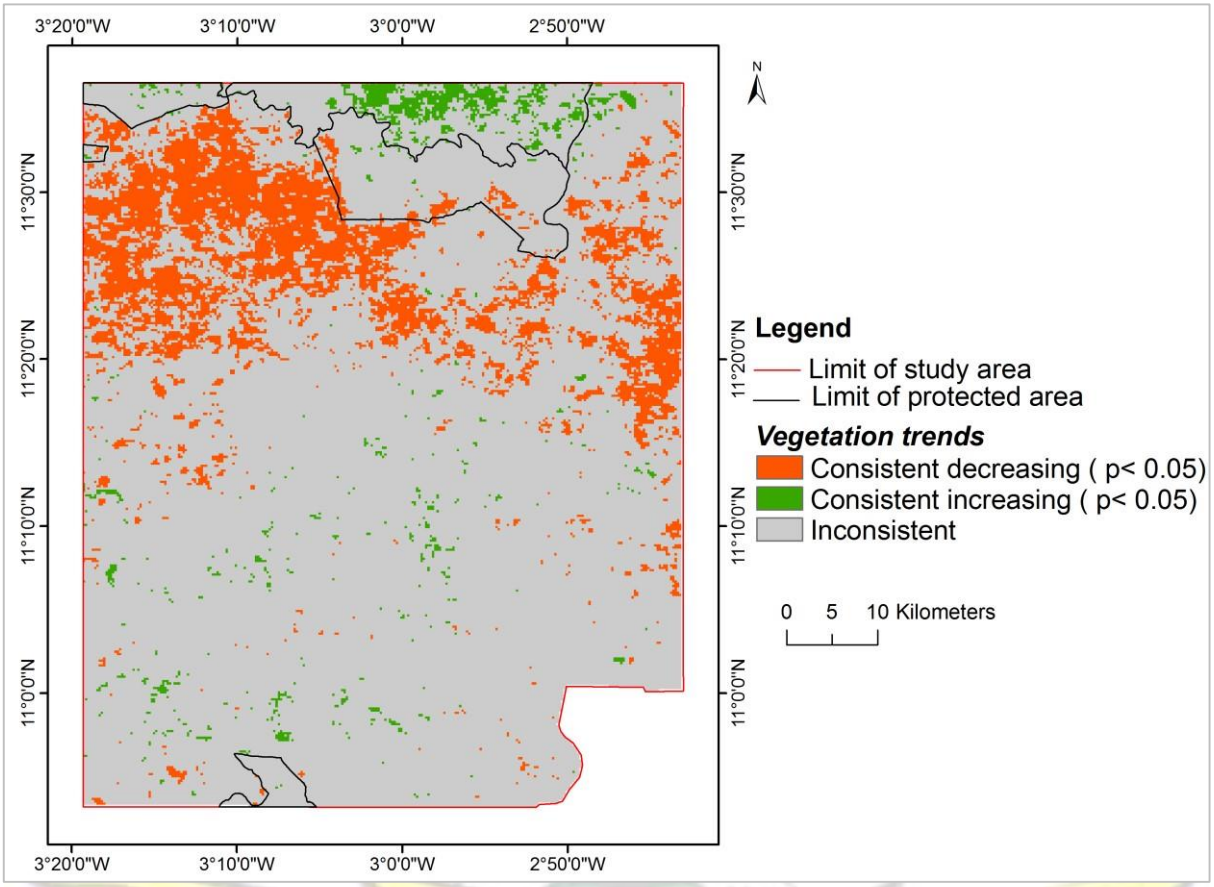

Figure 6. 5. Vegetation trends occurred in the study area (2000-2013)

Table 6. 5. Proportion of vegetation trends observed in the study area

	Significant consistent increasing	Significant consistent decreasing	Inconsistent	Total
Pixel count	1793	11408	68536	81737
Percentage	2.2	14	83.8	100

6.3.2. Distribution of vegetation trends according to LULC and LULCC

For all LULC classes, inconsistent trend was largely dominating (more than 70% of the area of each LULC) in the study area (Table 6.6). Among the detected trends, decreasing trajectory was more prominent than increasing trend. Agricultural area was more affected by decreasing trend (25.8%), whereas woodland was the least concerned by such a trend (4.8% of its area). However, woodland was the most affected by greening trend (4.2% of its area) while only 0.5 % of agricultural area and 1.5% of mixed vegetation exhibited that trend.

Areas under significant consistent decreasing trend were dominated by agricultural area (56.8%), followed by mixed vegetation (30.1%) and woodland (13.1%). This distribution was reversed regarding significant consistent increasing trend areas where 70.1%, 23.4% and 6.5% were covered by woodland, mixed vegetation and agricultural area respectively. Inconsistent vegetation trends were mostly found in woodland (40.8 %) and mixed vegetation (32.5%).

Regarding LULCC classes, Table 6.7 indicates that inconsistent trend was also largely dominating (More than 70% of the area of each LULCC), and decreasing trend was more prominent than increasing trend. Natural vegetation loss (26.9%) and stable non-natural vegetation (23.4%) were the most affected by decreasing trend and the two other classes (Stable natural vegetation and other change) by increasing trend. Table 6.7 also shows that most of the inconsistent trends (60.6%) are found in stable natural vegetation. The significant consistent increasing trend occurred mostly in stable natural vegetation (81.7%) followed by other change (11.2%). Natural vegetation loss and stable natural vegetation prevailed over the other classes on area affected by significant consistent decreasing trend with values of 36.3% and 33.3% respectively. These findings show that changes in LULC influence vegetation trend and highlight an association between increasing NDVI trend and stable natural vegetation and between decreasing NDVI trend and natural vegetation loss area.

Table 6. 6. Distribution of vegetation trends according to LULC

	Inconsistent (%)	Sig. consistent increasing (%)	Sig. consistent decreasing (%)	Total
Woodland	91	4.2	4.8	100
Mixed vegetation	85.4	1.6	13	100
Agricultural area	73.7	0.5	25.8	100
	Inconsistent (%)	Sig. consistent increasing (%)	Sig. consistent decreasing (%)	
Woodland	40.8	70.1	13.1	
Mixed vegetation	32.5	23.4	30.1	
Agricultural area	26.7	6.5	56.8	

Total	100	100	100

Table 6. 7. Distribution of vegetation trends according to LULCC classes

	Inconsistent (%)	Sig. consistent increasing (%)	Sig. consistent decreasing (%)	Total
Stable natural vegetation	88.1	3.1	8.8	100
Other change	89.2	2.2	8.6	100
Natural vegetation loss	72.7	0.4	26.9	100
Stable non-natural vegetation	76	0.6	23.4	100

	Inconsistent (%)	Sig. consistent increasing (%)	Sig. consistent decreasing (%)
Stable natural vegetation	60.6	81.7	33.3
Other change	11.7	11.2	6.8
Natural vegetation loss	14.9	3	36.3
Stable non-natural vegetation	12.8	4.1	23.6
Total	100	100	100

6.3.3. Random Forest modelling accuracy and variables contribution

The modelling error rate distribution per sample is presented in Figure 6.6. The error rate per sample was less than 6% with a mean of 5.2%. The total performance of the modelling was then estimated to be 94.8%. This result means that the model was able to discriminate efficiently significant consistent increasing trend areas from those under significant consistent decreasing trend.

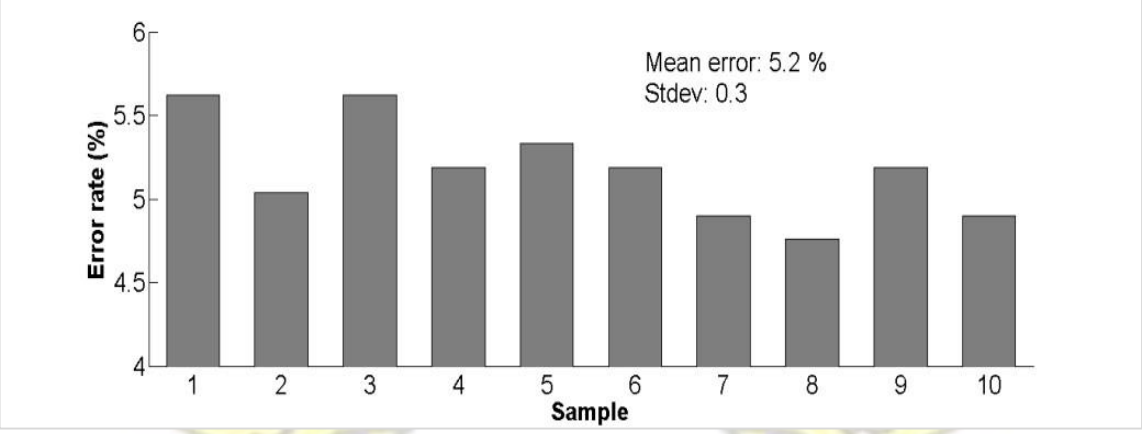

Figure 6. 6. Error distribution of significant consistent trends modelling per samples

The results of variables contribution to the modelling are illustrated by the boxplot in Figure 6.7. The boxplot shows the distribution of the MDA score values for each predictor through the 10 samples. It highlights the first, second (median) and third quartiles, minimum and

maximum values of the MDA score. Human footprint was remarkably the most important variable in the modelling for all the samples, followed by rainfall and geomorphological units. LULC and soil types were less important.

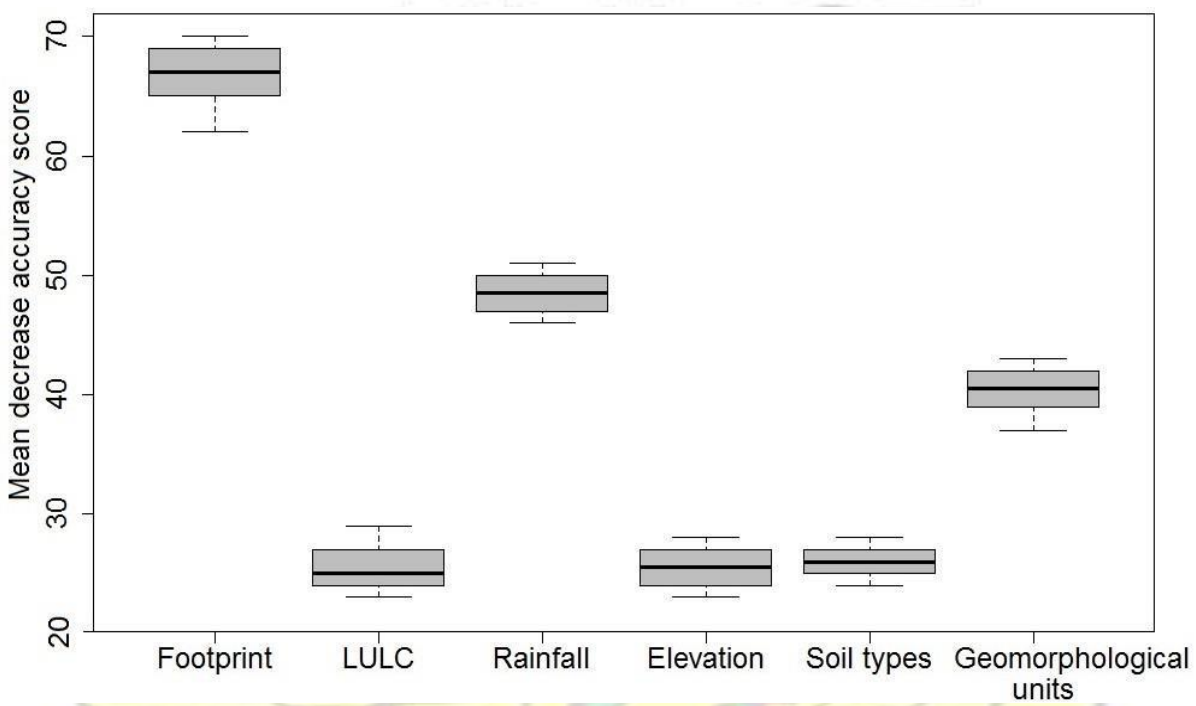

Figure 6. 7. Variables importance score for significant consistent trends modelling according to 10 samples

It is perceptible from Table 6.8 that human footprints distribution played a key role in the occurrence of significant consistent vegetation trends across the study area. Indeed, 55.8% of significant consistent increasing trends areas were characterised by absent or very low human footprint, only 4.6% were found in area under very high human footprint. In addition, significant consistent decreasing trends were less located in areas with absent or very low human footprint (1.2%), but they were mainly found in areas with medium (38.6%) and high (29.5%) human footprint.

Table 6. 8. Distribution of significant consistent vegetation trends according to human footprint

Footprint classes	Significant consistent increasing (%)	Significant consistent decreasing (%)
Absent or very low	55.8	1.2
Low	12.9	16
Medium	13.6	38.6
High	13.1	29.5
Very high	4.6	14.7
Total	100	100

6.3.4. Local population perception of vegetation trends during the last decade

The perception of local population of vegetation trend between 2000 and 2013 is in agreement with the results of satellite images processing. In all, 96.3% of household chiefs observed a reduction in vegetation cover in their environment, and only 2.7% noticed stability and 1% an increasing trend of vegetation cover (Figure 6.8). Cropland expansion, drought, wood extraction, mining and bushfire were frequently mentioned by local population as main causes of vegetation reduction; among those factors, cropland expansion, drought and wood extraction were largely identified to be the main threats of vegetation cover (Figure 6.9).

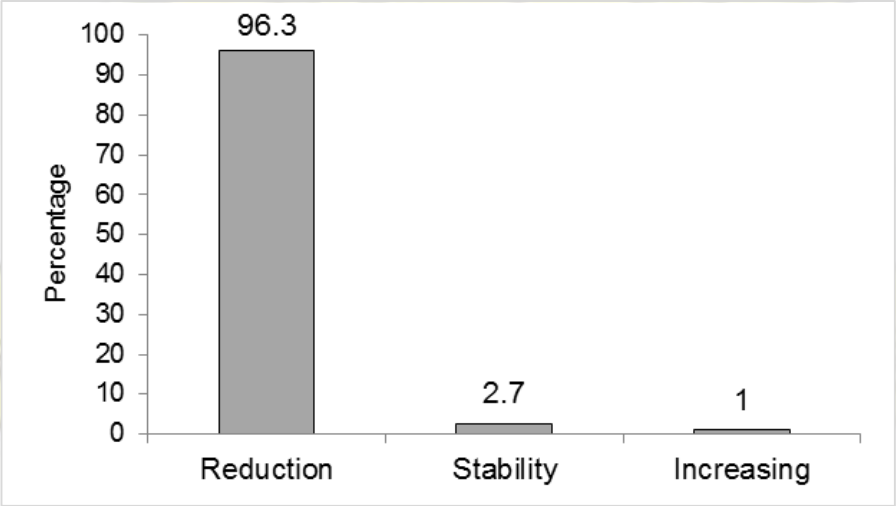

Figure 6. 8. Local population perception of vegetation trends in the study area

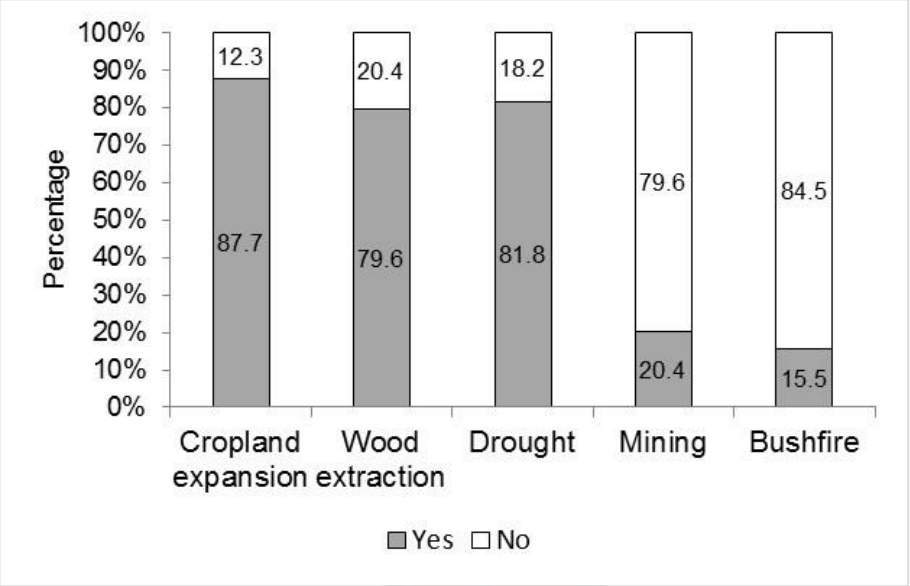

Figure 6. 9. Causes of vegetation reduction according to local population

Thirteen vegetation species were identified by local population as becoming rare in their environment; those species are *Nauclea latifolia, Tamarindus indica, Bombax costatum, Adansonia digitata, Loudetia simplex, Vitex doniana*, among other (Figure 6.10). However, *Nauclea latifolia* was mostly identified by household heads (60%) as the rarest specie, then *Tamarindus indica* (16.5%) and *Bombax costatum* (8%). Most of those species are used for medicine, food and construction. Some species (e.g. *Vitellaria paradoxa, Parkia biglobosa, Azadirachta indica and Faidherbia albida*) are more frequent in farmlands, also because of their medical and/or food usefulness, while other species are sacred and, therefore, prohibited to be cut down. *Diospyros mespiliformis*, *Gardenia erubescens* and *Berlinia grandiflora* were mostly pointed out as prohibited species from cutting down (Figure 6.11).

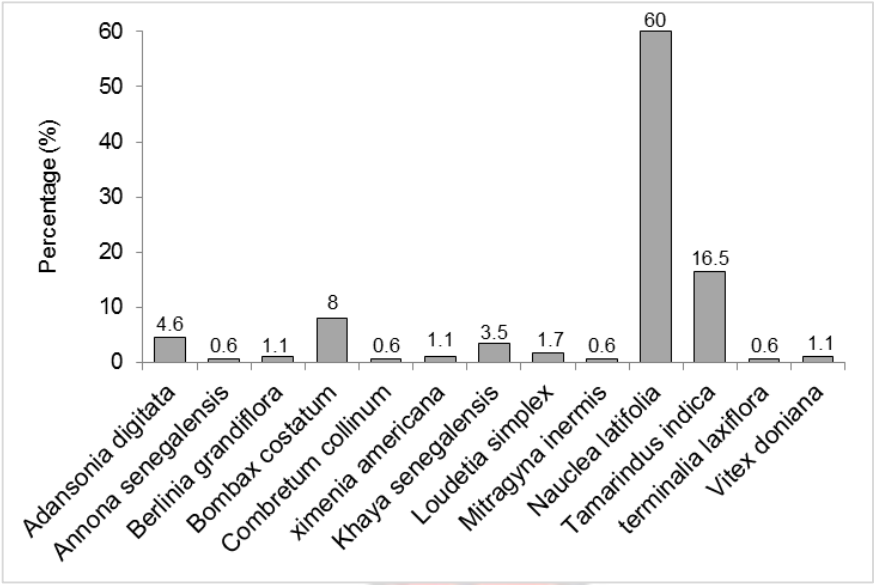

Figure 6. 10. Vegetation species becoming rare according to local population

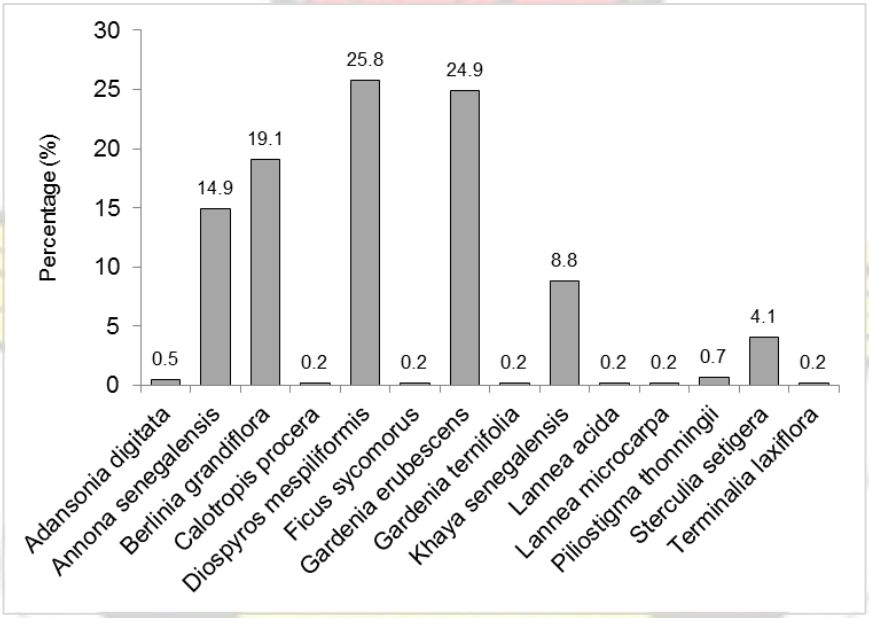

Figure 6. 11. Vegetation species prohibited for cutting according to local population

6.4. Discussion

In the study area, despite the observed domination of inconsistent dynamics of NDVI, patterns of significant consistent trends of vegetation were detected in the period 2000-2013 by the adopted approach. The prevailing of decreasing trajectories among the significant consistent trends highlights a progressive loss of vegetation cover in the study area. These results are in agreement with previous studies conducted across West Africa. For instance, Hountondji *et al.* (2005) found a consistently vegetation degradation during the period 19811999 over most of

the Sahel belt of Niger. In Burkina Faso, Hountondji *et al.* (2006) noted a domination of negative trend of vegetation in the period 1982-1999, which according to them, may reflect ongoing land degradation processes. However, the findings of this research contrast with the works by Leroux *et al*. (2014) and Traore *et al.* (2014) that found dominating increasing dynamics of vegetation among the detected significant trends in the Sahel and Sudan zones, and in the Bani river basin in Mali respectively. Kaptué *et al.* (2015) analysed changes in watershed-scale vegetation conditions in four regions of the Sahel from1983–2012 and also supported a greening trend across this region. However, they found strong regional differences in the extent and direction of change. The use of coarse satellite resolution images of 8 km (e.g. Olsson *et al.*, 2005; Traore *et al.*, 2014) remains an important weakness of those works, and in addition to the study area location, the assessment methods and the observation period, could explain the difference of results compared to the present study.

However, the results of other local studies (e.g. Braimoh, 2004; Ouedraogo *et al.*, 2010; Houessou *et al.*, 2013) conducted across the Sudan savannah with more accurate resolution images (e.g. Landsat, 30 m x 30 m resolution) give confidence to the findings achieved in this research, since they have noted a general reduction of natural vegetation mainly due to cropland expansion. This supports the fact that more than half (56.8%) of the significant consistent decreasing trend of vegetation in the study area were found in agricultural areas. This is potentially due to the expansion of croplands at the expense of natural vegetation, for instance between 1999 and 2011 as noted in chapter 4. Furthermore, the distribution of significant trends of NDVI according to the LULCC classes shows that changes in LULC influence vegetation productivity, although the observation periods in this study were slightly different: 1999-2011 for LULCC and 2000-2013 for NDVI trends.

In this study, natural vegetation loss includes conversions from woodland and mixed vegetation to other LULC types, and stable natural vegetation consists of stable woodland, stable mixed

vegetation as well as the conversions from one to another; therefore, the conversion from woodland to mixed vegetation, which is a regression of vegetation cover, could explain the presence of significant decreasing trend in stable natural vegetation (Table 6. 7). Besides, the LULCC class, “other change”, includes conversions between water, agricultural area and bare surface as well as from those classes to natural vegetation; thus, the conversion to natural vegetation is likely the reason of increasing vegetation trend in the class other change. Of course, anthropogenic land management also could have played a role in the observed trends of vegetation especially in areas of stable non-natural vegetation, such as stable agricultural area, where changing in crop types could influence NDVI trends. In addition, the resampling of the LULCC map from 30 m x 30 m to 250 mx 250 m resolution could have slightly influenced the results and could explained the small portion of greening area found in the LULCC class called natural vegetation loss. This research revealed that, at local scale, human is the major driver of the occurrence of significant consistent trends of vegetation in the southwest Burkina Faso. The results of the analyses showed that vegetation has higher development in areas less influenced by humans (e.g. Protected area of Deux Balle forest), but decreases in area more affected by human footprint. In the study area, shifting cultivation agriculture, wood harvesting, mining and bushfire are the main local practices that threat natural vegetation.

Local populations of the study area are aware of the environmental change occurring in their area and should be involved in the reforestation campaigns. Such a finding corroborates with the conclusion of Ouoba *et al.* (2014) in the Sahel region of Burkina Faso that noticed a good perception of local population regarding vegetation cover dynamics. For that purpose, indigenous knowledge should be incorporated into forest rehabilitation process for identifying endangered species in order to assure efficient biodiversity conservation. This awareness of

local population led them to undertake reforestation with assistance from the State. This could explain the few greenings observed in areas with important human footprint.

6.5. Conclusion

The assessment of vegetation trend is essential to understand the global environmental change. In West Africa, the trend of vegetation remains a debate in the scientific community. Suitable assessment methods with more accurate resolution satellite data set could bring out reliable conclusion about vegetation trends in this part of the world. In the southwest Burkina Faso, a study, which integrated temporal persistence analysis and Mann-Kendall's trend test to assess vegetation trends at local scale, revealed that the study area was predominated by patterns of inconsistent dynamics of vegetation in the period 2000-2013. Increasing and decreasing trends were detected, but the latter was largely dominant which was confirmed by local population. Anthropogenic pressure was the main driver of the occurrence of the detected trends in the study area. The findings also showed that changes in LULC influence vegetation trends. The adopted approach, which consisted of integrating temporal persistence analysis and Mann-Kendall's trend test to detect trend in MODIS NDVI 250 m has shown to be efficient and coherent with the landscape of the study area.

Chapter 7: Conclusions and Recommendations

7.1. General remarks

Forkuor (2014) found that late rainy season period was the most appropriate temporal window for croplands mapping in the Sudan savannah of West Africa. This finding can be extended to all the main LULC types of the Sudan savannah as reported in chapter 4. The addition of ancillary data to late rainy season image is more suitable to map LULC in the study region.

This combination of data significantly improves mapping accuracy and increases chance of using cloud free image as compared to combinations including multitemporal images. This provides an alternative for accurate LULC mapping in the Sudan savannah of West Africa. The availability of satellite images (e.g. Landsat) and environmental ancillary data, such as topographic (e.g. ASTER GDEM and SRTM) and climatic data (e.g. Worlclim data) is an asset that could facilitate the implementation of the combination of remote sensing image and ancillary data for LULC dynamics monitoring.

In the southwest of Burkina Faso, LULC dynamics between 1999 and 2011was characterised by expansion of agricultural area and bare surface combined with reduction of natural vegetation, which is an evidence of anthropogenic pressure on vegetation. Similar LULC dynamics have been observed elsewhere across the Sudan savannah of West Africa, for example, in southern Burkina Faso (Ouedraogo *et al.,* 2010), Benin Republic (Houessou *et al.,* 2013) and northern Ghana (Braimoh, 2004). Rainfall in the study area was dominated by near normal conditions of variability and with a non-significant rising trend, for instance, in the periods 1981-2012 and 2001-2012.

The response of the study area vegetation under those conditions of rainfall variability and Land Use/Cover Change was characterised by consistent and inconsistent trends of its productivity as indicated by NDVI trend assessment in the period 2000-2013 in chapter 6. The large prominence of decreasing trend (86.4%) among the detected consistent NDVI trends is a sign of an ongoing degradation of vegetation cover, which is a confirmation of previous studies (e.g. Hountondji *et al.,* 2006). The increasing trend of vegetation was mostly found in protected areas, which reveals the relevant role played by those areas in the context of anthropogenic and climatic pressures on vegetation. The findings in this thesis showed that, in the study region, changes in LULC influence vegetation productivity. For instance, it has been observed that conversions from natural vegetation (Woodland and mixed

vegetation) to other LULC types (e.g. agricultural area, bare surface) are associated with loss of vegetation productivity (decreasing of NDVI values), while stable natural vegetated LULC favours the increase of vegetation productivity (increasing NDVI values). This is in support of Leroux *et al*. (2014) that found that cropland expansion at the detriment of natural vegetation leads to a decrease in NDVI values in the Sudan area of West Africa.

The inconsistent trend of vegetation observed in the study area is likely due to anthropogenic land management practices and also due to rainfall variability. Indeed rainfall fluctuation strongly influences the dynamics of vegetation indices such as NDVI and EVI that are both good indicators of vegetation in the southwest of Burkina Faso (see chapter 5). The good performance of NDVI observed in this study shows that saturation and background material effects on NDVI signal are insignificant in the study area. This finding is in contrast with the conclusions of Farrar *et al.* (1994) and Liu and Huete (1995). However, this result is in support of the findings of Fensholt (2004) who found that in semi-arid Senegal the problem of background contamination on vegetation indices from soil is not severe.

Rainfall was found by some authors to govern the detected trends of vegetation at large scale in West Africa (e.g. Hermann *et al.*, 2005b; Leroux *et al*., 2014). However, this study suggests that at local scale anthropogenic pressure is the main driving factor. Such a result agrees with the conclusion of Ouedraogo *et al.* (2010) that stated that population size and distribution explain land cover change in the southern Burkina Faso, particularly the conversion from natural vegetation to cropland. The predominance of near normal rainfall conditions and non-significant rising trend of rainfall in the period 2001-2012 stress the key role played by human activities on the reduction of vegetation between 2000 and 2013 in the study area. Despite their disturbing effect, local population also contributed to the regeneration of some areas by reforestation activities. Alternative sources of energy, such as millet and sorghum stalks, are

used by farmers for cooking instead of wood. Those practices attest to the awareness of local population to environmental degradation.

Vegetation trends according to remote sensing processing agree with the local population perception, which gives confidence to the remote sensing method employed in this study. Simonelo *et al.* (2008) have shown the capacity of the temporal persistent analysis to efficiently capture vegetation dynamics with coarse satellite images (e.g. NOAA/AVHRR 8 km spatial resolution) in the Mediterranean area. However, the present research also found that the integration of temporal persistent analysis with Mann-Kendall's trend test produces consistent results in the Sudan savannah (e.g. in the southwest of Burkina Faso) when using MODIS NDVI at 250 m resolution. This performance of MODIS NDVI confirms previous analysis (e.g. Fensholt and Sandholt, 2005; Fensholt *et al.*, 2006) that claimed that MODIS NDVI was a better proxy for vegetation cover in the savannah of West Africa.

7.2. Summary of key findings

The response of vegetation dynamics to rainfall variability and land use in the southwest of Burkina Faso has been evaluated in this study by combining remote sensing observations and local population perception. Specifically, changes occurring in LULC have been determined based on random forest classification of Landsat images (1999, 2006 and 2011) and ancillary data. The results showed that late rainy season period was more suitable to map LULC types in the southwest Burkina Faso. Multi-temporal data classification significantly performed better than the classification of mono-temporal data in the study area. In addition, the inclusion of environmental ancillary data improved multi-temporal classification and also significantly enhanced mono-temporal image classification accuracies. No significant difference was observed between the performance of multi-temporal classification and its combination with

ancillary data as well as the combination of mono-temporal image and environmental ancillary data. These findings suggest that the combination of ancillary data and mono-temporal image from late rainy season reduces the data requirements as compared to multi-temporal data classification. The result of this study is relevant to the Sudan savannah of West Africa where atmospheric condition is a limitation to the availability of quality multi-temporal satellite images. Between 1999 and 2011, agricultural area and bare surface have increased in the study area, whereas there was a reduction in woodland and mixed vegetation; for example the loss of natural vegetation was about 17.9% ± 2.5% in the same period.

The inter-annual variability of rainfall in the period 1981-2012 and its relationship with vegetation dynamics have also been determined in the southwest Burkina Faso by using NDVI and EVI as vegetation indicators. The findings highlighted that, in the period 19812012, the study area was frequently under mild dry and mild wet rainfall events with intermittent occurrence of extreme events. A non-significant rising rainfall trend was predominant particularly in the periods 1981-2012 and 2001-2012. Furthermore, vegetation dynamics was strongly related to rainfall, and NDVI was found to be slightly better correlated to rainfall than EVI in the study region.

Lastly, the trends of vegetation dynamics in the study area were assessed by integrating temporal persistence analysis and Mann-Kendall's trend test to detect trends in MODIS NDVI 250 m data (2000-2013) which was used as proxy for vegetation productivity. Furthermore, local population perception of vegetation trends (2000-2013) was also determined based on a random survey of household heads. The results revealed that the study area was largely characterised by inconsistent vegetation dynamics (83.8%) within the period 2000-2013. Decreasing trend (14 %) was particularly found in agricultural area and in high and medium human footprint areas, while increasing trend (2.2 %) was observed mainly in woodland and areas less affected by human activities. The distribution of vegetation trends was

mainly explained by human footprint, which makes human to be the main driver of vegetation trends in the study region. Field survey showed that cropland expansion, wood harvesting, mining and bushfire were the principal anthropogenic activities that threaten natural vegetation. The perception of the local population was in agreement with the remote sensing observations.

In general, in the observation period, the vegetation of the study area was found to have reduced, and this is more because of unsustainable land use than rainfall conditions. This calls for more sustainable land use management practices in the southwest of Burkina Faso in order to safeguard natural environment and livelihood of local population.

7.3. Main contributions to research

In the first place, this work has determined a suitable period and accurate combination of spatial data to classify LULC in the Sudan savannah especially in the southwest of Burkina Faso. The acquisition of satellite image from inadequate temporal windows and the use of less accurate classification method are among the majors sources of LULC mapping errors in West Africa. For the southwest of Burkina Faso, the use of satellite image acquired from late rainy season period (e.g. October) combined with environmental ancillary data reduces LULC mapping error and is more appropriate for this region.

Secondly, the study provided the validation of EVI in the Sudan Savannah of Burkina Faso regarding its ability to express the response of vegetation to rainfall. The strong positive correlation of EVI and NDVI with rainfall is an indication that both indices are reliable in southwest of Burkina Faso.

Thirdly, this thesis contributed to the debate on vegetation trend in West Africa particularly in the Sudan savannah and confirmed a predominant degradation trend of vegetation cover.

At local scale, human activities are the main drivers of consistent vegetation trends.

Furthermore, the study demonstrated that the temporal persistence analysis combined with

Mann-Kendall's trend test performs well with MODIS NDVI at 250 m in assessing vegetation dynamics in the Sudan savannah and can be used for further investigations in other spots across West Africa.

7.4. Recommendations

7.4.1. For research

- ✓ Satellite image from late rainy season (e.g. October) should be used for mono-temporal (single date) LULC classification in the Sudan savannah, as it reduces the confusion between LULC classes. However, for LULC mapping in the Sudan savannah, this study recommends the combination of satellite image from late rainy season period and environmental ancillary data. Future studies could assess the spatial transferability of the performance of such a combination of data in other zones across West Africa.
- ✓ The integration of temporal persistence analysis with Mann-Kendall's trend test can be employed to monitor vegetation dynamics in the Sudan savannah of West Africa, and the testing of this method in the other climatic zones in West Africa will be interesting for future research. Furthermore, future projection of vegetation trends in the study area and beyond is also a relevant opportunity for further research.

7.4.2. For policies

- ✓ The LULCC and vegetation trends maps presented in this study can serve as decision making tools to enforce laws on deforestation and carbon emission into the atmosphere. These maps can be used to support ongoing reforestation campaigns and to take appropriate decisions for sustainable land use management and practices in the southwest of Burkina Faso.
- ✓ Education of local populations on the impact of deforestation on climate change would be necessary by employing a participatory approach.

Bibliography

Adjonou, K., Djiwa, O., Kombate, Y., Adzo Dzifa Kokutse, A. D. and Kokou, K. 2010. Etude de la dynamique spatiale et structure des forêts denses sèches reliques du Togo: implications pour une gestion durable des aires protégées. *International Journal of Biological and Chemical Sciences*, 4(1): 168-183.

Aduah, M.S. and Aabeyir, R. 2012. Land cover dynamics in WA municipality, upper west region of Ghana. *Research Journal of Environmental and Earth Sciences*, 4(6): 658– 664.

Aggarwal, S. 2003a. Principles of Remote Sensing. *in* M.V.K. Sivakumar, P.S. Roy, K. Harmsen and S.K. Saha *(*eds.), *Satellite Remote Sensing and GIS Applications in Agricultural Meteorology*, World Meteorological Organisation, Geneva, 23-38.

Aggarwal, S. 2003b. Earth resource satellites. *in* M.V.K. Sivakumar, P.S. Roy, K. Harmsen and S.K. Saha (eds.), *Satellite Remote Sensing and GIS Applications in Agricultural Meteorology*, World Meteorological Organisation, Geneva, 39-65.

Akar, O. and Güngör, O. 2012. Classification of multispectral images using Random Forest algorithm. *Journal of Geodesy and Geoinformation*, 1(2):105-112.

Akognongbe, A., Abdoulaye, D., Vissin, E.W. and Boko, M. 2014. Dynamique de l'occupation du sol dans le bassin versant de l'Oueme à l'exutoire de Bétérou (Bénin). *Afrique Science*, 10(2): 228-242.

Al-Ahmadi, F. S. and Hames, A. S. 2009. Comparison of Four Classification Methods to Extract Land Use and Land Cover from Raw Satellite Images for Some Remote Arid Areas, Kingdom of Saudi Arabia. *Earth Science*, 20(1): 167-191.

Alajlan, N., Bazi, Y., Melgani, F., Yager, R.R. 2012. Fusion of supervised and unsupervised learning for improved classification of hyperspectral images. *Information Sciences*, 217: 39-55.

Alcaraz-Segura, D., Chuvieco, E., Epstein, H.E., Kasischke, E.S., & Trishchenko, A. 2010. Debating the greening vs. browning of the North American boreal forest: differences between satellite datasets. *Global Change Biology*, 16: 760-770.

Amekudzi, L.K., Yamba, E.I., Preko, K.,. Asare, E.O., Aryee, J., Baidu, M. and Codjoe, S.N.A. 2015. Variabilities in Rainfall Onset, Cessation and Length of Rainy Season for the Various Agro-Ecological Zones of Ghana. *Climate*, 3: 416-434.

Amri, R., Zribi, M., Lili-Chabaane, Z., Duchemin, B., Gruhier, C. and Chehbouni, A. 2011. Analysis of Vegetation Behavior in a North African Semi-Arid Region, Using SPOTVEGETATION NDVI Data, *Remote Sensing*, 3: 2568-2590.

Anyamba, A. and Tucker, C.J. 2005. Analysis of Sahelian vegetation dynamics using NOAAAVHRR NDVI data from 1981–2003. *Journal of Arid Environments*, 63: 596–614.

Anderson, R., Hardy, E. E., Roach, J. T. and Witmer, R. E. 1976. A land use and land cover classification system for use with remote sensor data. Sioux Falls, USA: USGS Professional Paper 964.

Ardli, E.R. and Wolff, M. 2009. Land use and land cover change affecting habitat distribution in the Segara Anakan lagoon, Java, Indonesia. *Regional Environmental Change*, 9: 235–243.

Arouna, O., Toko, I., Djogbénou C. P. and Sinsin, B. 2011. Comparative analysis of local populations' perceptions of socio-economic determinants of vegetation degradation in sudano-guinean area in Benin (West Africa). *International Journal of Biodiversity and Conservation*, 3(7): 327-337.

Bado, B.V., Bationo, A., Lompo, F., Traore, K., Sedogo, M.P. and Cescas, M.P. 2012. Long term effects of crop rotations with fallow or groundnut on soil fertility and succeeding sorghum yields in the Guinea Savannah of West Africa. In *Lessons learned from Longterm Soil Fertility Management Experiments in Africa*; Springer Netherlands, Berlin, Germany.

Bamba, A., Dieppois, B., Konaré, A., Pellarin, T., Balogun, A., Dessay, N., Kamagaté, B., Issiaka Savané, I. and Diédhiou, A. 2015. Changes in Vegetation and Rainfall over West Africa during the Last Three Decades (1981-2010). *Atmospheric and Climate Sciences*, 5: 367-379

Bamba, I. 2010. *Anthropisation et dynamique spatio-temporelle de paysages forestiers en Republique Democratique du Congo*. Thèse de Doctorat, Universite Libre de Bruxelles.

Barrett, C.B., Reardon, T., and Webb, P., 2001. Nonfarm income diversification and household livelihood strategies in rural Africa: concepts, dynamics, and policy implications. *Food Policy*, 26(4):315–331.

Bhagat, V.S., 2012. Use of remote sensing techniques for robust digital change detection of land: a review. *Recent Patents on Space Technology*, 2: 123–144.

Bibi, U.M., Kaduk, J. and Balzter, H. 2014. Spatial-Temporal Variation and Prediction of Rainfall in Northeastern Nigeria, *Climate*, 2: 206-222.

Blanzieri E. and Melgani F. 2008. Nearest neighbor classification of remote sensing images with the maximal margin principle. *IEEE Transactions on Geoscience and Remote Sensing*, 46:1804-1811.

Boateng, P.K. 2013. Agricultural production, land-use/cover change and the desertification debate in the West African Savannah: An adapted political ecology approach. *Journal of Arts and Humanities*, 2(8): 21–35.

Bobée, C., Ottlé, C., Maignan, F., de Noblet-Ducoudré, N., Maugis, P., Lézine, A.-M. and Ndiaye, M. 2012. Analysis of vegetation seasonality in Sahelian environments using MODIS LAI, in association with land cover and rainfall. *Journal of Arid Environments*, 84: 38-50.

Boeglin, J.-L. 1990. *évolutions minéralogique et géochimique des cuirasses ferrugineuses de la région de Gaoua (Burkina Faso)*. Thèse de Doctorat, Université Louis Pasteur.

Bouriaud, O., Leban, J.M. and Deleuze, C. 2005. Intra-annual variations in climate influence growth and wood density of Norway spruce. *Tree Physiology*, 25: 651–660.

Bowman A.W. and Azzalini A. 1997. *Applied Smoothing Techniques for Data Analysis*. Oxford, Oxford University Press.

Braimoh, A.K. 2004. Seasonal migration and land-use change in Ghana. *Land Degradation and Development. 15:* 37–47.

Braimoh, A.K. and Vlek, P.L.G. 2005. Land-Cover Change Trajectories in Northern Ghana. *Environmental Management*, 36(3): 356–373.

Breiman, L. 1996. Bagging predictors. *Maching Learning*, 24: 123–140.

Breiman, L. 2001. Random forests. *Maching Learning*, 45: 5–32.

Bunn, G. A. and Goetz, S.J. 2006. Trends in Satellite-Observed Circumpolar Photosynthetic Activity from 1982 to 2003: The Influence of Seasonality, Cover Type, and Vegetation Density. *Earth Interactions*, 12: 1-19.

Calle, M.L and Urrea, V. 2010. Letter to the Editor: Stability of Random Forest importance measures. *Briefings in bioinformatics*, 12(1): 86-89.

Callo-Concha, D., Gaiser, T., Webber, H., Tischbein, B,Müller, M. and Ewert, F. 2013. Farming in the West African Sudan Savanna: Insights in the context of climate change. *African Journal of Agricultural Research*, 8(38): 4693-4705.

Callo Concha, Daniel; Gaiser, Thomas; Ewert, Frank.2012. *Farming and cropping systems in the West African Sudanian Savanna. WASCAL research area: Northern Ghana, Southwest Burkina Faso and Northern Benin.* Bonn, No. 100.

Camberlin, P. and Diop, M. 2003. Application of daily rainfall principal component analysis to the assessment of the rainy season characteristics in Senegal. *Climate Research*, 23: 159–169.

Capra, A., Consoli, S. and Scicolone, B. 2013. Long-Term Climatic Variability in Calabria and Effects on Drought and Agrometeorological Parameters. *Water Resource Management*, 27: 601–617

Carrão, H., Gonçalves, P. & Caetano, M., 2008. Contribution of multispectral and multitemporal information from MODIS images to land cover classification. *Remote Sensing of Environment*, 112(3), 986-997.

Carreiras, J.M.B., Pereira, J.M.C. and Shimabukuro, Y.E. 2006. Land-cover Mapping in the Brazilian Amazon Using SPOT-4 Vegetation Data and Machine Learning Classification Methods. *Photogrammetric Engineering and Remote Sensing*, 72(8): 897–910.

Chase, T.N., Pielke, R.A., Kittel, T.G.F., Nemani, R.R. and Running, S.W. 1999. Simulated impacts of historical land cover changes on global climate in northern winter. *Climate Dynamics*, 16: 93–105.

Chatfield, C. 2003. *The Analysis of Time Series: An Introduction*. 5th ed. Chapman & Hall, London, U.K.

Chen, G., Hay, G.J., Carvalho and Wulder, M. 2012. Object-based change detection. *International Journal of Remote Sensing*, 33(14): 4434–4457.

Chen, H., Guo, S., Xu, C-Y. and Singh, V.P. 2007. Historical temporal trends of hydroclimatic variables and runoff response to climate variability and their relevance in water resource management in the Hanjiang basin. *Journal of Hydrology*, 344: 171– 184.

Chen, J., Gong, P., He C., Pu, R.and Shi, P. 2003. Land-Use/Land-Cover Change Detection Using Improved Change-Vector Analysis. *Photogrammetric Engineering & Remote Sensing*, 69(4): 369–379.

Chesworth, W. (Ed.). 2008. *Encyclopedia of soil science*. Springer Science & Business Media.

Colditz, R. R., Conrad, C., Wehrmann, T., Schmidt, M. and Dech, S. TiSeG: 2008. A Flexible Software Tool for Time-Series Generation of MODIS Data Utilizing the Quality Assessment Science Data Set. *IEEE transactions on geoscience and remote sensing*, 46(10): 3296-3308.

Colditz, R.R., Conrad, C. and Dech, S.W. 2011. Stepwise Automated Pixel-Based Generation of Time Series Using Ranked Data Quality Indicators. *IEEE Journal of Selected Topics in Applied Earth Observations and Remote Sensing*, 4(2): 272-280.

Compaore, H. 2006. The impact of savannah vegetation on the spatial and temporal variation of the actual evapotranspiration in the Volta Basin, Navrongo, Upper East Ghana. *Ecology and Development Series*, 36.

Congalton, R.G. and Green, K. 2009. *Assessing the Accuracy of Remotely Sensed Data: Principles and Practices*; CRC Press: London, UK.

Conrad, C., Dech, S., Dubovyk, C., Fritsch, S., Klein, D., Löw, F., Schorcht, G. and Zeidler, J. 2014. Derivation of temporal windows for accurate crop discrimination in heterogeneous croplands of Uzbekistan using multitemporal RapidEye images. *Computers and Electronics in Agriculture*, 103: 63–74.

Cord, A., Conrad, C., Schmidt, M. and Dech, S. 2010. Standardized FAO-LCCS land cover mapping in heterogeneous tree savannas of West Africa. *Journal of Arid Environments*, 74: 1083–1091.

Cui, X., Gibbes, C., Southworth, J. and Waylen, P. 2013. Using Remote Sensing to Quantify Vegetation Change and Ecological Resilience in a Semi-Arid System. *Land*, 2: 108130.

Cutler, D.R., Edwards, T.C., Beard, K.H., Cutler, A., Hess, K.T., Gibson, J. and Lawler, J.J. 2007. Random forests for classification, Ecology, 88, pp. 2783–2792.

Da, D.E.C., Thombiano, L. et Boni, A. 2009. La dynamique des paysages à Oursi. *Cahier du CERLESH*, 26: 167-186.

Dardel, C., Kergoat, L., Hiernaux, P., Mougina, E., Grippa , M. and Tucker, C.J. 2014. Regreening Sahel: 30 years of remote sensing data and field observations (Mali, Niger). *Remote Sensing of Environment*, 140: 350–364.

Davenport, M.L. and Nicholson, S.E. 1993. On the relation between rainfall and the Normalized Difference Vegetation Index for diverse vegetation types in East Africa. *International Journal of Remote Sensing*, 14(12): 2369–2389.

Deer P.J., Eklund P. 2003. A Study of Parameter Values for a Mahalanobis Distance Fuzzy Classifier. *Fuzzy Sets and Systems*, 137: 191-213.

Delves, L.M., Wilkinson, R., Oliver, C.J., and White, R.G., 1992. Comparing the performance of SAR image segmentation algorithms. *International Journal of Remote Sensing*, 13(11): 2121– 2149.

Deng, C. and Wu, C. 2013. A spatially adaptive spectral mixture analysis for mapping subpixel urban impervious surface distribution. *Remote Sensing of Environment*, 133: 62–70.

Deng, J.S., Wang, K., Deng,Y.H. and Qi, G.J. 2008. PCA-based land-use change detection and analysis using multitemporal and multisensory satellite data. *International Journal of Remote Sensing*, 29: 4823–4838.

Derbile, E. K., 2010. *Local Knowledge and Livelihood Sustainability under Environmental Change in Northern Ghana*. PhD thesis, University of Bonn, 296 p.

Dewan, A.M. and Yamaguchi, Y. 2009. Using remote sensing and GIS to detect and monitor land use and land cover change in Dhaka Metropolitan of Bangladesh during 1960– 2005. *Environmental Monitoring and Assessment*, 150: 237–249.

Dhakal, A. S., Amada, T., Aniya, M. and Sharm, R. R. 2002. Detection of areas associated with flood and erosion caused by a heavy rainfall using multitemporal Landsat TM data. *Photogrammetry of Engineering Remote Sensing*, 68: 233-239.

Dhodhi, M.K., Saghri J.A., Ahmad I., and Ul-Mustafa R. 1999. D-ISODATA: A Distributed Algorithm for Unsupervised Classification of Remotely Sensed Data on Network of Workstations. *Journal of Parallel and Distributed Computing*, 59: 280-301.

di Gregorio, A.D. and Jansen, L. J. 2005. *Land Cover Classification System, Classification Concepts and User Manual, Software Version 2*. In: Food and Agriculture Organization of the United Nations, Environmental and Natural Resources Series Rome. Available online:http://www.fao.org/docrep/003/x0596e/x0596e00.HTM (accessed on 1 July 2015).

Dipama, J.M. 2005. Analyse de la dynamic du couvert vegetal par photographie aeriennes et images Landsat dans la province de la Kompienga (Burkina Faso). *Cahiers du CERLESHS*, 23: 51-66.

Dodge, Y. 2010. *The Concise Encyclopedia of Statistics*, Springer, New York

Duadze, S.E.K. 2004. *Land Use and Land Cover Study of the Savannah Ecosystem in the Upper West Region (Ghana) Using Remote Sensing*; Bonn: Cuvillier Verlag Göttingen, Germany.

Dwivedi R.S., Kandrika S., Ramana K.V. 2004. Comparison of Classifiers of Remote- Sensing Data for Land-Use/Land-Cover Mapping. *Current Science*, 86: 328-335.

Efiong, J. 2011. Changing Pattern of Land Use in the Calabar River Catchment, Southeastern Nigeria. *Journal of Sustainable Development*, 4(1): 92-102.

Eklundh, L. 1998. Estimating relations between AVHRR NDVI and rainfall in East Africa at 10-day and monthly time scales. *International Journal of Remote Sensing*, 19(3): 563568.

ENVI, 2009. *Atmospheric Correction Module: QUAC and FLAASH User's Guide, Version 4.7*. Available online: https://www.exelisvis.com/portals/0/pdfs/envi/Flaash_Module.pdf (accessed on 1 July 2015).

FAO, 1998. *SDdimensions: Environment: Geoinformation, monitoring and assessment. Sustainable development Department (SD)*, Food and Agriculture Organization of The United Nations (FAO). Rome

FAO, 1999. *Sahel Weather and Crop Situation 1999, Global Information and Early Warning System on Food and agriculture*. Report No 4. Available online: ftp://ftp.fao.org/docrep/fao/003/x3004e/x3004e00.pdf (accessed on 1 July 2015).

FAO, 2006. *World reference base for soil resources, 2006: a framework for international classification, correlation, and communication*. Food and Agriculture Organization of the United Nations. Rome.

Farrar, T.J., Nicholson, S.E. and Lare, A.R. 1994. The influence of soil type on the relationships between NDVI, rainfall, and soil moisture in semiarid Botswana. II. NDVI response to soil moisture. *Remote Sensing of Environment*, 50(2): 121–133.

Fensholt, R. 2004. Earth observation of vegetation status in the Sahelian and Sudanian West Africa: comparison of Terra MODIS and NOAA AVHRR satellite data. *International Journal of Remote Sensing*, 25(9): 1641–1659.

Fensholt, R. and Rasmussen, K. 2011. Analysis of trends in the Sahelian 'rain-use efficiency' using GIMMS NDVI, RFE and GPCP rainfall data, *Remote Sensing of Environment*, 115: 438–451.

Fensholt, R. and Sandholt, I. 2005. Evaluation of MODIS and NOAA AVHRR vegetation indices within situ measurements in a semi-arid environment. *International Journal of Remote Sensing*, 26(12): 2561–2594.

Fensholt, R., Rasmussen, K., Nielsen, T.T. and Mbow, C. 2009. Evaluation of earth observation based long term vegetation trends — Intercomparing NDVI time series trend analysis consistency of Sahel from AVHRR GIMMS, Terra MODIS and SPOT VGT data. *Remote Sensing of Environment*, 113: 1886–1898.

Fensholt, R., Sandholt, I. and Stisen, S. 2006. "Evaluating MODIS, MERIS, and VEGETATION –Vegetation Indices Using in situ Measurements in a Semiarid Environment." *IEEE Transactions on Geoscience and Remote Sensing*, 44(7): 1774–1786.

Fisher, P. 1997. The Pixel: A Snare and a Delusion. *International Journal of Remote Sensing*, 18: 679-685.

Foody, G.M. 2002. Status of land cover classification accuracy assessment. Remote Sensing of Environment, 80: 185 – 201.

Forkel, M., Carvalhais, N., Verbesselt, J., Mahecha, M.D., Neigh, C.S.R. and Reichstein, M. 2013. Trend Change Detection in NDVI Time Series: Effects of Inter-Annual Variability and Methodology. *Remote Sensing*, 5: 2113-2144.

Forkuor, G. 2014. *Agricultural Land Use Mapping in West Africa Using Multi-sensor*. PhD thesis, Julius-Maximilians-Universität Würzburg, 175 p.

Forkuor, G., Conrad, C., Thiel, M., Ullmann, T. and Zoungrana, E. 2014. Integration of optical and Synthetic Aperture Radar imagery for improving crop mapping in Northwestern Benin, West Africa. *Remote Sensing*, 6: 6472–6499.

Forkuor, G., Conrad, C., Landmann, T. and Thiel, M., 2013. *Improving agricultural land use mapping in West Africa using multi-temporal Landsat and RapidEye data*. In: Borg, E., Daedelow, H., Johnson, R. (Eds), 5th RapidEye Science Archive (RESA) - From the Basics to the Service. GITO: Berlin, pp. 57-72.

Förster, M., Schmidt, T., Schuster, C. and Kleinschmit, B. 2012. Multi-temporal detection of grassland vegetation with RapidEye imagery and a spectral-temporal library. *Geoscience and Remote Sensing Symposium (IGARSS)*, 2012 IEEE International, Munich, 22-27 July 2012.

Friedl, M. A., Sulla-Menashe, D., Tan, B., Schneider, A., Ramankutty, N., Sibley, A. and Huang, X. 2010. MODIS Collection 5 global land cover: Algorithm refinements and characterization of new datasets. *Remote Sensing of Environment*, 114: 168–182.

Galford, G.L., Melillo, J., Mustard, J.F., Carlos E. P. Cerri, C.E.P. and Cerri, C.C. 2010. The Amazon Frontier of Land-Use Change: Croplands and Consequences for Greenhouse Gas Emissions. *Earth Interactions*, 14(15): 1-24.

Galiano, L., Martınez-Vilalta, J. and Lloret, F. 2010. Drought-Induced Multifactor Decline of Scots Pine in the Pyrenees and Potential Vegetation Change by the Expansion of Cooccurring Oak Species. *Ecosystems*, 13: 978–991.

Gao, X., Huete, A. R., Ni, W. and Miura, T. 2000. Optical–biophysical relationships of vegetation spectra without background contamination. *Remote Sensing of Environment*, 74(3): 609– 620.

Garza-Gisholt, E., Hemmi, J.M., Hart, N. S. and Collin S.P. 2014. A Comparison of Spatial Analysis Methods for the Construction of Topographic Maps of Retinal Cell Density. *PLoS ONE*, 9(4): e93485.

Garzelli, A. and Nencini, F. 2007. Panchromatic sharpening of remote sensing images using a multiscaleKalman filter, *Pattern recognition*, 40(12): 3568–3577.

Gaughan, A.E., Stevens, F.R., Gibbes, C., Southworth, J. and Binford, M.W. 2012. Linking vegetation response to seasonal precipitation in the Okavango–Kwando–Zambezi catchment of southern Africa, *International Journal of Remote Sensing*, 33(21): 6783–6804.

Gemmer, M., Becker, S., Jiang, T., 2004. Observed monthly precipitation trends in China 1951–2002. *Theoretical and Applied Climatology*, 39: 21–37.

Gessner, U., Naeimi, V., Klein, I., Kuenzer, C., Klein, D. and Dech, S. 2013a. The relationship between precipitation anomalies and satellite-derived vegetation activity in Central Asia. *Global and Planetary Change*, 110: 74–87.

Gessner, U., Machwitz, M., Conrad, C. and Dech, S. 2013b. Estimating the fractional cover of growth forms and bare surface in savannas. A multi-resolution approach based on regression tree ensembles. *Remote Sensing of Environment*, 129: 90–102.

Ghofrani, Z., Mokhtarzade, M., Sahebi, M.R. and Beykikhoshk, A. 2014. Evaluating coverage changes in national parks using a hybrid change detection algorithm and remote sensing. *Journal of Applied Remote Sensing*, 8: 1-16.

Gislason, P.O., Benediktsson, J.A. and Sveinsson, J.R. 2006. Random Forests for land cover classification. *Pattern Recognition Lett*ers, 27(4): 294–300.

Gray, C. L. 2005. What kind of intensification? Agricultural practice, soil fertility and socioeconomic differentiation in rural Burkina Faso. *The Geographical Journal*, 171(1): 70–82.

Guay, K.C., Beck, P.S., Berner, L.T., Goetz, S.J., Baccini, A. and Buermann W. 2014. Vegetation productivity patterns at high northern latitudes: a multi-sensor satellite data assessment. *Global Change Biology*, 20(10):3147-3158.

Guinko, S.1984. *Végétation de la Haute Volta*. Thèse de Doctorat, Es Science, université BordeauxIII.

Gunderson, L.H., 2000. Ecological resilience—in theory and application. *Annual Review of Ecology and Systematic*, 31: 425–439.

Gyau-Boakye, P. and Tumbulto, J.W., 2006. Comparison of rainfall and runoff in the humid southwestern and the semiarid northern savannah zone in Ghana. *African Journal of Science and Technology*, 7 (1): 64–72.

Haertel, V., Shimabukuro, Y. E., and Almeida-Filho, R., 2004. Fraction images in multitemporal change detection. *International Journal of Remote Sensing*, 25(23): 5473–5489.

Harris, A., Carrb, A.S. and Dashc, J. 2014. Remote sensing of vegetation cover dynamics and resilience across southern Africa. *International Journal of Applied Earth Observation and Geoinformation*, 28: 131–139.

Hadgu, G., Tesfaye, K., Mamo, G. and Kassa, B. 2013. Trend and variability of rainfall in Tigray, Northern Ethiopia: Analysis of meteorological data and farmers' perception. *Academia Journal of Agricultural Research*, 1(6): 088-100.

Hayes, D.J. and Sader, S.A. 2001. Comparison of ChangeDetection Techniques for Monitoring Tropical Forest Clearing and Vegetation Regrowth in a Time Series. *Photogrammetric Engineering & Remote Sensing*, 67(9): 1067-1075.

Hein L. and de Ridder, N. 2006. Desertification in the Sahel: a reinterpretation. *Global Change Biology*, 12: 751–758.

Hein, L., de Ridder, N., Hiernaux, P., Leemans , R., de Witd, A. and Schaepman, M. 2011. Desertification in the Sahel: Towards better accounting for ecosystem dynamics in the interpretation of remote sensing images. *Journal of Arid Environments*, 75: 1164-1172.

Herrmann, S. M., Anyamba, A. and. Tucker, C.J. 2005a. Recent trends in vegetation dynamics in the African Sahel and their relationship to climate. *Global Environmental Change*, 15: 394–404.

Hermann, S. M., Anyamba, A. and Tucker, C. J. 2005b. Exploring relationship between rainfall and vegetation dynamics in the Sahel using coarse resolution satellite data. *Proceedings of International Symposium on Remote Sensing of Environment*, June 20- 24, St. Petersburg, 2005.

Herold, M., Woodcock, C.E., Loveland, T.R., Townshend, J., Brady, M., Steenmans, C. and Schmullius, C.C. 2008. Land-cover observations as part of a Global Earth Observation System of Systems (GEOSS): Progress, Activities, and prospects. *IEEE Systems Journal*, 2: 414–423.

Higginbottom, T.P. and Symeonakis, E. 2014. Assessing Land Degradation and Desertification Using Vegetation Index Data: Current Frameworks and Future Directions. *Remote Sensing*, 6: 9552-9575.

Hobbs, R. J. 1990. Remote sensing of spatial and temporal dynamics of vegetation. *Ecological Studies*, 79: 203-219.

Horning, N. 2010. Random forests: An algorithm for image classification and generation of continuous fields data sets. *In Proceedings of the International Conference on Geoinformatics for Spatial Infrastructure Development in Earth and Allied Sciences*, Osaka, Japan, 9–11 December 2010.

Hostert, P., Roder, A. and Hill, J. 2003. Coupling spectral unmixing and trend analysis for monitoring of long-term vegetation dynamics in Mediterranean rangelands. *Remote Sensing of Environment*, 87:183–197.

Houessou, L.G., Teka, O., Imorou, I.T., Lykke, A.M. and Sinsin, B. 2013. Land use and Land-cover change at "W" Biosphere Reserve and its surroundings areas in Benin Republic (West Africa). *Environment and Natural Resources Research,* 3(2): 87–101.

Houghton, R.A., Hackler, J.L. and Lawrence, K.T. 1999. The U.S. carbon budget: Contribution from land-use change. *Science,* 285: 574–578.

Hountondji, Y.C, Sokpon, N. and Ozer, P. 2006. Analysis of the vegetation trends using low resolution remote sensing data in Burkina Faso (1982–1999) for the monitoring of desertification. *International Journal of Remote Sensing,* 27(5): 871–884.

Hountondji, Y.-C., Nicolas, J., Sokpon, N. and Ozer, P. 2005. Mise en évidence de la resilience de la végétation sahélienne par télédétection basse resolution au Niger à la suite d'épisodes de sécheresse. *BELGEO*, 4: 499-516.

Huang, C. and Townshend, J. R. G. 2003. A stepwise regression tree for nonlinear approximation: applications to estimating subpixel land cover. *International Journal of Remote Sensing*, 24(1): 75-90.

Huete, A., Didan, K, Miura, T., Rodriguez, E.P., Gao, X. and Ferreira, L.G. 2002. Overview of the radiometric and biophysical performance of the MODIS vegetation indices. *Remote Sensing of Environment*, 83(1-2): 195–213.

Huete, A.R., Van Leeuwen, W.J.D., Hua, G., Qi, J. and Chehbouni, A. 1992. Normalization of multidirectional red and NIR reflectances with the SAVI. *Remote Sensing of Environment*, 41(2-3): 143-154.

Hussain, M., Chen, D., Cheng, A., Wei, H. and Stanley, D. 2013. Change detection from remotely sensed images: From pixel-based to object-based approaches. *ISPRS Journal of Photogrammetry and Remote Sensing*, 80: 91–106.

Im, J. and Jensen, J., 2005. A change detection model based on neighborhood correlation image analysis and decision tree classification. *Remote Sensing of Environment*, 99(3): 326–340.

INSD. 2011. *La région du Sud-Ouest en chiffres*. Institut National de la Statistique et de la Demographie du Burkina Faso, Ouagadougou.

INSD, 2007. *Résultats préliminaires du recensement général de la population et de l'habitat de 2006*. Direction de la Demographie, Institut National des Statistiques et de la Demographie (INSD), Ouagadougou.

IPCC, 2012. *Managing the Risks of Extreme Events and Disasters to Advance Climate Change Adaptation*. Cambridge University Press, Cambridge, UK, and New York, NY, USA, 582 p.

IPCC, 2007. *IPCC fourth assessment report: climate change 2007*. IPCC, Geneva, Switzerland.

Ishappa, M.R. and Aruchamy, S. 2010. Spatial Analysis of Rainfall Variation in Coimbatore District Tamilnadu using GIS. *International Journal of Geomatics and Geosciences*, 1(2): 106-118.

Jaagus, J., 2006. Climatic changes in Estonia during the second half of the 20th century in relationship with changes in large-scale atmospheric circulation. *Theorotical and Applied Climatology*, 83: 77–88.

Jamali, S. 2014. *Analyzing Vegetation Trends with Sensor Data from Earth Observation Satellites*. PhD thesis, Lund University, Sweden.

Jamali, S., Seaquist, J., Ardö, J. and Eklundh, L. 2011. Investigating temporal relationships between rainfall, soil moisture and MODIS-derived NDVI and EVI for six sites in Africa. *Savanna*, 21: 547–550.

Jamali, S., Seaquist, J., Eklundh, L. and Ardö, J. 2014. Automated mapping of vegetation trends with polynomials using NDVI imagery over the Sahel. *Remote Sensing of Environment*, 141: 79–89.

Jia, K., Liang, S., Wei, X., Zhang, L., Yao, Y. and Gao, S. 2014. Automatic land-cover update approach integrating iterative training sample selection and a Markov Random Field model. *Remote Sensing Letters*, 5(2):148–156.

Jiang, H., Zhao, D., Cai, Y., An, S. 2012. A Method for Application of Classification Tree Models to Map Aquatic Vegetation using Remotely Sensed Images from Different Sensors and Dates. *Sensors*, 12: 12437-12454.

Kabba, V.T.S. and Li, J. 2011. Analysis of Land Use and Land Cover Changes, and Their Ecological Implications in Wuhan, China. *Journal of Geography and Geology*, 3(1):104-118.

Kansiime, M.K., Wambugu, S.K. and Shisanya, C.A. 2013. Perceived and Actual Rainfall Trends and Variability in EasternUganda: Implications for Community Preparedness and Response. *Journal of Natural Sciences Research*, 3(8): 179-194.

Kaptué, A.T., Prihodko, L. and Hanan, N.P. 2015. On regreening and degradation in Sahelian watersheds. Proceedings of the national academy of sciences, 112(39): 12133–12138.

Kärdi, T. 2007. Remote sensing of urban areas: linear spectral unmixing of Landsat Thematic Mapper images acquired over Tartu (Estonia). *Proceedings of the Estonian Academy of Sciences, Biology and Ecology*, 56(1):19-32.

Kasei, R., Diekkruger, B. and Leemhuis, C. 2010. Drought frequency in the Volta Basin of West Africa. *Sustainability Science*, 5(1): 89–97.

Kavzoglu T. and Mather P.M. 2003. The Use of Backpropagating Artificial Neural Networks in Land Cover Classification. *International Journal of Remote Sensing*, 24: 4907-4938.

Key, T., Warner, T.A., McGraw, J.B. and Fajvan, M.A.F. 2001. A Comparison of Multispectral and Multitemporal Information in High Spatial Resolution Imagery for Classification of Individual Tree Species in a Temperate Hardwood Forest. *Remote Sensing of Environment*, 75: 100–112.

Klein, D and Roehrig, J. 2006. How does vegetation respond to rainfall variability in a semihumid West African in comparison to a semi-arid East African environment?

Proceedings of the 2nd Workshop of the EARSeL SIG on Land Use and Land Cover, Bonn, 28-30 September 2006.

Knauer, K., Gessner, U., Dech, S.and Kuenzer, C. 2014. Remote sensing of vegetation dynamics in West Africa. *International Journal of Remote Sensing*, 35(17): 6357–6396.

Kumar, M. 2003. Digital image processing. *in* M.V.K. Sivakumar, P.S. Roy, K. Harmsen and S.K. Saha (eds.), *Satellite Remote Sensing and GIS Applications in Agricultural Meteorology*, World Meteorological Organisation, Geneva, pp. 81-102.

Kumar, Y. and Sahoo, G. 2012. Analysis of Parametric & Non Parametric Classifiers for Classification Technique using WEKA. *International Journal of Information Technology and Computer Science*, 7: 43-49.

Lambin, E. F. 1997. Modeling and monitoring land-cover change processes in tropical regions. *Progress in Physical Geography*, 21(3): 375–393.

Lambin, E.F. and Ehrlich, D. 1996. The surface temperature-vegetation index space for land cover and land-cover change analysis. *International Journal of Remote Sensing*, 17: 463-487.

Lambin, E.F., Geist, H.J. and Lepers, E., 2003. Dynamics of Land-Use and Land-Cover Change in Tropical Regions. *Annual Review of Environment and Resources*, 28: 205241.

Landmann, T. and Dubovyk, O. 2014. Spatial analysis of human-induced vegetation decline over eastern African using a decade (2001-2011) of medium resolutionMODIS timeseries data. *International Journal of Applied Earth Observation and Geoinformation*, 33: 76-82.

Lanfredi, M., Simonielloa, T. and Macchiato, M. 2004 Temporal persistence in vegetation cover changes observed from satellite: Development of an estimation procedure in the test site of the Mediterranean Italy. *Remote Sensing of Environment*, 93: 565–576.

Langley, S.K, Cheshire, H.M. and Humes, K.S. 2001. A comparison of single date and multitemporal satellite image classifications in a semi-arid grassland. *Journal of Arid Environment*, 49: 401–11.

Laux, P., Kunstmann, H. and Bardossy, A. 2008. Predicting the regional onset of the rainy season in West Africa. *International Journal of Climatology*, 28: 329–342.

Le Barbé, L., Lebel, T. and Tapsoba, D. 2002. Rainfall Variability in West Africa during the Years 1950–90. *Journal of Climate*, 15(2): 187-202.

Lebel, T. and Ali, A. 2009. Recent trends in the Central and Western Sahel rainfall regime (1990– 2007). *Journal of Hydrology*, 375: 52–64.

Leroux, L., Bégué, A. and Lo, S.D. 2014. Regional analysis of crop and natural vegetation in West Africa based on NDVI metrics. *International Geoscience and Remote Sensing Symposium (IGARSS)*, July 18, 2014.

Li, B., Li Zhang, Yan, Q. and Xu, Y. 2014. Application of piecewise linear regression in the detection of vegetation greenness trends on the Tibetan Plateau. *International Journal of Remote Sensing*, 35(4): 1526–1539.

Li, B., Yu, W. and Wang, J. 2011. An Analysis of Vegetation Change Trends and Their Causes in Inner Mongolia, China from1982 to 2006. *Advances in Meteorology*, 2011: 1-8.

Li, M., Zang, S., Zhang, B., Li, S. and Wu, C. 2014. A Review of Remote Sensing Image Classification Techniques: the Role of Spatio-contextual Information. *European Journal of Remote Sensing*, 47: 389-411.

Li, Z., Li, X., Weia, D., Xub, X. and Wanga, H. 2010. An assessment of correlation on MODIS-NDVI and EVI with natural vegetation coverage in Northern Hebei Province, China. *Procedia Environmental Sciences*, 2: 964–969.

Liaw A. and Wiener M. 2002. Classification and regression by random Forest. *R News*, 2: 18–22.

Lillesand, T.M. and Kiefer, R.W. 1987. *Remote Sensing and Image Interpretation*, Sec. Ed., John Wiley and Sons, Inc. Toronto.

Lillesand, T.M., Kiefer R.W. and Chipman J.W. 2004. *Remote Sensing and Image Interpretation*. Ed. 5. John Wiley and Sons Ltd.

Lillesand, T.M., Kiefer, R.W. and Chipman, J.W. 2008. *Remote Sensing and Image Interpretation*. 6th. ed: John Wiley and Sons, Inc.

Liu, H.Q. and Huete, A.R. 1995. A feedback based modification of the NDV I to minimize canopy background and atmospheric noise. *IEEE Transactions on Geoscience and Remote Sensing*, 33(2): 457-465.

Liu, W. and Wu, E.Y. 2005. Comparison of non-linear mixture models: sub-pixel classification. *Remote Sensing of Environment*, 94:145–154.

Loosvelt, L., Petersb, J., Skriverc, H., Lievensa, H., Van Coillie, M.B.F., De Baets, B. and Verhoesta, N.E.C. 2012. Random Forests as a tool for estimating uncertainty at pixellevel in SAR image classification. *International Journal of Applied Earth Observation and Geoinformation*, 19: 173–184.

Löw, F., Conrad, C. and Michel, U. 2015. Decision fusion and non-parametric classifiers for land use mapping using multi-temporal RapidEye data. *ISPRS Journal of Photogrammetry and Remote Sensing*, 108: 191–204

Lu, D., Li, G. and Moran, E. 2014. Current situation and needs of change detection techniques. *International Journal of Image and Data Fusion*, 5(1): 13–38.

Lu, D., Li, G., Moran, E. and Hetrick, S. 2013. Spatiotemporal analysis of land-use and landcover change in the Brazilian Amazon. *International Journal of Remote Sensing*, 34(16): 5953–5978.

Lu, D., Hetrick, S., Moran, E. and Li, G. 2012. Application of time series Landsat images to examining Land Use/Cover dynamic change. *Photogrammetric Engineering & Remote Sensing*, 78(7): 747–755.

Lu, D., Batistella, M., and Moran, E., 2008. Integration of Landsat TM and SPOT HRG images for vegetation change detection in the Brazilian Amazon. *Photogrammetric Engineering and Remote Sensing*, 74(4): 421–430.

Lu, D., Mausel, P., Batistella, M. and Moran, E. 2005. Land-cover binary change detection methods for use in the moist tropical region of the Amazon: a comparative study. *International Journal of Remote Sensing*, 26(1): 101–114.

Lu, D., Mausel, P., Brondizio, E. and Moran, E. 2004. Change detection techniques. *International Journal of Remote Sensing*, 25(12): 2365–2407.

Lu, D. and Weng, Q. 2004. Spectral Mixture Analysis of the Urban Landscape in Indianapolis with Landsat ETM+ Imagery. *Photogrammetric Engineering & Remote Sensing*, 70(9): 1053–1062.

Lu, H., Raupach, M.R., Mc Vicar, T.R. and Barrett, D.J. 2003. Decomposition of vegetation cover into woody and herbaceous components using AVHRR NDVI time series. *Remote Sensing of Environment*, 86(1): 1-18.

Lucio, P.S., Molion, L. C. B., Valadão, C. E. A., Conde, F.C., Ramos, A. M. and de Melo, M.L.D., 2012. Dynamical Outlines of the Rainfall Variability and the ITCZ Role over the West Sahel. *Atmospheric and Climate Sciences*, 2(3): 337-350.

Lunetta, R.S. and Balogh, M.E. 1999. Application of Multi-Temporal Landsat 5 TM Imagery for Wetland Identification. *Photogrammetric Engineering & Remote Sensing*, 65(11): 1303-1310.

Lunetta, R.S., Knight, J.F., Ediriwickrema, J., Lyon, J.G. and Worthy, L.D. 2006. Land-cover change detection using multi-temporal MODIS NDVI data. *Remote Sensing of Environment*, 105: 142–154.

Lupo, F., Reginster, I. and Lambin, E. F. 2001. Monitoring land-cover changes in West Africa with SPOT Vegetation: Impact of natural disasters in 1998-1999. *International Journal of Remote Sensing*, 22(13): 2633-2639.

Machwitz, M., Gessner, U., Conrad, C., Falk, U., Richters, J. and Dech, S. 2015 Modelling the gross primary productivity of West Africa with the regional biomass model RBM+, using optimized 250 m MODIS FPAR and fractional vegetation cover information. *International Journal of Applied Earth Observation and Geoinformation*, 43:177-194.

Manandhar, R., Odeh, I.O.A. and Ancev, T. 2009. Improving the accuracy of land use and land cover classification of Landsat data using post-classification enhancement. *Remote Sensing*, 1: 330–344.

Marconcini M., Camps-Valls G., Bruzzone L. 2009. A Composite Semisupervised SVM for Classification of Hyperspectral Images. *IEEE Geoscience and Remote Sensing Letters*, 6: 234-238.

Martiny, N., Richard, Y. and Camberlin, P. 2005, Interannual persistence effects in vegetation dynamics of semiarid Africa. *Geophysical Research Letters*, 32(L24403): 1-4.

Mas, J.-F. 1999. Monitoring land-cover changes: a comparison of change detection techniques. *International Journal of Remote Sensing*, 20(1): 139–152.

Mas, J.F., Pérez-Vega, A., Ghilardi, A., Martínez, S., Loya-Carrillo, J.O and Vega, E. 2014. A suite of tools for assessing thematic map accuracy. *Geography Journal*, 2014: 1-10.

Mbow, C., Brandt, M., Ouedraogo, I., de Leeuw, J. and Marshall, M. 2015. What Four Decades of Earth Observation Tell Us about Land Degradation in the Sahel? *Remote Sensing*, 7: 4048-4067.

McIver, D.K. and Friedl, M.A. 2002. Using Prior Probabilities in Decision-tree Classification of Remotely Sensed Data. *Remote Sensing of Environment*, 81: 253-261.

McKee, T. B., Doesken, N. J. and Kleist, J. 1993.The relationship of drought frequency and duration to time scales. *8th Conference on Applied Climatology*, 17–22 January, Anaheim, CA.

Mellor, A., Haywood, A., Stone, C. and Jones, S. 2013. The Performance of Random Forests in an Operational Setting for Large Area Sclerophyll Forest Classification. *Remote Sensing*, 5: 2838-2856.

Mena, C.F. 2008. Trajectories of Land-use and Land-cover in the Northern Ecuadorian Amazon: Temporal Composition, Spatial Configuration, and Probability of Change. *Photogrammetric Engineering and Remote Sensing*, 74(6): 737–751.

Méndez-Barroso, L.A., Vivoni, E.R., Watts, C.J. and Rodríguez, J.C. 2009. Seasonal and interannual relations between precipitation, surface soil moisture and vegetation dynamics in the North American monsoon region. *Journal of Hydrology*, 377: 59–70.

Mennis, J. 2001. Exploring relationships between ENSO and vegetation vigor in the southwest USA using AVHRR data. *International Journal of Remote Sensing*, 22: 3077 – 3092.

Mickelson, J.G. Jr., Civco, D.L. and Silander, J.A. Jr. 1998. Delineating forest canopy species in the northeastern United States using multi-temporal TM imagery. *Photogrammetric Engineering and Remote Sensing*, 64(9): 891–904.

Middleton, N.J. and Thomas, D.S.G. 1997, *World atlas desertification*, Edward Arnold, London, UK.

Mondal, A., Kundu, S., Chandniha, Surendra Kumar Shukla, R. and Mishra, P. 2012. Comparison of Support Vector Machine and Maximum Likelihood Classification Technique using Satellite Imagery. *International Journal of Remote Sensing and GIS*, 1(2): 116–123.

Morten, L. and Fensholt, R. 1999. The spatio-temporal relationship between rainfall and vegetation development in Burkina Faso. *Danish Journal of Geography*, 2: 43-55.

Morton, D.C., DeFries, R.S., Shimabukuro, Y.E., Anderson, L.O., Arai, E., del Bon EspiritoSanto, F., Freitas, R. and Morisette, J. 2006. Cropland expansion changes deforestation dynamics in the southern Brazilian Amazon. *Proceeding of the National Academy of Sciences of the USA*, 103(39): 14637–14641.

Mundia, C. N. and Aniya, M. 2006. Dynamics of land use/cover changes and degradation of Nairobi City, Kenya. *Land Degradation and Development*, 17(1): 97–108.

Muhlbauer, A., Spichtinger, P. and Lohmann, U. 2009. Application and comparison of robust linear regression methods for trend estimation. *Journal of Applied Meteorology and Climatology*, 48:1961-1970.

Murthy, C.S., Raju, P. V. and Badrinath, K.V.S. 2003. Classification of wheat crop with multi-temporal images: performance of maximum likelihood and artificial neural networks. *International Journal of Remote Sensing*, 24(23): 4871–4890.

Myint, S.W., Gober, P., Brazel, A., Grossman-Clarke, S. and Weng, Q. 2011. Per-pixel vs. object based classification of urban land cover extraction using high spatial resolution imagery. *Remote Sensing of Environment*, 115(5): 1145–1161.

Nacoulma, B.M.I., Schumann, K., Traore, S., Bernhardt-Romermann, M., Hahn, K., Wittig, R. and Thiombiano, A. 2011. Impacts of land-use on West African savanna vegetation: a comparison between protected and communal area in Burkina Faso. *Biodiversity and Conservation*, 20: 3341–3362.

Neeti, N. and Eastman, J.R. 2011. A contextual mann-kendall approach for the assessment of trend significance in image time series. *Transactions in GIS*, 15: 599-611.

Nezlin, N.P., Kostianoy, A.G. and Li, B. 2005. Inter-annual variability and interaction of remote-sensed vegetation index and atmospheric precipitation in the Aral Sea region. *Journal of Arid Environments*, 62: 677–700.

Nicholson, S. E. 2005. On the question of the "recovery" of the rains in the West African Sahel. *Journal of Arid Environment*, 63: 615–641.

Nicholson, S.E. 2001. Climatic and environmental change in Africa during the last two centuries. *Climate Research*, 17: 123–144.

Nicholson, S.E. 2013. The West African Sahel: A Review of Recent Studies on the Rainfall Regime and Its Interannual Variability. *ISRN Meteorology*, 2013: 1-32.

Nicholson, S.E., Davenport, M.L. and Maloa, A.R. 1990. A comparison of the vegetation response to rainfall in the sahel and east africa, using normalized difference vegetation index from NOAA AVHRR. *Climatic Change*, 17(2): 209-241.

Nicholson, S.E., Tucker, C.J. and Ba, M.B. 1998. Desertification, Drought, and Surface Vegetation: An Example from the West African Sahel. *Bulletin of the American Meteorological Society*, 79(5): 815-829.

Nicodemus, K.K. 2011. Letter to the editor: On the stability and ranking of predictors from random forest variable importance measures. *Brief Bioinformatics*, 12: 369–373.

Nightingale, J.M. and Phinn, S.R. 2003. Assessment of Relationships Between Precipitation and Satellite Derived Vegetation Condition Within South Australia. *Australian Geographical Studies*, 41(2): 180–195.

Nordberg, M.L. and Evertson, J. 2003. Vegetation index differencing and linear regression for change detection in a Swedish mountain range using Landsat TM and ETM+ imagery. *Land Degradation & Development*, 16: 139–149.

Obot, N. I., Chendo, M. A. C., Udo, S. O. and Ewona I. O. 2010. Evaluation of rainfall trends in Nigeria for 30 years (1978-2007). *International Journal of the Physical Sciences*, 5(14): 2217-2222

Odekunle, T.O. 2004. Rainfall and the length of the growing season in Nigeria. *International Journal of Climatology*, 24: 467–479.

Odjugo, P.A.O. 2010. General Overview of Climate Change Impacts in Nigeria. *Journal of Human Ecology*, 29(1): 47-55.

Olofsson, P., Foody, G.M., Heroldc, M., Stehman, S.V., Woodcock, C.E. and Wulder, M.A. 2014. Good practices for estimating area and assessing accuracy of land change. *Remote Sensing of Environment,*148: 42–57.

Olofsson, P., Foody, G.M., Stehman, S.V. and Woodcock, C.E. 2013. Making better use of accuracy data in land change studies: Estimating accuracy and area and quantifying uncertainty using stratified estimation. *Remote Sensing of Environment,* 129: 122–131.

Oloukoi, J., Mama, V.J. and Agbo, F.B. 2006. Modélisation de la dynamique de l'occupation des terres dans le département des collines au Benin. *Télédétection*, 6(4): 305-323.

Olsson, L., Eklundh, L. and Ardo, J. 2005. A recent greening of the Sahel—trends, patterns and potential causes. *Journal of Arid Environments*, 63: 556–566.

Olusegun, C.F. and Adeyewa, Z.D. 2013. Spatial and Temporal Variation of Normalized Difference Vegetation Index (NDVI) and Rainfall in the North East Arid Zone of Nigeria. *Atmospheric and Climate Sciences*, 3: 421-426.

Orekan,V.O.A. 2007. *Implementation of the local land-use and land-cover change model CLUE-s for Central Benin by using socio-economic and remote sensing data.* PhD thesis, University of Bonn.

Ouedraogo, I., Runge, J., Eisenberg, J., Barron, J. anf Sawadogo. S. 2014. The re-greening of the Sahel: Natural cyclicity or human-induced change? *Land* (3): 1075–1090.

Ouedraogo, I., Tigabu, M., Savadogo, P., Compaore, H., Oden, P.C. and Ouadba, J.M. 2010. Land cover change and its relation with population dynamics in Burkina Faso, West Africa. *Land degradation and development*, 21: 453–462.

Ouoba, A.P., Da, E.C.D. and Paré, S. 2014. Perception locale de la dynamique du peuplement ligneux des vingt dernières années au Sahel burkinabé. Vertigo, 14(2): DOI : 10.4000/vertigo.15131.

Ouoba, A.P. 2013. Changements climatiques, dynamique de la végétation et perception paysanne dans le Sahel burkinabè. Thèse de Doctorat, université de Ouagadougou, 305 p.

Owusu, K., Waylen , P. and Qiu, Y. 2008. Changing rainfall inputs in the Volta basin: implications for water sharing in Ghana. *GeoJournal*, 71(4): 201-210.

Ozdarici, A.O., Akar, O. and Gungor, O. 2012. Evaluation of Random Forest method for agricultural crop classification, *European Journal of Remote Sensing* ,45: 421-432.

Pal, M. and Mather P.M. 2005. Support Vector Machines for Classification in Remote Sensing. *International Journal of Remote Sensing*, 26: 1007-1011.

Panthou, G. Vischela, T. and Lebela, T. 2014. Recent trends in the regime of extreme rainfall in the Central Sahel. *International Journal of Climatology*, 34: 3998–4006.

Peng, J., Xu, Y. and Cai, Y. and Xiao, H. 2011. Climatic and anthropogenic drivers of Land Use/Cover Change in fragile karst areas of southwest China since the early 1970s: a case study on the Maotiaohe watershed. *Environmental Earth Sciences*, 64: 2107–2118.

Pettorelli, N., Vik, J.O., Mysterud, A., Gaillard, J-M., Tucker, C.J. and Stenseth, N.C. 2005. Using the satellite-derived NDVI to assess ecological responses to environmental change. *TRENDS in Ecology and Evolution*, 20(9): 503-510.

Pouliot, D., Latifovic, R. and Olthof, I. 2009. Trends in vegetation NDVI from 1 km AVHRR data over Canada for the period 1985–2006. *International Journal of Remote Sensing*, 30(1): 149–168.

Prince, S.D., Wessels, K.J., Tuckerw, C.J. and Nicholson, S.E. 2007. Desertification in the Sahel: a reinterpretation of a reinterpretation. *Global Change Biology*, 13:1308–1313.

Puletti, N., Perria R. and Storchi P. 2014. Unsupervised classification of very high remotely sensed images for grapevine rows detection. *European Journal of Remote Sensing*, 47: 45-54.

Rai, R. K., Upadhyay, A. and Ojha, C. S. P. 2010. Temporal Variability of Climatic Parameters of Yamuna River Basin: Spatial Analysis of Persistence, Trend and Periodicity. *Open Hydrology Journal*, 4:184-210.

Rao, K.Y., Stephen, M.J. and Phanindra, D.S. 2012. Classification Based Image Segmentation Approach. *International Journal of Computer Science and Technology*, 3(1): 658–660.

Raziei, T., Bordi, I. and Pereira, L. S. 2013. Regional Drought Modes in Iran Using the SPI:

The Effect of Time Scale and Spatial Resolution. *Water Resource Management*, 27:1661–1674

Reenberg, A., Oksen, P. and Svendsen, J. 2003. Landuse changes vis-à-vis agricultural development in Southeastern Burkina Faso: the field expansion dilemma. *Geografisk Tidsskrift-Danish Journal of Geography*, 103: 57-69.

Reese, H. 2011. *Classification of Sweden's Forest and Alpine Vegetation Using Optical Satellite and Inventory Data*, Doctoral Thesis Swedish University of Agricultural Sciences.

Richard, Y. and Poccard, I. 1998. A statistical study of NDVI sensitivity to seasonal andinterannual rainfall variations in Southern Africa. *International Journal of Remote Sensing*, 19(15): 2907-2920.

Rodriguez-Galiano, V.F., Chica-Olmo, M., Abarca-Hernandez, F., Atkinson, P.M. and Jeganathan, C. 2012a. Random Forest classification of Mediterranean land cover using multi-seasonal imagery and multi-seasonal texture. *Remote Sensing of Environment*, 121: 93–107.

Rodriguez-Galiano, V.F., Ghimire, B.; Rogan, J., Chica-Olmo, M. and Rigol-Sanchez, J.P. 2012b. An assessment of the effectiveness of a random forest classifier for land-cover classification. *ISPRS Journal of Photogrammetry and Remote Sensing*, 67: 93–104.

Rogan, J., Miller, J., Stow, D., Franklin, J., Levien, L. and Fischer, C. 2003. Land-cover change monitoring with classification trees using landsat TM and ancillary data. *Photogrammetric Engineering & Remote Sensing*, 69(7): 793–804.

Ruelland, D., Dezetter, A., Puech, C. and Ardoin_Bardin, S. 2008. Long_term monitoring of land cover changes based on Landsat imagery to improve hydrological modelling in West Africa. *International Journal of Remote Sensing*, 29(12): 3533–3551.

Sala, O.E., Chapin, F.S., Armesto, J.J., Berlow, E., Bloomfield, J., Dirzo, R., Huber-Sanwald, E., Huenneke, L.F., Jackson,R.B., Kinzig, A., Leemans, R., Lodge, D.M., Mooney, H.A., Oesterheld, M., Poff, N.L., Sykes, M.T., Walker, B.H., Walker, M. and Wall, D.H. 2000. Global biodiversity scenarios for the year 2100. *Science*, 287: 1770–1774.

Sanderson, E.W., Jaiteh, M., Levy, M.A., Redford, K.H., Wannebo, A.V. and Woolmer, G. 2002. The Human Footprint and the Last of the Wild. *BioScience*, 52(10): 891-904.

Sandwidi, W.J.P. 2007. *Groundwater potential to supply population demand within the Kompienga dam basin in Burkina Faso*. PhD thesis, University of Bonn.

Sanfo, S. 2010. *Politiques publiques agricoles et lutte contre la pauvreté au Burkina Faso: le cas de la région du Plateau Central*. Doctoral dissertation. Universite Paris 1 Panthéon _ Sorbonne. Paris. France.

Sarr, B. 2012. Present and future climate change in the semi-arid region of West Africa: a crucial input for practical adaptation in agriculture. *Atmospheric Science Letters*, 13(2): 108–112.

Sawadogo, H., Zombre, N. P., Bock, L. and Lacroix, D. 2008. Évolution de l'occupation du sol de Ziga dans le village de Yatenga (Burkina Faso) à partir de photos aériennes. *Télédétection,* 8(1): 59-73.

Schlüte, T. 2008. *Geological Atlas of Africa: With Notes on Stratigraphy, Tectonics, Economic geology, Geohazards, Geosites, and Geoscientific education of each country*. 2nd edition, Springer, 301 p.

Sesnie, S.E., Hagell, S.E., Otterstrom, S.M., Chambers, C.L. and Dickson B.G. 2008. SRTMDEM and Landsat ETM+ data for mapping tropical dry forest cover and biodiversity assessment in Nicaragua. *Revista Geográfica Acadêmica*, 2(2): 53–65.

Shalaby, A. and Tateishi, R. 2007. Remote Sensing and GIS for Mapping and Monitoring Land Cover and Land-use Changes in the Northwestern Coastal Zone of Egypt. *Applied Geography,* 27: 28-41.

Simoniello, T., Lanfredi, M., Liberti, M., Coppola, R. and Macchiato, R. 2008. Estimation of vegetation cover resilience from satellite time series. *Hydrology and Earth System Sciences*, 12: 1053–1064.

Sims, D.A., Luo, H., Hastings, S., Oechel, W.C., Rahman, A.F. and Gamon, J.A. 2006. Parallel adjustments in vegetation greenness and ecosystem CO2 exchange in response to drought in a Southern California chaparral ecosystem. *Remote Sensing of Environment,* 103(30): 289–303.

Singh, A. 1989. Digital change detection techniques using remotely sensed data. *International Journal of Remote Sensing*, 10: 989–1003.

Singh, N. and Mulye, S. S. 1991. On the relations of the rainfall variability and distribution with the mean rainfall over India. *Theoretical and Applied Climatology*, 44(3): 209-221.

Skole, D. and Tucker, C. 1993: Tropical deforestation and habitat fragmentation in the Amazon: Satellite data from 1978 to 1988. *Science*, 260: 1905–1910.

Smith, L.C. 2000. Trends in Russian Arctic river-ice formation and breakup, 1917 to 1994. *Physical Geography*, 20(1): 46–56.

Sobrino, J. and Julien, Y. 2011. Global trends in NDVI-derived parameters obtained from GIMMS data. *International journal of remote sensing*, 32: 4267-4279.

Son, N.T., Chen, C.F., Chen, C.R., Minh, V.Q. and Trung, N.H. 2014. A comparative analysis of multitemporal MODIS EVI and NDVI data for large-scale rice yield estimation. *Agricultural and Forest Meteorology*, 197: 52–64.

Sop, T.K. and Oldeland, J. 2011. Local perceptions of woody vegetation dynamics in the context of a 'greening sahel': a case study from Burkina Faso. *land degradation and development*, DOI: 10.1002/ldr.1144.

SP/CONEDD, 2011. *Elaboration du PANA Programmatique du Burkina Faso : Etudes de modélisation climatique, d'évaluation des risques et d'analyse de la vulnérabilité aux changements climatiques,* MEDD, Ouagadougou.

Spiekermann, R., Brandt, M. and Samimi, C. 2015. Woody vegetation and land cover changes in the Sahel of Mali (1967–2011). *International Journal of Applied Earth Observation and Geoinformation*, 34: 113–121.

Stehman, S.V. 2012. Impact of sample size allocation when using stratified random sampling to estimate accuracy and area of land-cover change. *Remote Sensing Letters*, 3: 111– 120.

Stehman, S.V. and Czaplewski, R.L. 1998. Design and analysis for thematic map accuracy assessment: Fundamental principles. *Remote Sensing of Environment*, 64: 331–344.

Thackway, R. and Lesslie, R. 2006. Reporting vegetation condition using the Vegetation Assets, States and Transitions (VAST) framework. *Ecological Management and Restoration*, 7: S53-S62.

Thakur, S., Singh, A. and Suraiya, S. 2012. Comparison of Different Image Classification Techniques for Land Use Land Cover Classification: An Application in Jabalpur District of Central India. *International Journal of Remote Sensing and GIS*, 1(1): 26-31.

Tottrup, C. and Rasmussen, M. S. 2004. Mapping long-term changes in savannah crop productivity in Senegal through trend analysis of time series of remote sensing data. *Agriculture, Ecosystems and Environment*, 103: 545–560.

Tottrup, C., Rasmussen, M.S., Eklundh, L. and Jönsson, P., 2007. Mapping fractional forest cover across the highlands of mainland Southeast Asia using MODIS data and regression tree modelling. *International Journal of Remote Sensing*, 28(1): 23–46.

Traore, S.S., Landmann, T., Forkuo, E.K. and Traore, P.C.S, 2014. Assessing Long-Term Trends In Vegetation Productivity Change Over the Bani River Basin in Mali (West Africa). *Journal of Geography and Earth Sciences*, 2(2): 21-34.

Trietz, P. and Howarth, P. 2000. Integrating spectral, spatial and terrain variables for forest ecosystem classification. *Photogrammetric Engineering & Remote Sensing*, 66(3): 305–317.

Turner, B.L.I., Skole, D., Sanderson, S., Fischer, G., Fresco, L. and Leemans, R. 1995. *LandUse and Land-Cover Change*. IGBP Report, N° 35, HDP Report N° 7. Stockholm and Geneva, IGBP and HDP.

UNESCO, 1973. *International classification and mapping of vegetation, series 6, Ecology and conservation*, Paris 92p.

USGS, 2014. *MODIS Reprojection Tool Web Interface (MRTWeb)*. Available online: https://mrtweb.cr.usgs.gov/ (access on 12 June 2014).

Van de Giesen, N., Liebe, J. and Jung, G. 2010. Adapting to climate change in the Volta Basin, West Africa. *Current science*, 8: 1033–1037.

Viera, A.J. and Garrett, J.M. 2005. Understanding Interobserver Agreement: The Kappa Statistic. *Family Medecine*, 37(5): 360-363.

Vintrou, E., Bégué, A., Baron, C., Saad, A., Seen, D.L. and Traoré, S.B. 2014. A Comparative Study on Satellite- and Model-Based Crop Phenology in West Africa. *Remote Sensing*, 6: 1367-1389.

Vitousek, P.M., Mooney, H.A., Lubchenco, J. and Melillo, J.M.1997. Human domination of earth's ecosystems. *Science*, 277: 494–499.

Vittek, M., Brink, A., Donnay, F., Simonetti, D. and Desclée, B. 2014. Land Cover Change Monitoring Using Landsat MSS/TM Satellite Image Data over West Africa between 1975 and 1990. *Remote Sensing*, 6: 658-676.

von Storch, H. and Zwiers, F. 1999. *Statistical analysis in climate research*. Cambridge university press.

Vuille, M. 2011. Climate Variability and High Altitude Temperature and Precipitation. *in* Singh, V.P., Singh, P. Haritashy, U.K. (eds.), *Encyclopedia of Snow, Ice and Glaciers*, Springer, pp. 153-156,

Wardell, D.A., Reenberg, A. and Tottrup, C. 2003. Historical footprints in contemporary landuse systems: forest cover changes in savannah woodlands in the Sudano-Sahelian zone. *Global Environmental Change*, 13: 235–254.

Wardlow, B.D. and Egbert, S.L. 2010. A comparison of MODIS 250-m EVI and NDVI data for crop mapping: a case study for southwest Kansas. *International Journal of Remote Sensing*, 31(3): 805–830.

WASCAL, 2015. *Doctoral Program Climate Change and Land Use*. Available online: http://www.wascal.org/graduate-programs/climate-change-and-land-use/(accessed on 13 November 2015).

Washington-Allen, R.A., Ramsey, R. D., West, N.E. and Norton, B.E. 2008. Quantification of the ecological resilience of drylands using digital remote sensing. *Ecology and Society*, 13: 1-33.

Waske, B. and Braun M. 2009. Classifier ensembles for land cover mapping using multi temporal SAR imagery. *ISPRS Journal of Photogrammetry and Remote Sensing*, 64: 450-457.

Weih, R.C., Jr. and Riggan, N.D., Jr. 2010. Object-Based Classification vs. Pixel-Based Classification: Comparitive Importance of Multi-Resolution Imagery. *Proceedings of GEOBIA 2010: Geographic Object-Based Image Analysis*, Ghent, Belgium, 29 June–2 July 2010; 38. Part 4/C7, p. 6.

Weng, Q., Hu, X. and Lu, D. 2008. Extracting impervious surface from medium spatial resolution multispectral and hyperspectral imagery: A comparison. *International Journal of Remote Sensing*, 29: 3209–3232.

Wessels, K.J., Bergh, F.V.D. and Scholes, R.J. 2012. Limits to detectability of land degradation by trend analysis of vegetation index data. *Remote Sensing of Environment*, 125: 10–22.

Wessels, K.J., Prince, S.D., Malherbe, J., Small, J., Frost, P.E. and VanZyl, D. 2007. Can human-induced land degradation be distinguished from the effects of rainfall variability? A case study in South Africa. *Journal of Arid Environment*. 68: 271–297.

Whiteside, T.G. Boggs, G.S. and Maier S.W. 2011 Comparing object-based and pixel-based classifications for mapping savannas. *International Journal of Applied Earth Observation and Geoinformation*, 13(6): 884–893.

Wright, J.B., Hastings, D.A., Jones, W.B., and Williams, H.R., 1985. *Geology and mineral resources of West Africa*. Allen & Unwin, London.

Xian, G., Homer, C. and Fry, J. 2009.Updating the 2001 National Land Cover Database land cover classification to2006 by using Landsat imagery change detection methods. *Remote Sensing of Environment*,113: 1133–1147.

Xie, Y., Sha, Z. and Yu, M. 2008. Remote sensing imagery in vegetation mapping: a review. *Journal of Plant Ecology*, 1(1): 9-23.

Xu, M., Cao, C., Zhang, H., Guo, J., Nakane, K., He, Q., Guo, J., Chang, C., Bao, Y., Gao, M. and Li. X. 2010. Change detection of an earthquake-induced barrier lake based on remote sensing image classification. *International Journal of Remote Sensing*, 31(13): 3521–3534.

Yang, L., Xian, G., Klaver, J.M. and Deal, B. 2003. Urban Land-Cover Change Detection through Sub-Pixel Imperviousness Mapping Using Remotely Sensed Data. *Photogrammetric Engineering and Remote Sensing*, 69(9): 1003–1010.

Yuan, F., Sawaya, K.E., Loeffelholz, B.C. and Bauer, M.E., 2005. Land cover classification and change analysis of the Twin Cities (Minnesota) Metropolitan Area by multitemporal Landsat remote sensing. *Remote sensing of Environment*, 9(2): 317-328.

Yuan, J. and Niu, Z. 2008. Evaluation of atmospheric correction using FLAASH. *In Proceedings of the Earth Observation and Remote Sensing Applications*, Beijing, China, June 30–July 2 2008.

Yüksel, A., Akay, A.E. and Gundogan, R. 2008. Using ASTER Imagery in Land Use/Cover Classification of Eastern Mediterranean Landscapes According to CORINE Land Cover Project. *Sensors*, 8: 1237-1251.

Zanotta, D.C. and Haertel, V., 2012. Gradual land cover change detection based on multitemporal fraction images. *Pattern Recognition*, 45: 2927–2937.

Zeng, B. and Yang, T-B. 2009. Natural vegetation responses to warming climates in Qaidam Basin 1982–2003. *International Journal of Remote Sensing*, 30(21): 5685–5701.

Zeng, N., King, A.W., Zaitchik, B., Wullschleger, S.D., Gregg, J., Wang, S. and KirkDavidoff, D. 2013. Carbon sequestration via wood harvest and storage: An assessment of its harvest potential. *Climatic Change*, 118(2): 245-257.

Zhang, B., Li, S., Wu, C., Gao, L., Zhang, W. and Peng, M. 2012. A neighbourhoodconstrained k-means approach to classify very high spatial resolution hyperspectral imagery. *Remote Sensing Letters*, iFirst: 1–10.

Zhang, J. 2010. Multi-source remote sensing data fusion: status and trends. International Journal of Image and Data Fusion, 1(1): 5–24.

Zhang, J., Rivard, B., Sanchez-Azofeifa, A. and Castro-Esau, K. 2006. Intra- and inter-class spectral variability of tropical tree species at La Selva, Costa Rica: Implications for species identification using HYDICE imagery. *Remote Sensing of Environment*, 105: 129–141.

Zhang, X., Friedl, M.A., Schaaf, C.B., Strahler, A.H. and Liu, Z. 2005. Monitoring the response of vegetation phenology to precipitation in Africa by coupling MODIS and TRMM instruments. *Journal of Geophysical Research*, 110: 1-14.

Zhang, X., Friedl, M.A., Schaaf, C.B., Strahler, A.H., Hodges, J.C.F., Gao, F., Reed, B.C. and Huete, A. 2003. Monitoring vegetation phenology using MODIS. *Remote Sensing of Environment*, 84: 471–475.

Zhao, B., Yan, Y.N., Guo, H.Q., He, M.M., Gu, Y.J. and Li, B. 2009. Monitoring rapid vegetation succession in estuarine wetland using time series MODIS-based indicators: An application in the Yangtze River Delta area. *Ecological Indicators*, 9(2): 346–356.

Zhao, Y., He, C. and Zhang, Q. 2012. Monitoring vegetation dynamics by coupling linear trend analysis with change vector analysis: a case study in the Xilingol steppe in northern China. *International Journal of Remote Sensing*, 33(1): 287–308.

Zheng, N. and Xue, J. 2009. *Statistical Learning and Pattern Analysis for Image and Video Processing*. Springer-Verlag London Limited.

Zhou, J., Civico, D. L. and. Silander, J. A. 1998. A wavelet transform method to merge Landsat TM and SPOT panchromatic data, *International Journal of Remote Sensing*, 19(4): 743-757.

Zombre, P.N. 2006. Evolution de l'occupation des terres et localisation des sols nus dans le centre nord du Burkina Faso. *Télédétection*, 5(4): 285-297.

Zoungrana, B. J-B., Conrad, C., Amekudzi, L.K., Thiel, M., Da, E.D., Forkuor, G. and Löw, F. 2015a. Multi-Temporal Landsat Images and Ancillary Data for Land Use/Cover Change (LULCC) Detection in the Southwest of Burkina Faso, West Africa. *Remote Sensing*, 7: 12076-12102.

Zoungrana, B. J-B., Conrad, C., Amekudzi, L.K., Thiel, M. and Da, E.D. 2015b. Land Use/Cover Response to Rainfall Variability: A Comparing Analysis between NDVI and EVI in the Southwest of Burkina Faso, *Climate*, 3: 63-77.

Appendices

Appendix 1. LULC types in the study area. **a** and **b**) Agricultural areas, **c**) Artificial water body, **d**) Woodland along river, **e**) Mixed vegetation, **f**) Bare surface

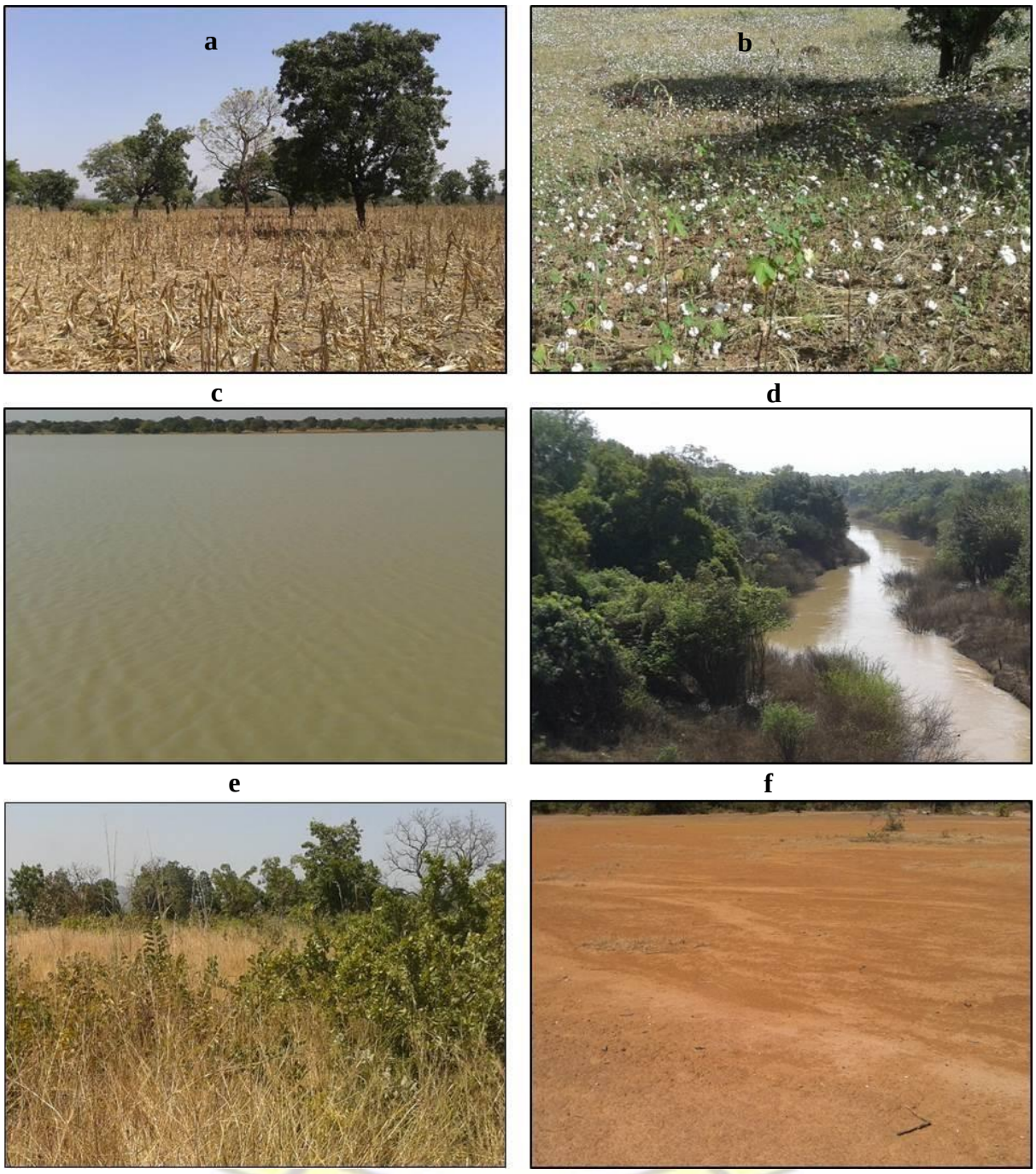

Appendix 2. Impact of anthropogenic pressures on vegetation cover in the study area

Bushfire

Harvested Wood

Artisanal mining area

Area progressively losing its vegetation

Appendix 3. Questionnaire addressed to household

I. GENERAL ASPECT

1.Village (Name)…… **Household number……..**

2.Size of household (number of members)…….....

3.Did you born here? Yes ☐ No ☐

4. If no where do you come from?.....

4.What is your main activity?.....

5. what do you produce ……....

II. CLIMATE VARIABILITY

1.What do you think about the rainfall evolution in your village?

Reduction ☐ Stability ☐ Increasing ☐

2.What is the occurring of drought in your village?

Scarce ☐ sometimes ☐ often ☐ very often ☐

3. Do you know something about climate change? Yes ☐ No ☐

III. VEGETATION COVER EVOLTION

1.What do you think about vegetation cover evolution in the village and its surrounding?

Reduction ☐ Stability ☐ Increasing ☐

2. If reduction what are the causes according to you?

Cropland dynamic ☐ fuelwood extraction ☐ drought ☐ other

……..

3. Are there species which became rare in your environment?

Yes ☐ No ☐ If yes, cite.....

3. Are there species that are prohibited from cutting down?

Yes ☐ No ☐ If yes, cite.....

IV. AGRICULTURAL PRACTICES AND VEGETATION COVER

1- Do you practice slash and burn? (Slash and burn)

Yes ☐ No ☐

2- Do you practice bushfire? Yes ☐ No ☐

3. What are other farming practices that you do?

4- Do you cut all the trees in your farm or some of them?

All ☐ Some ☐

5- Which kind of tree do you leave in your farm?

Type of tree	Food	Medicinal	sacred	Other
	☐	☐	☐	☐
Examples				